ACCRI Theme 4:

Contrails and Contrail-Specific Microphysics

Andrew Heymsfield
National Center for Atmospheric Research
Boulder, Colorado
heyms1@ucar.edu

Darrel Baumgardner
Universidad Nacional Autónoma de México
Mexico City, Mexico
darrel@servidor.unam.mx

Paul DeMott
Colorado State University
Ft. Collins, Colorado
pdemott@lamar.colostate.edu

Piers Forster
School of Earth and Environment
University of Leeds, Leeds, LS2 9JT, UK
P.M.Forster@leeds.ac.uk

Klaus Gierens
DLR-Institut für Physik der Atmosphäre
Oberpfaffenhofen, D-82234 Wessling, Germany
klaus.gierens@dlr.de

Bernd Kärcher
DLR-Institut für Physik der Atmosphäre
Oberpfaffenhofen, 82234 Wessling, Germany
bernd.kaercher@dlr.de

Andreas Macke
Leibniz-Institut für Meereswissenschaften
IFM-GEOMAR
D-24105 Kiel, Germany
amacke@ifm-geomar.de

EXECUTIVE SUMMARY

Theme 4 of the ACCRI, "Contrails and Contrail-Specific Microphysics", reviews the current state of understanding of the science of contrails: 1) how they are formed, 2) their microphysical properties as they evolve, 3) how they develop into contrail cirrus and if their microphysical properties can be distinguished from natural cirrus, 4) their radiative properties and how they are treated in global models and 5) the ice nucleating properties of soot aerosols and whether these aerosols can nucleate cirrus crystals.. Key gaps and underlying uncertainties in our understanding of contrails and their effect on local, regional and global climate are identified and recommendations are provided for research activities that will remove or decrease these uncertainties.

Contrail formation is described by a simple equation that is a function of atmospheric temperature and pressure, specific fuel energy content, specific emission of water vapor and the overall propulsion efficiency. Thermodynamics is the controlling factor for contrail *formation* whereas the physico-chemistry of the emitted particles acts in a secondary role. The criteria for contrail formation determine whether a contrail will form but does not predict whether the contrail will persist or spread into an extensive cirrus-like cloud.

Contrail ice crystals are captured within the downward-travelling vortex pair generated by the aircraft, descending with an average speed of about 2 m/s, which induces adiabatic compression, heating, and sublimation. This phase reduces the ice particle concentration and the contrail will persist and spread only possible if the ambient air is supersaturated with respect to ice.

At formation, the ice number concentration ($\sim 10^4$-10^5 cm^{-3}) and size (several tenths of μm) are mainly determined by the plume cooling rates. During the early stages of a contrail's development, the total ice crystal concentrations are of order 10^3-10^4 cm^{-3} and mean diameters of 5 μm. In the vortex (descending) phase, the concentrations diminish to an order of 10-100 cm^3 and mean sizes increase up to 10 μm diameter. Continued evolution of the size distributions depends on the ambient relative humidity. Observations of the ice crystal shapes during the early phase of contrail formation and beyond are sparse yet important for estimating the radiative properties of young contrails.

When a contrail is first formed the aircraft's contribution of water vapor to the contrail is appreciable. Soon thereafter the ice water content (IWC) increases and is modulated based on the ambient (environmental) water vapor density. The IWC can be quantified using a simple model that converts the ambient (environmental) water vapor supersaturation into condensate.

The fate of a contrail depends on the environmental relative humidity with respect to ice (RHi). In an ice supersaturated environment, contrail microphysical properties are similar to natural cirrus, i.e., concentrations of ice crystals larger than 100 μm in diameter are of order 10-100 l^{-1} and the habits are bullet rosettes; however, many previous measurements of size distributions in the presence of ice crystals several hundred microns and above have been dominated by artifacts resulting from the shattering of crystals on the microphysical probes' inlets. It is therefore difficult to differentiate the particle size distributions (PSD) in cases where large crystals exist in contrails, and that the time and transition toward natural cirrus properties is not well defined based on current data.

Soot particles emitted by aircraft jet engines may perturb cirrus properties and alter cirrus coverage without contrail formation being involved. Aircraft engine exhaust that does not form contrails, and contrails that evaporate, provide sources of enhanced aerosol particle number concentrations directly in regions where cirrus may be forming. Consideration also needs to be given to the role of prior contrail and cloud processing on "preactivating" exhaust ice nuclei.

The nucleation process(es) involved in producing cirrus ice crystals from aircraft exhaust soot aerosols when contrails do not form or from residual soot following contrail evaporation are highly uncertain. Ice formation by black carbon particles in general remains poorly understood. Most studies have been conducted at temperatures warmer than 235K and only a few have carefully quanti-

fied the freezing fraction of soot particles on a single particle basis. Furthermore, the studies most relevant to cirrus formation have used idealized soot particles of unknown relevance to aircraft exhaust soot. Thus, in contrast to the level of knowledge of the composition of aircraft exhaust emissions reflected in the literature, relatively little is known about their role in ice formation, motivating a strong need for further systematic laboratory and in-situ studies.

Aviation soot emissions may change the number of ice crystals in cirrus by several tens of percent according to global model studies; however, due to the limited and inconclusive results on ice nucleating behavior of soot particles, global models that address soot-induced cirrus can only provide preliminary parametric studies exploring possible uncertainties of changes in cirrus properties.

Radiative forcing from contrails depends on many factors: contrail coverage, ice water path, optical properties, geometry, time of day, size and location, age and persistence, background cloudiness and surface albedo. Contrails reflect solar radiation leading to a negative forcing and absorb/trap longwave radiation causing a positive forcing. The net forcing of a contrail is expected to be a positive forcing; however, the cancellation of shortwave and longwave terms of roughly equal magnitude means that the radiative impact is very sensitive to any error in either term. After coverage, which is poorly known, ice water path and optical properties are the largest sources of uncertainty

Most contrail-related subscale processes are not represented in current large-scale models, with the notable exception of the thermodynamic conditions for contrail formation. Until recently GCMs have not carried ice supersatuation, so estimates of available ice have had to be obtained from parameterizations that assume that ice exists above a relative humidity threshold less than 100%. These schemes are also diagnostic as one timestep does not know about contrails at any previous timesteps; therefore, assumptions are also needed about contrail lifetime. The lack in climate models of physical and radiative interaction between contrails and their moist environment renders impossible a meaningful determination of global contrail effects on the water budget in the upper troposphere. Constraining the radiatively important ice crystal size and the IWC or the optical depth of contrails is needed before an accurate estimate of global contrail radiative forcing can be made. While several additional factors including ice crystal shape add to the uncertainty in the radiative forcing, it is the contrail coverage, the IWC and the crystal size that are key to providing an accurate forcing estimate.

The IPCC fourth assessment estimated the linear contrail radiative forcing for 2005 to be 0.01 Wm^{-2} but with a low level of scientific understanding and a factor of three uncertainty in its magnitude. Clearly, significant refinements to the estimates will require improvements in the knowledge and representations of (a) contrail and cirrus ice microphysics and radiative properties, (b) the global distribution of upper-tropospheric ice supersaturation, and (c) improved treatment of contrail and cirrus microphysics, radiation, aerosols, vertical motions driving ice supersaturation, and interactions of contrails with their environment, in global models. Acquiring the information that is needed to make these improvements will require targeted field studies and new instruments that overcome the uncertainties and limitations that impeded previous studies.

1 INTRODUCTION AND BACKGROUND

The continuing growth of airborne transportation is accompanied by increased emissions of gases and particles whose impact on climate, regionally and globally, remains highly uncertain due to limited information on the emission properties and the complex physical processes that govern how these emissions interact with the environment over multiple spatial and temporal scales (Wuebbles, 2006). Given the projection that the demand for air transportation services could grow by a factor of three by 2025 (Next Generation Air Transportation System, 2004), it is imperative that the environmental impact of the current fleet of aircraft is evaluated so that the impact of further growth can be accurately assessed.

Linear contrails, products of aircraft emissions in the upper atmosphere, are arguably the most visible human influence on the Earth's climate. They are high level ice clouds formed under specific atmospheric conditions that usually have more of a climate warming influence by trapping longwave radiation rather than a cooling effect by reflecting incoming solar radiation.. The environmental conditions determine whether they appear at all and if they do appear, whether they persist from minutes to hours and if they spread to form wide decks of cirrus-like clouds or even act to seed or enhance clouds that have already formed. The studies that have attempted to quantify their warming effect suggest that the climate forcing could be comparable to that from aviation's CO2 emissions, but the magnitude is uncertain.

This section of the SSWP, "contrails and contrail-specific microphysics" assesses the current understanding of the science of contrail formation, what we know about their microphysical and radiative properties as a function of time following their formation, and the limitations and uncertainties that are obstacles to accurately predicting how contrails from current and future aircraft fleets impact regional and global climate change. The discussions herein reflect those that were outlined for contrail formation and climate impact during the 2006 workshop on aviation and its impact on climate change (Wuebbles, 2006). They are presented here in greater scientific detail and additional information is presented on the current state of information from field projects that measured contrail properties and much more attention is given to in-situ instrumentation for measuring contrail properties and the limitations associated with these sensors.

2 REVIEW OF THE SPECIFIC THEME

2.1 *Current state of science*

2.1.1 *Range of conditions for formation of contrails, their persistence and evolution into cirrus.*

Contrail formation is determined almost exclusively by basic thermodynamics and the atmospheric conditions in which engine emissions are released. Contrail formation is described by a simple equation containing atmospheric temperature and pressure, specific fuel energy content, specific emission of water vapour and the so-called overall propulsion efficiency. This equation is known as the Schmidt-Appleman-Criterion (SAC), which has been formulated in a convenient format by Schumann (1996) based on earlier work by Schmidt (1941) and Appleman (1953). The SAC states that a contrail forms during the plume expansion process if the mixture of exhaust gases and ambient air transiently reaches or surpasses saturation with respect to liquid water. The fact that the mixture must reach water saturation (and not only ice saturation or any other relative humidity) is the only empirical component of the thermodynamic approach and it is the only part that is related to the ice-forming properties of emitted particles. It simply means that the emitted particles act primarily as cloud condensation nuclei (CCN) and are poor ice forming nuclei (IN), i.e. they first activate into liquid droplets that freeze afterwards. The validity of the SAC description has been demonstrated and confirmed from various research flights (Busen and Schumann, 1995; Kärcher et

al., 1998; Jensen et al., 1998; IPCC 1999). These validations also demonstrate that the thermodynamics is the controlling factor for contrail *formation*, not the physico-chemistry of the emitted particles; however, as we note later, the latter does exert a weak influence on contrail *properties*.

The mixing process is assumed to take place isobarically, so that on a T (absolute temperature) – e (partial pressure of water vapour in the mixture) diagram the mixing (phase) trajectory appears as a straight line. The slope of the mean phase trajectory in the turbulent exhaust field, G (units Pa/K), is characteristic for the respective atmospheric situation and aircraft/engine/fuel combination and given by

$$G = \frac{EI_{H2O} p c_p}{\varepsilon Q (1-\eta)}$$

where ε is the ratio of molar masses of water and dry air (0.622), c_p is the isobaric heat capacity of air (1004 J/kg K) and p is the ambient air pressure. G depends on the emission index of water vapour, EI_{H2O} (1.25 kg per kg kerosene burnt), the chemical heat content of the fuel, Q (43 MJ per kg of kerosene), and on the overall propulsion efficiency, η, of the aircraft engine. Modern airliners have a propulsion efficiency of approximately 0.35, and therefore produce contrails in less cold air than older aircraft (Schumann, 2000). Improved jet engine technology may therefore enhance contrail formation.

One can formulate the SAC condition as a criterion for the maximum temperature, T_c, that would allow contrail formation for given conditions of the ambient relative humidity and pressure:

$$T_c(G,e) = T_{LM}(G) - \frac{e^*[T_{LM}(G)] - e}{G} \qquad (1)$$

where e is the ambient water vapor partial pressure, e^* is the saturation vapor pressure (wrt liquid water) and T_{LM} the maximum temperature that allows contrail formation when the ambient relative humidity (wrt water) is 100% (i.e. $e=e^*$). There is a large degree of uncertainty in predicting T_c because of the uncertainties in determining the parameters that control the magnitude and behaviour of G. One particularly difficult quantity to measure is η. It varies from aircraft to aircraft, cannot be accurately determined at ground conditions and is more difficult to evaluate at cruise altitudes. As shown in Fig. 1 for errors in T_c due to uncertainties in η, a typical uncertainty in η of 0.02 leads to an uncertainty in T_c of about ±0.5 K. This error propagates into the uncertainty in the relative humidity calculated from water vapor pressure measurements, i.e. at upper tropospheric temperatures, such an error in T_c of ±0.5 K corresponds to an error in the threshold relative humidity of about ±5% (in RH units).

The SAC only determines contrail formation and not what follows, i.e. its persistence or evolution into extensive, cirrus-like cloud. Persistence is possible only if the ambient air is supersaturated with respect to ice such that once formed, ice crystals in the plume can grow until the air becomes subsaturated.

2.1.2 *Chemical and microphysical mechanisms that determine the evolution of emissions from the engine exit to plume dispersion*

The initial composition of jet contrails are determined by processes occurring within approximately one wingspan behind the aircraft: chemical and water activation of combustion particles, i.e. soot aerosols, and the subsequent formation of ice on some of these particles (Kärcher et al., 1996). The contribution of soot particles to contrail formation at temperatures near T_c was inferred from theoretical studies in the cooling plume of the homogeneous freezing potential of fully liquid, volatile acidic plume particles that start forming before the threshold conditions for ice formation (Kärcher et al., 1995). It was found that volatile particles do not freeze homogeneously in plumes that are barely supersaturated with respect to water as a result of their very small sizes (a few nm) relative to soot particles (> 10 nm). Soot is formed from sulphurous and carbonaceous compounds during combustion. The sulphurous component, in the form of sulphuric acid, H_2SO_4, increases together with water vapour by condensation after emission (Kärcher, 1998), potentially altering the ice nucleation process involving soot particles; however, if there is sufficient moisture

in the plume as it rapidly cools, the soot particles can acquire a liquid water coating that instantaneously freezes into ice once the plume achieves water supersaturation. This can occur even if hygroscopic H_2SO_4 particles are absent and the soot surfaces have poor water adsorption properties, similar to graphite (Kärcher et al., 1996). In the latter case, the degree of required water supersaturation may depend on the hydrophilic/hydrophobic character of the soot particles (Popovicheva et al., 2007). It was also concluded, based on an observation of contrail formation very close to T_c (Busen and Schumann, 1995), that soot particles with H_2SO_4/H_2O coatings may nucleate ice heterogeneously slightly below water saturation (Kärcher et al., 1996); however, due to the extremely rapid increases in relative humidity, such a small difference in ice nucleation behavior does not significantly affect the SAC criteria within the uncertainties of measurements that determine T_c. In contrast, an assumption of near perfect ice nucleation of exhaust soot, i.e. contrail formation at or substantially above plume ice saturation, would clearly contradict observational evidence (Kärcher et al., 1998).

The number concentration ($\sim 10^4$-10^5 cm^{-3}) and size (fractions of a micrometer) of contrail ice particles at formation is mainly determined by the very high plume cooling rates of order 1000 K/s (Kärcher et al., 1998). Soot particle concentrations in aircraft plumes are typically of this order (Petzold et al., 1998b, 1999) and, once frozen, are sufficiently high to shut off further ice nucleation by depleting the excess water vapor. This predominant dynamical control renders the ice nucleation properties of the particles in the contrail plume relatively unimportant. Increasing the fuel sulphur content leads to more rapid growth of soot particle coatings and potentially activates the entire soot particle reservoir (Schumann et al., 1996; Gierens and Schumann, 1996). Cold ambient temperatures and increased fuel sulphur content lead to slightly more and smaller contrail particles, also because homogeneous freezing of the more numerous water-activated liquid exhaust droplets that take dominance over soot-induced ice formation (Kärcher et al., 1998). Some further turbulent mixing with ambient air and depositional growth of contrail ice particles occurs until the capture of individual plumes in the vortices suppresses the mixing. At this point, the majority of the ice crystals are still very small (diameters < 1 μm) but their concentration has decreased to $\sim 10^3$-10^4 cm^{-3}. The processes that occur during the downward displacement and break-up of wake vortices are thought to be primarily responsible for the observed variability in the number concentrations of young contrail ice particles. Numerical studies (Sussmann and Gierens, 1999) show that a variable fraction of the initial ice crystals sublimate during the vortex phase, depending on the ambient humidity, temperature, stability and turbulence.

Contrail ice crystals are captured within the downward-travelling vortex pair. They descend with an average speed of about 2 m/s that implies adiabatic compression and heating. The heating can be computed assuming a dry adiabatic lapse rate (which can be safely assumed since the evaporating ice mass and latent heating is small) such that a vertical displacement of 300 m heats the air by 3 K and decreases the relative humidity (wrt ice) by 30% within the plume. Hence, a fraction of the contrail ice sublimates during the vortex phase unless the ambient RH exceeds 130%. Surviving fractions of contrail ice (by number and mass) of the order 10^{-3} at ice saturation increase in a power law fashion with increasing supersaturation (Unterstrasser et al., 2007). The power law exponent increases strongly with ambient temperature such that the relationship between the surviving ice fraction and supersaturation becomes more sensitive as the temperature increases.

The adiabatic sinking of the vortex pair leads to a baroclinic instability around the upper stagnation point of the pair. Ice crystals can escape from the vortex system and remain behind. The ice in this so-called secondary wake (which is merely a small fraction of the initially produced ice) is not subject to adiabatic compression and survives when the ambient air is supersaturated, resulting in a faint but persistent contrail. This contrail consists either of the ice in the secondary wake plus the ice that survives the adiabatic heating in the primary vortex or of the secondary wake alone. The numerical studies indicate a broad range of initial conditions (ice mass and number concentration) for the later evolution of contrails.

2.1.3 *Role of emission characteristics and plume processes on the large-scale aviation impact*

As detailed above, nascent contrail properties are not very sensitive to the emission characteristics of kerosene-fuelled jet engines as the initial number of contrail ice particles is limited by the very high cooling rates in the plume rather than by soot emission indices. The slight

alteration of nascent contrail properties by high sulphur emissions is of little practical relevance given that the fuel sulphur content is expected to decrease rather than increase in the future (Wuebbles, 2006). These conclusions might be tempered if future alterations to fuels and combustion parameters would enhance the ice nucleating properties of soot particles (see section 2.1.4); however, the expected impact of changes in things like fuel additives is negligible (Gierens, 2007). The most influential factors that modify contrail properties are those that occur during and after vortex break-up as previously described in 2.1.2. The contrail-to-cirrus transition is further controlled by the moisture fields (the topic of key theme 3) and the distribution of vertical shear in the horizontal wind. The generation of individual contrail-cirrus may be sensitive to vertical gradients of thermodynamic parameters and turbulence levels. In heavily travelled regions within or near flight corridors persistent contrails do not appear as single objects whereby the spreading of multiple contrails leads to contrail decks in which the evolution of one contrail cannot be considered separately from the others.

2.1.4 *Potential for cirrus formation/modification due to aviation soot emissions*

Soot particles emitted by aircraft jet engines, in the absence of contrail formation, may also perturb cirrus properties and alter cirrus coverage. Aircraft engine exhaust that does not form contrails and contrails that evaporate provide sources of enhanced concentrations of aerosol particles in regions where cirrus may eventually form. The potential perturbation likely occurs on regional scales because the residence time of aerosols in the upper tropopause is of the order of days to several weeks, depending on the location of the emissions, the season and the latitude. This aerosol indirect effect is mentioned within the Intergovernmental Panel on Climate Change Fourth Assessment Report (Denman et al. 2007) As such it is an atmospheric component that has medium potential impact on overall aerosol forcing of climate but with very low understanding. The magnitude of the cloud perturbation (e.g. changes in ice cloud particle effective radius) depends on the ice nucleating ability of the released soot particles, on the efficiency of existing aerosol particles to nucleate ice, on temporal interactions of the soot particles with ambient gases and aerosols, on the abundance of water vapor (H_2O), and on dynamic processes setting the stage for the generation of clouds in ice supersaturated regions (Haag and Kärcher, 2004). In fact, an understanding of cirrus formation itself is tantamount to estimating any aircraft soot impact on cirrus.

A good level of understanding of the key, microphysical factors in cirrus formation has evolved over the last 20 years. An important process for ice formation in cirrus is homogeneous freezing of liquid-containing aerosol particles. This process for sulfuric acid and other liquid aerosols appears to be at least quantitatively well understood (Sassen and Dodd, 1988; Heymsfield and Sabin, 1989; Jensen and Toon, 1994; Koop et al., 2000; DeMott, 2002; Lin et al. 2002; Möhler et al., 2003; Haag et al., 2003; Koop, 2004). Pure liquid droplets (or highly diluted liquid aerosol particles) freeze with predictable nucleation rates at water saturation and at approximately 235K Haze particles freeze in a similar manner at progressively more subsaturated conditions as the temperature decreases. Presumably, this process sets an upper bound (Fig. 2) on the ice supersaturation conditions needed for cirrus cloud formation in the upper troposphere, without other factors that might inhibit ice formation by this process. During cirrus formation there is a competition between homogeneous freezing of soluble aerosol particles and potentially more efficient heterogeneous ice nucleation by some fraction of insoluble aerosol particles, such as dust (e..g., Zuberi et al. 2002; DeMott et al. 2003a,b; Richardson et al. 2007), crystallized organic and inorganic phases of soluble aerosols (e.g., Zuberi et al., 2001; Abbatt et al., 2006; Zobrist et al., 2006; Shilling et al., 2006; Beaver et al., 2006) or soot (e.g., Kärcher et al. 1996; Jensen and Toon, 1997; DeMott et al. 1997; Kärcher et al. 2007). This competition is constrained by the available water vapor and therefore only a fraction of all aerosols can influence the microphysical composition of cirrus. Thus the dynamics that drives supersaturation and the aerosols that drive ice nucleation are intertwined in cirrus much as in any cloud (Kärcher and Ström, 2003; Haag and Kärcher, 2004).

On the premise that aircraft soot particles are effective ice nuclei (IN) under conditions that do not already favor homogeneous freezing of liquid aerosol particles and that cirrus formation is dynamically triggered by slow synoptic uplift, cloud resolving simulations have shown that the resulting cirrus are more stable and have different areal coverage and optical properties than cirrus formed on liquid particles in the absence of aircraft soot (Jensen and Toon, 1997). The main

problem associated with assessing the role of aircraft soot in cirrus cloud formation is to unambiguously demonstrate that ice nucleates mainly on the primary exhaust soot particles or secondary particles formed by condensation and coagulation. Designing airborne measurements that help resolve this problem is very challenging. In fact, it must be noted that no direct atmospheric studies have yet validated the impacts of both homogeneous and heterogeneous freezing on cirrus formation directly in the atmosphere, i.e. matching measurements with predictions of cloud ice particle distributions directly from aerosol and dynamical properties. Such a "closure" experiment requires high resolution measurements of aerosol composition, IN, relative humidity, vertical motion, and cloud ice particle size distribution. All of these are technically challenging.

Atmospheric variability in vertical winds below the synoptic scale often seems to control the cooling rates of air parcels containing ice-forming particles (Kärcher and Ström, 2003), challenging the validity of the common assumption that cirrus formation is triggered by slow synoptic uplift. The cooling rate history determines the relative contributions of heterogeneous and homogeneous ice nucleation and how many aerosol particles nucleate to form cirrus ice crystals (DeMott et al., 1997; Gierens, 2003; Kärcher and Lohmann, 2003; Kärcher et al., 2006). Atmospheric cooling rates are difficult to determine experimentally and to describe and predict by models. Taken together, this renders a separate experimental evaluation of dynamical and aerosol effects on cirrus formation very difficult.

Measurements have indicated that regions of the upper troposphere are sometimes highly supersaturated with respect to ice, exceeding values typically required for, at temperatures warmer than needed for homogeneous freezing. There are possible physical mechanisms for such high supersaturations (e.g., Jensen et al., 2005; Peter et al., 2006); however, measuring humidity at low temperatures remains challenging and global prediction of ice supersaturation is still in its infancy. Fortunately, in the extratropics at altitudes where most current air traffic occurs, observed levels of supersaturation are consistent with homogeneous ice nucleation as outlined by Koop et al. (2000).

The following sections review the present state of knowledge of the ice nucleation potential of aircraft exhaust particles based on laboratory and field studies and scenarios for the potential for cirrus modification due to aircraft emissions.

2.1.4.1 *Laboratory evidence regarding ice formation by black carbon particles and aircraft exhaust soot*

Ice formation by black carbon particles in general remains poorly understood. It is further necessary in this regard to distinguish what is known about ice formation by soot particles in general and what is known about those particularly relevant to aircraft emissions. In the former case, it is apparent that some black carbon containing particles act as ice nuclei, as carbonaceous particles have been found as one of the major types of apparent nuclei of ice crystals formed on aerosols sampled from the background upper troposphere and cold regions of the lower troposphere (Chen et al. 1998; Rogers et al. 2001). The efficiency of black carbon particles acting as IN depends very sensitively, but in unclear ways, on temperature and supersaturation, the soot size and surface oxidation characteristics, and as for any ice nucleus on the mechanism of ice formation (DeMott 1990; Gorbunov et al. 2001; Diehl and Mitra, 1998; Möhler et al. 2005a,b; Dymarska et al. 2006). Most studies have been focused at temperatures warmer than 235K and only a few have carefully quantified the freezing fraction of soot particles on a single particle basis. Only a few other laboratory studies have addressed the ice nucleation properties of soot particles at lower temperatures (DeMott et al. 1999; Möhler et al. 2005a,b). Furthermore, the studies most relevant to cirrus formation have used idealized soot particles of unknown relevance to aircraft exhaust soot. Thus, in contrast to the level of knowledge of the composition of aircraft exhaust emissions reflected in the literature, relatively little is known about their role in ice formation.

Figure 2, adapted from Kärcher et al. (2007) summarizes studies of soot ice formation in the cirrus regime. Results from DeMott et al. (1999) for commercial black carbon particles (240 nm mode diameter "lamp black" from Degussa Corporation, Frankfurt/Main, Germany) frozen in a continuous flow diffusion chamber are indicated by DS in the figure. The aerosol particles were treated in some cases by exposure to H_2SO_4 molecules to simulate contrail and atmospheric processing. Untreated particles and those with lower H_2SO_4 coverage ("monolayer") activated ice

only at a relative humidity close to water saturation. With greater H_2SO_4 coverage ("multilayer") ice nucleation by 1% of the particles occurred for ice saturation ratios (S_i) less than required for homogeneous freezing of soluble particles (Koop et al., 2000) at T<220 K. Although the mechanism that apparently renders multilayer-treated DS as more efficient IN is unclear at the moment, it does not appear to be present for untreated or thinly coated particles.

Möhler et al. (2005a) used fractal-like, agglomerated soot particles (100 nm mode diameter) from a graphite spark generator (GS in Fig. 2) for ice nucleation studies in the AIDA cloud chamber of Forschungszentrum Karlsruhe. Untreated GS particles showed S_i thresholds (0.1-0.3% freezing) far below the homogeneous freezing threshold conditions. Coating with H_2SO_4 (volume fractions of 20-80%) drove threshold ice formation conditions significantly higher, toward the homogeneous freezing condition compared to the untreated GS particles.

In contrast to these results favoring a possible role of soot particles as low temperature deposition and immersion freezing nuclei are results for actual collected and re-dispersed combustor soot containing particles (Koehler et al. 2008), smaller soot-containing particles from high temperature stove combustion of jet fuel (DeMott et al. 2002) and soot-containing biomass combustion particles (DeMott et al. 2008). In all of these cases the soot particles were present within internally mixed particles that included soluble organic and inorganic matter. These results, for arguably more realistic atmospheric particles, indicate no special ice nucleating properties to initiate freezing for S_i lower than required for homogeneous freezing in the cirrus temperature regime. Ice formation conditions are indistinguishable or inhibited with respect to homogeneous freezing.

Hydrophilic and hydrophobic organic carbon (OC) is also present in aircraft-emitted aerosols (Demerdjian et al. 2007) or is contained in ambient aerosols that ultimately mix with and contribute to the chemical composition of the plume particle mixtures. Möhler et al. (2005b) employed the AIDA chamber to investigate the ice nucleation ability of soot particles with different OC content generated in a propane burner with different fuel-to-air ratios. Flame soot particles with 16% OC mass content (FS16 in Fig. 2) nucleated ice at S_i only modestly below and indistinguishable from homogeneous freezing thresholds whereas ice was initiated from flame soot with 40% OC content (FS40 in Fig. 2) at S_i values exceeding those required for homogeneous freezing. Although these experiments indicate suppressed IN activity for certain thicker OC coatings, the general impact of OC may depend on the nature of the combustion process and fuel, e.g. IN activity may differ for jet fuel combustion versus biomass burning.

The noted differences in the IN activity of soot particles appear related to different physical or chemical surface properties of the various particles. Most aircraft emitted soot particles are smaller than 100 nm in diameter and have highly complex chemistry. The apparent lack of IN activity of particles representative of those found in jet exhaust is informative; however the lack of understanding of the physical and chemical mechanisms of this activity suggests strong caution on generalizing behaviors in the ambient upper troposphere. The role of prior contrail and cloud processing of exhaust ice nuclei, i.e. "preactivation" (Roberts and Hallett, 1968), also needs to be better understood and taken into account. Clearly there is a strong need for further systematic laboratory and in-situ studies.

2.1.4.2 *Atmospheric evidence for aircraft soot impact on cirrus*

Evidence exists that cirrus ice crystal residue particles sampled from within aircraft corridors contain enhanced numbers of soot particles (Ström and Ohlsson, 1998). Nevertheless, this observation alone is insufficient to demonstrate that soot particles have actually played a role in the process of ice formation. Instead, soot could be included as a passive tracer within freezing aerosol particles or could be scavenged by ice crystals after the cloud has formed. More recent studies inferred strong differences between the S_i formation conditions of cirrus between the Northern and Southern hemispheres (Ström et al. 2003; Haag et al. 2003; Kärcher and Ström, 2003), but this could not be clearly attributed to either aircraft or other anthropogenic aerosols. Nevertheless, the number concentrations of cirrus ice crystals and the insoluble residuals of these crystals were found to increase proportionally (Seifert et al. 2004).

Only a single study of the concentrations and chemical composition of ice nuclei in and out of aircraft exhaust trails has been made directly (Chen et al. 1998). The aircraft IN instrument could only measure to temperatures at the warm limit of most cirrus clouds (~235K). In this temperature regime no difference was seen in the carbonaceous component of ice nuclei in and out of plumes. As in the background free troposphere, crustal, carbonaceous and metallic particles dominated the compositions of heterogeneous ice nuclei. The only difference in composition within exhaust trail regions was in the numbers of metallic particles. This could indicate a source from aircraft due to the presence of metal in combustion particles from jet engines (Demerdjian et al. 2007). Nevertheless, the concentrations of ice nuclei within dry contrails were indistinguishable from those in the ambient free troposphere. This result is emphasized in Fig. 3, where the correlation coefficient of IN, condensation nuclei (CN) and NO are shown for the data set taken during the NASA Subsonic Cloud and Contrail Effects Special Study (SUCCESS) experiment (Rogers et al. 1998; Rogers et al. 2008). While CN and NO concentrations show some positive correlation, IN at T>235K correlate with neither. It is not known if these results can be extrapolated to lower temperatures.

In-situ measurements of the ice nucleation efficacy of exhaust have never been obtained for the temperature conditions representative of contrail or cirrus formation. There is a glaring scientific need for improved real-time measurement capabilities of ice nucleation involving ambient aerosols at cirrus levels. It is also notable that ground based studies of aircraft emissions, such as the PARTEMIS program (Wilson et al. 2004; Petzold et al. 2005), have studied the CCN activity of exhaust particles, but never the IN activities.

Despite the limited and inconclusive results from the afore mentioned laboratory studies, soot particles continue to be prescribed in model simulations as a major source of IN ice formation with the consequence that these particles indirectly affect climate model simulations to a major extent (Lohmann, 2002; Lohmann and Diehl, 2006). Specific to aircraft effects is the study of Hendricks et al. (2005) who found that, by assuming all aircraft soot particles act as efficient IN, aviation causes a reduction of cirrus ice crystal number concentrations. The reduction occurs at NH midlatitudes and ranges between 10 and 60%, in terms of annual means. How this impact ensues can be inferred from the specifics of the soot-cirrus interaction scenario discussed in the next section.

2.1.4.3 *Cirrus formation scenarios and implications of aircraft soot-cirrus interactions*

Kärcher et al. (2007) considered the competition between aircraft generated soot particles, other ice nuclei in the upper troposphere and the homogeneous freezing process for liquid aerosol particles using a physically-based parameterization scheme for cirrus formation in adiabatically rising air parcels. This paper recognized that in order to have an important role as heterogeneous ice nuclei soot particles from aircraft emissions must compete with other known ice nucleators in the upper troposphere. Mineral dust particles, including those expected to be representative of the atmosphere, are known to act as efficient heterogeneous IN over a wide range of temperature conditions (Zuberi et al., 2002; Hung et al., 2003; Archeluta et al., 2005; Möhler et al., 2006; Knopf and Koop, 2006; Kanji and Abbatt, 2006). Field observations also indicate that mineral particles, fly ash and metallic particles far from their source regions may serve at times as IN in cirrus clouds - in some cases without being associated with significant acidic or other condensed components (Heintzenberg et al., 1996; Chen et al., 1998; DeMott et al., 2003a; Sassen et al., 2003; Cziczo et al., 2004; Twohy and Poellot, 2005; Richardson et al., 2007).

Figure 4, from Kärcher et al. (2007), provides a description of the expected role of aircraft soot particles on cirrus formation provided that the ice nucleation behavior of such soot particles can be fully quantified. In the absence of such quantitative information an idealized, single threshold values for IN activation was assumed for that study. As a general conclusion from the above-mentioned laboratory studies of mineral dust particles, onset ice saturation values for heterogeneous nucleation on dust particles are as low as S_i =1−1.25 in cirrus conditions; however, S_i is1.3−1.4 for smaller dust particles and 1.35−1.5 for kaolinite and montmorillonite immersed in aqueous $(NH_4)_2SO_4$ droplets. These values can be used to constrain the competition between ice formation by soot particles and other atmospheric ice nuclei. The total number densities of ice crystals, n_i, as a function of soot particle number density, n_s is shown in Fig. 4. Besides n_s, other crucial parameters that were varied in the calculations were: (i) the vertical wind speed, w, ranging from purely

synoptic uplift (top panel) via mean values typically observed on the mesoscale (middle panel) to lee wave or convective forcing (bottom panel); (ii) the abundance of mineral dust particles as indicated by the legends, with concentrations n_d increasing with w; and (iii) the threshold ice saturation ratios S_{cr} for ice nucleation by the soot particles as given at the top of the figure, whereby the highest value is below but close to the homogeneous freezing threshold. The results are insensitive to variations of the liquid particle properties. Other assumptions about IN sizes are based on observational evidence, as described by Kärcher et al. (2007).

In all panels in Fig. 4 the black curves denote the dependence of n_i versus n_s without interference by dust particles. In the limit of small n_s, n_i arises exclusively from homogeneous freezing of liquid particles and soot does not play any role in ice formation. The number of ice crystals formed by homogeneous freezing increases from 0.05 cm^{-3} to 10 cm^{-3} when the updraft speed increases from 5 cm s^{-1} to 100 cm s^{-1}, highlighting the sensitivity of n_i on the cooling rate. Increasing n_d in this limit (from black via blue to red curves) decreases n_i roughly by a factor of 2 (blue curves) and 5 (red curves) in each panel. These ice crystals, forming early (at lower S) during cooling, enhance the water vapor losses due to depositional growth and thereby reduce the rate of increase of supersaturation leading to fewer liquid particles freezing homogeneously.

Given that soot-induced changes in cirrus are not readily observable, if they indeed exist, the next section and those that follow return to a discussion of contrail cirrus.

2.1.5 *Contrail and cirrus cloud observations*

Contrail microphysical properties—the ice water content (IWC), the total ice particle surface area (A) or extinction (σ), total ice particle number concentration (N_t), ice particle size distributions (PSD), ice particle mean number and mass or volume-weighted diameters ($\bar{D}, \bar{D}_{m,\,v}$) and ice particle shapes have been reported in a number of published articles over the past three decades. These observations and the instruments used to collect the data, are shown in Table 1. Section 2.2.4 and Table 4 further elaborates on the measurement techniques used to collect contrail data and their limitations. The studies to date have sampled contrails properties from their inception (Goodman et al., 1998; Schröder et al., 2000) through to their development into contrail cirrus for periods of an hour or later (Knollenberg, 1972; Heymsfield et al., 1998; Lawson et al., 1998; Poellot et al., 1999; Schröder et al., 2000, Atlas et al., 2006). The observations span the temperature range -78C (Gao et al., 2004) to -30C (Gayet et al., 1996). Contrail ice crystals have been captured, preserved and analyzed (Goodman et al., 1998) and imaged with high-resolution digital cameras (Lawson et al., 1998). Most observations to date have measured the microphysical properties with optical 1-D light scattering (e.g., FSSP) or 2-D imaging (e.g., 2D-C) probes.

In the discussion below, we report ice water content (IWC) and ice particle size distributions (PSD) measured in contrails, compare them to those in cirrus clouds and address the question of whether contrail and natural cirrus can be differentiated.

2.1.5.1 *Ice Water Content*

The ice water content of contrails has largely been estimated from particle size distributions measured by optical spectrometer probes (see Section 2.2.4). This calculation requires assumptions about the ice crystal shapes and their masses and is subject to a factor of two or more uncertainties[1] that extend beyond the issues of measuring contrail PSD (Section 2.2.4). Direct measurements of the IWC can now be made by such probes as a counterflow virtual impactor (CVI, Twohy et al., 1997) and the Fast In situ Stratospheric Hygrometer (FISH). Early on in the lifetime of a contrail, however, the ice crystals are often smaller five microns, the lower size limit that can be collected by

[1] Early on in the lifetime of a contrail the PSD are dominated by small ice crystals, which, for the calculations of the IWC, are considered to be solid ice spheres for lack of information on crystal masses (e. g., Schröder et al., 2000). This can lead to obvious uncertainties and usually overestimates IWC by up to a factor of two to three (see crystals collected in contrails ~40 to 80 seconds after the contrail was generated, Goodman et al., 1998).

CVI and related bulk samplers, or fall below the IWC (~0.001 g m^{-3}) that can be detected by them. Details of their operating principles are given in Section 2.2.4.

Schumann (2002) summarized most IWC estimates in contrails and fit the temperature (T)-dependent relationship to these observations:

$$IWC(g/m^3) = \exp(6.97+0.103T[^{\circ}C])\times 10^3. \quad (2)$$

This curve, plotted in Fig. 5, is derived from data that spans the temperature range -67 to -30C and IWC from 0.001 to 0.07 g/m^3, encompassing the majority of published contrail data acquired to date.

To explain the magnitude of the IWCs observed in contrails, Meerkötter et al. (1999) modeled the "potential IWC" as half of the available condensate between the vapor density at the point of ice nucleation (~140-160%, depending on the temperature) and the vapor density at ice saturation (see Fig. 1). This model is supported by the observations (see Fig. 5). The Schumann curve fit and Meerkötter et al. model indicate that there is a factor of ten decrease in the observed or potential IWC as temperatures (T) are reduced from -40ºC, the warmest possible contrail formation temperature, to -70C.

The potential IWC is a useful empirical representation of the IWC. In practice, however, wake and environmental turbulence produces mixing of contrail and ambient air. The contrail ice crystals are free to draw upon supersaturation in the environment, if present, for growth. Using a large eddy simulation (LES), Lewellen and Lewellen (2001) modeled air motion, moisture and ice crystal size distributions in contrails forming under a range of ambient relative humidities with respect to ice (RHi). Initially, the vortex pair generated by an aircraft descends rapidly for several hundred seconds. The positive buoyancy acquired by the vortex systems' descent through the stratified atmosphere produces Brunt-Vaisala oscillations that are damped by turbulence and mixing between the plume and the environmental air. When the environment is supersaturated with respect to ice, the IWC tends to increase by entrainment of moist air as the volume of the plume expands, its value set by the excess moisture above the ice saturation level. According to Lewellen and Lewellens' model simulations, the ratio of the actual IWC in the plume to its equilibrium value, given by the difference between the vapor density in the environment and its saturation value at the given temperature, is nearly unity throughout the contrail plume. There are obvious exceptions to this estimate, e.g., in the plume center or near the edges .

The representation of potential IWC therefore should account for the ambient humidity. As an approximation, we can take

$$IWC=\rho_a[X_i(RH_i/100-1)], \quad (3)$$

where ρ_a is the density of air, X_i is the saturation mixing ratio with respect to ice at the ambient temperature and RH_i is in percent. This presumes that there is considerable supersaturation in the environment such that the dominant source of condensed water is the ambient supersaturation and not the aircraft exhaust, as assumed by Appleman (1953) and others since. The curves in Fig. 5 show the IWC as a function of temperature for the expected range of RHi for ice supersaturated layers in the upper troposphere. For a standard atmosphere this result is well-described by the relationship

$$IWC(g/m^3) = (RH_i/100-1)*\exp(a_o+a_1T+a_2T^2), \quad (4)$$

where a_0=-3.4889, a_1=0.05588 and a_2=6.268x10^{-4}; T here is in $^{\circ}$C.

We have reanalyzed some of the best in-situ contrail data collected to date to explore how well Eq. (3) predicts observations of the IWC within contrails. Some of the most reliable observations come from the 12 May 1996 SUCCESS case study when the DC-8 generated a contrail while flying in a racetrack pattern in highly ice supersaturated, cloud-free air (Heymsfield et al., 1998). Some 20 and 40 minutes after the initial contrail pass the DC-8 returned through the contrail, sampling it in a

racetrack pattern. These penetrations occurred long after the times required for the wake vortices to develop oscillations that mixed the contrail plume with the environmental air, i.e. these samples can be considered as taken from the later stage of contrail evolution. The DC-8 then sampled the contrail particles as they grew in the ice supersaturated air (as ascertained from a TDL hygrometer) for almost two hours following contrail formation. The accuracy of the TDL hygrometer was established to be +/-5% based on contrail crossings and wave cloud penetrations at temperatures between -40 and -65C.

The track of the DC-8 during these three penetrations (Pens. 1-3) is shown in Fig. 6a. The temperature during Pen. 1 was a mean of -50.2 C (Fig. 6b), 2.2^0C cooler than during Pen. 2. Pen. 2 was an average of 250 m higher than the generation height, indicating that portions of the contrail had risen at an average rate of 11 cm/s between penetrations. Because the concentration of trace species NO and NOy measured from the DC-8 (Campos et al., 1998) were much above the ambient environmental values (see symbols, bottom of Figs. 6b-d, with high NO regions identified in Heymsfield et al., 1998 as NO>100 ppb) and the contrail cloud was in the shape of a racetrack, we know with certainty that we were within the contrail generated during Pen. 1. The environment was highly supersaturated, RH_i>100%, during the contrail generation run (Fig. 6c). The RH_i values approached the limit for homogeneous ice nucleation at these temperatures of about 160% (see Heymsfield et al., 1997 and others), although ice particles were rarely sampled (see later). Abrupt excursions of the RH_i trace during Pen. 2—from high values to nearly ice saturation and visa versa--clearly indicated turbulent patches of ice mass associated with the contrail plume. Pen. 3 was largely outside of the contrail with only brief encounters during climb and descent through locations of high NO. Following the third penetration the DC-8 sampled crystals descending and growing in the highly ice supersaturated air below the contrail.

The IWC measured by the CVI (Twohey et al., 1997) indicates that there was initially no IWC in the environment (Fig. 6d). [The CVI should have detected IWC above 0.001 g/m^3 because these crystals would have been cirrus crystals, with most of them above the CVI "cut" size of about 5-6 microns]. Abrupt fluctuations were noted in the IWC during Pen. 2 and larger fluctuations during Pen. 3. Particle sizes were primarily above the CVI "cut" size for both penetrations, as discussed in the next subsection.

The potential IWC—derived from Eq. (2), is shown for Pen. 1 in Fig. 6d. The mean potential IWC for Pen 1 was 0.0086+/- 0.00023 g/m^3 (Fig. 6d). In the regions of high NO, the IWC measured by the CVI for Pen. 2 was a mean of 0.0074 +/- 0.003 g/m^3. Given that the IWCs were close to the detection threshold of the CVI and some particles could have been below the particle "cut" size of the CVI, the model and measurements agreed well.

Fig. 7 shows an expanded view of the measured and potential IWC and RHI during Pen. 2 where, throughout the region, pockets of high NO were measured. There is consistency between the aircrafts' NO signature (i. e., the contrail plume), detection of IWCs by the CVI and the reduction in RH to near 100%. The tailing off of the measured IWC at the end of each contrail penetration is due to hysteresis of the CVI--where residual IWC remains in the CVI's detection chamber following passage through a cloud. In the contrail-free regions the potential IWC is close to the values in adjacent contrail regions and the RHI is significantly elevated above ice saturation. Although the growth of the ice in the contrail portions developed from near supersaturation at earlier times, it is clear from Pen. 1 that the potential and measured IWCs were comparable.

On 13 July 2001 during the CRYSTAL-FACE field campaign in southern Florida the NASA WB57 aircraft flew a straight-track (Fig. 8a) at temperatures near -75C (Fig. 8b). The environment was highly ice supersaturated (Fig. 8c), and the WB57F produced a contrail. There has been considerable discussion on the accuracy of the RH measurements during this penetration because the peak values exceeded the threshold for ice production through homogeneous nucleation. A more conservative estimate would be 20% lower than the measured values (dotted line, Fig. 8c). A low IWC was measured and derived from the FSSP and CAS PSD during the penetration (Fig. 8d) and ice concentrations given later are shown to be very low. There was considerable potential IWC.

The WB57 turned and penetrated its contrail (Fig. 8e), encountering regions of high NO that tagged the contrail presence. The temperature trace on the return leg was a mirror image of the trace from the first penetration (Fig. 8f). Ice supersaturation was considerably lower than during the initial sampling and when reduced by 20% it agrees with the expectation that RH_i is about 100%

within a contrail. The measured and derived IWCs are about three times larger than those from the initial penetration and are within 30% of the potential IWC from the first penetration.

The IWCs measured during the SUCCESS and CRYSTAL-FACE contrail cases, discussed above for the periods when the aircraft were in regions of high NO following the initial contrail generation run, are shown in Fig. 9. Given the high RH_i noted in each of the cases—nearly 160%, the measured peak IWCs are consistent with Eq. (2). The IWCs are lower than they otherwise may have been because of the five second averaging times used in Fig. 9 to get a reliable value from the PSD.

These observations for young, non-precipitating contrails can be compared to measurements of the IWC in cirrus and in ice crystals falling out into ice supersaturated air below contrail (i. e., contrail cirrus). Heymsfield (2007, hereafter H07) report on IWCs acquired during nineteen Lagrangian spiral descents from the top to base of mid and low-latitude ice clouds (Fig. 9b) made during several field experiments where the IWCs were measured directly in most instances. A total of 5000 data points, spanning the temperature range -65 to 0C, are included in this data set. All but four of the spirals are from cirrus clouds generated by in-situ vertical motions; the others, identified in the figure, were outflow generated by deep convection. These observations improve upon earlier estimates of IWC(T) because they are measured directly rather than derived from PSD (with assumptions about crystal masses) and they are from contiguous penetrations of cloud from top to bottom rather than random samples. An additional ice cloud data set—from the WB57F during CRYSTAL-FACE (discussed earlier but for natural cirrus), provides measurements primarily in the -60 to -80C temperature range.

Many of the natural cirrus exhibit IWCs much above the theoretical values, signifying that most of this ice has been transported upwards from below in deep convection. For example, the red points in Fig. 9b are from all of the Lagrangian spirals through anvils in the H07 study. The majority of the points in H07 are from in-situ generated cirrus and for the most part fall within the confines of the theoretical curves.

For the 12 May 1996 contrail produced during SUCCESS the DC-8 followed the development of ice particles for almost an hour as they fell into the highly supersaturated air (RH_i were 120-140%) below the contrail (Heymsfield et al., 1998). This provided an opportunity to observe the crystals as they developed downwards into typical bullet-rosette type shapes. As shown in Fig. 9b the IWCs conform to the observations for natural cirrus following along the theoretical curves for the given RH_i in the environment.

2.1.5.2 *Ice Particle Size Distributions*

The studies listed in Table 1 examined the characteristics of ice particle size distributions in early contrails through to contrail cirrus. Goodman et al. (1998) found the ice particle size distributions some 40 to 80 seconds after contrail generation at a temperature near -61C to be nearly unimodal with a mean volume diameter below 20 microns and a concentration range of 6 to 13 cm^{-3}. A comprehensive examination of contrail crystal characteristics from seconds to greater than an hour after generation was conducted by Schröder et al. (2000). Shortly after generation the concentrations are of order 1000 cm^{-3} and diameters about a micrometer. In the presence of ice supersaturations in the contrail generation zone and for temperatures in the -50 to -55C range, aging over a one hour period leads to larger mean diameters, about eight micrometers, and reduced concentrations due to plume mixing, of about 10-15 cm^3. Heymsfield et al. (1998) sampled a contrail for more than an hour from the time of its generation by the NASA DC-8 (see discussion and figures in previous section). Temperatures in the environment were about -52C and RH_i approached 160%. The total ice concentrations within the contrail were 10-100 cm^{-3} and the concentrations of ice crystals >50 μm reached 10-100 l^{-1}. The concentrations for > 50 μm crystals are comparable to those found in the > 50 μm sizes in the Knollenberg (1972) and Gayet et al. (1996) studies. As suggested by Heymsfield et al. (1998) favorable conditions for contrails to develop cirrus-like microphysics include a largely cirrus-free environment, a sustained growth period for crystals in high supersaturated conditions and sustained upward vertical motions leading to a deep layer of high ice supersaturation. Such conditions are likely to have been present in the environment in the study of ice virga developing from contrails (e.g., Knollenberg, 1972 and Atlas, 2006).

A detailed examination of the data from the 12 May 1996 case from SUCCESS provides considerable insight into the microphysical properties of contrails that develop into contrail cirrus and to the issues that are raised about particle probes in Section 2.3.4. Prior to the contrail generation the MASP sampled total concentrations (Nt, > 1 μm[2].) of order 10 cm^{-3} (Fig. 10a). In the virga falling from the contrail following Pen. 3, where the NO concentrations < 100 ppb, Nt were of order 10-20 cm^{-3}. Few particles were measured during the contrail generation run (Pen. 1). During Pen 2, where NO concentrations indicated prior passage of the DC-8 aircraft, Nt were clearly enhanced, to 20-80 cm^{-3}.

Ice water contents measured above the CVI's cut size of about 5 μm are several hundredths g/m^3 prior to Pen. 1 (Fig. 10b). In the virga falling from the contrail following Pen. 2 there is a steady increase in the IWC as the DC-8 circled downwards in the contrail cirrus crystals falling into highly ice supersaturated air (see Fig. 6). The crystals in the contrail were accumulating mass as they developed downwards.

Recent studies and the discussion below in Section 2.3.4 point to a potential high bias in ice concentrations measured in sizes $\leq$ 50 μm due to shattering of larger particles on the inlets of the probes like the MASP and FSSP. Heymsfield (2007) argues that a nearly constant fraction of the ice mass in large particles swept out by the small particle probes' forward surfaces is shattered and enters the probe's sensing area where it is registered as real particles and developed a linear relationships to express these dependencies of the form

$$\text{IWC (FSSP or MASP)}=\text{IWC(small particles, real)}+C*\text{IWC(large particles)}, \quad (5)$$

where *C* is an empirically-derived coefficient, IWC(small particles) is the IWC that we are trying to measure and IWC(large particles) is the IWC measured by the 2D probes. Heymsfield (2007) suggests that IWC measured by the CVI can be substituted for IWC(large particles) because IWC(FSSP or MASP) is usually 10% or less of the CVI IWC. The scaled MASP IWCs in Fig. 10b are found from Eq. (3) by assuming that the IWC(small particles, real) is 0 g/m^3 and that C is given by the mean ratio of IWC(MASP)/IWC(CVI) for the times in Fig. 10 where the NO < 100 ppb, indicating ambient (contrail-unperturbed) air. IWC(MASP) is derived from the MASP PSD> 1 μm, assuming that the particles are solid ice spheres. What is most noticeable is that where NO < 100 ppb there is excellent agreement between IWC(CVI) and C*IWC(MASP), strongly suggesting that IWC(small particles) is negligible relative to the shattering term. In strong contrast, the scaled MASP IWCs are almost an order of magnitude larger than those from the CVI during Pen. 2, the first contrail penetration. This strongly argues that IWC (small particles) dominates in this case and that shattering is producing a negligible contribution to IWC(MASP). These details are further illustrated in Fig. 10c, which shows the ratio of the IWC derived from the MASP PSD to those measured by the CVI, with points indicating the regions of high NO and dotted lines indicating the mean ratio for "low" and high NO regions.

Fig. 11a shows the ratio of the total number concentration measured by the MASP to the total number concentration derived from the 2D-C imaging probe (for sizes 100 μm and above). Noteworthy is the near absence of >100 μm particles during the contrail generation run (Pen. 1) and the first sampling of the contrail particles during Pen. 2. Following Pen. 3, the DC8 sampled the virga falling from the contrail it generated (see time after 88000 sec). The concentrations of 2D-C particles decreased as the DC-8 descended. This is partially attributable to size sorting. Because the smaller crystals have a slower sedimentation velocity than the larger ones—20 versus 80-100 cm/s, the smaller ones are left behind. Furthermore, as shown by Heymsfield et al. (1998), the largest contrail particles for this case developed downwards through aggregation. This would have also reduced the concentrations.

Figs. 11b-f show the development of the PSD from the first penetration of the contrail (see times for the 5-sec average samples, top of Fig. 11a) through to sampling at its lowest levels. Initially, the PSD were narrow (Fig. 11b). The PSD broadened downwards in the contrail cirrus, with crystals > 1 mm developing.

[2] Restricting sizes to > 1 μm virtually restricts the concentrations to those for ice particles; aerosols and haze particles tend to be smaller.

Using a combination of the direct measurements of the IWC from the CVI and the total concentrations measured separately by the MASP and 2D-C probe, we can derive the mean mass-weighted diameter from $D_m=[6/pi*IWC(CVI)/N_t]^{0.333}$. Because N_t will always be dominated by MASP particles and the concentration is suspect in regions where large particles are present, we can bound the possible range of D_m and evaluate its uncertainty by deriving D_m separately for the MASP and 2D probes. Further, we must use data only from the CVI above its detection threshold, about 0.004 g/m^3. As Fig. 12 shows, in the contrail generation region D_m is dominated by the MASP particles and is of the order of 10 μm; these estimates can be considered to be reliable. In the zone of fallout of the contrail particles, there is almost an order of magnitude spread in the D_m values. Although these regions are likely to be dominated by the 2D IWCs and therefore those D_m values are likely to be reliable, the shattering issue is likely to produce a large uncertainty in D_m.

2.1.5.3 *Formation of contrail cloud layers*

A long-standing observation in regions of heavy air-traffic is that contrails tend to appear in groups rather than as single objects (Kuhn, 1970; Carleton and Lamb, 1986; Bakan et al., 1994; Duda et al., 2004). While the contrails spread they gradually merge into an almost solid interlaced sheet, a contrail deck. Kuhn (1970) estimated an average thickness of 500 m for such decks over Barbados and California, a value that is also the measured average thickness of ice supersaturated layers over the mid-latitude meteorological station of Lindenberg, Germany (Spichtinger et al., 2003a). Ice supersaturation is often formed by synoptic scale uplifting (e.g. Spichtinger et al. 2005a) which would favor contrail deck development, e.g., Knollenberg (1972) observed an extensive contrail deck developing ahead of a massive upslope snowstorm along the front range. There is only one simple process study of contrail deck development (Gierens, 1998) that only considers the spread dynamics but not the contrail microphysics.

Individual contrails spread horizontally and vertically with rates depending on ambient conditions. Freudenthaler et al. (1995) measured horizontal spreading rates in the range 18 to 140 m/min with a scanning lidar in time frames up to one hour. The average spreading rate determined by Duda et al. (2004) for a contrail outbreak over the Great Lakes region on September 9, 2000 was 45 m/min, i.e. in the middle of the range given by Freudenthaler et al. (1995). Cross sectional areas were observed to increase with rates between 3500 and 25000 m^2/s. Vertical growth rates are often limited by the thickness of the supersaturated layer, in particular at the lower contrail edge, but growth rates up to 18m/min have been measured with the lidar. Vertical growth of contrails is sensitive to the ambient profile of potential temperature (stability) and to radiative heating or cooling within the body of the contrail. Gierens and Jensen (1998) modeled how a contrail can rise 400 m through a very dry layer because the potential temperature at flight altitude was higher than in the layers above leading to strong buoyancy of the plume when it reached the unstable layers. Jensen et al. (1998) showed in other simulations that strong radiative heating of a thick contrail causes a 5 cm/s uplift of the contrail, resulting in a total uplifting of several 100 meters within an hour. Atlas et al. (2006) found convective turrets developing in contrails, probably as a result of radiative heating. In contrast, latent heating seems unimportant for the dynamical evolution of contrails even in cases with substantial supersaturation (hence substantial ice growth).

Contrail spreading is controlled mainly by wind shear and ambient humidity. Under conditions of relatively little supersaturation contrail spreading can make them subvisible clouds. Under sufficiently moist conditions (more than 125% RH_i) horizontal contrail spreading is affected by processes that control the vertical growth of contrails, the taller a contrail, the more effective the wind-shear. Strong turbulence, e.g., clear air turbulence, with Richardson numbers of Ri ~ 0.1 causes 20-fold increase of the vertical diffusivity D_v, compared to a calm background situation (Dürbeck and Gerz, 1996). In contrast, turbulence is unimportant for the horizontal diffusivity D_h. Dürbeck and Gerz (1995, 1996) conducted numerical experiments to determine the typical range of diffusion constants in the free troposphere. Typical values are: D_h [5,20]m^2/s and D_v [0,0.6]m^2/s (in calm situations). In cases with wind shear there is also a slant diffusion parameter D_s, which is typically 0.4 $(D_h*D_v)^{0.5}$. D_h increases with atmospheric stability but D_v decreases because turbulent diffusion has to work against gravity. The simulations also show contrail width increasing approximately linearly with time for as long as half a day. One should note here, however, that the

simulations used a passive mass-less tracer. The results are not completely applicable for contrail to cirrus transformation when ice crystals are sedimenting.

2.1.5.4 *Summary of contrail and contrail cirrus microphysics*

The following summarizes the observations of subsections 1-3:

- Total ice crystal concentrations in the initial stages of contrail formation are of order 10^3-10^4 cm^{-3} in the center of the plume.
- During the early contrail dispersion phase, which begins some five minutes after contrail generation, N_t is of the order of 10-100 cm^{-3}.
- Observations of the ice crystal shapes during the initial contrail formation are sparse. The available observations suggest that when micrometer size they may be irregularly shaped, not spherical. Quasi-spherical, droxtal shapes have also been observed (Schröder et al., 2002).
- Contrail crystal shapes evolve to those observed in natural cirrus that develop under the same conditions, i.e. bullet rosettes when the environment is supersaturated with respect to ice.
- Direct measurements of ice water contents during the early contrail dispersion phase, when the IWC is dominated by particles five micrometers in diameter or larger (depending upon the temperature), are the most reliable. The IWC measurement, together with the measured ice crystal concentrations, allows a reliable determination of the median volume diameter of the PSD.
- A conceptual model for IWC production during the contrail dispersion phase that converts all of the (ice) supersaturated vapor condensate is consistent with a reanalysis of measurements from the SUCCESS and CRYSTAL-FACE field campaigns spanning the -50 to -75C temperature range.

2.2 *Present state of measurements and data analysis*

2.2.1 *Current understanding of possible past trends in contrail and cirrus coverage and their association with aviation traffic*

A long-standing question in relation to air traffic has been whether aviation increases the average cloudiness and whether it affects other weather parameters like daily sunshine duration and temperature range. More cirrus, formed from contrails, is potentially possible because 10 - 20% of the atmosphere, at typical subsonic flight altitudes, is cloud-free but ice-supersaturated (Gierens et al. 1999).

Boucher (1999) took ground and ship based cloud observations for the period 1982-1991 and grouped them into early (1982-1986) and late (1987-1991) periods. He then correlated the differences, late minus early, of cirrus frequency of occurrence, ΔC (change in cloudiness), in 3°× 3° grid boxes with the aviation fuel consumption, F, in the same grid boxes. He found a positive correlation between ΔC and F. The highest ΔC occurred in major air flight corridors, NE USA (+13.3%/decade) and the North Atlantic Flight Corridor (+7.1%/decade). This study concluded that effects of volcanoes, long term changes in relative humidity or climate variations related to the North Atlantic Oscillation (NAO) could not explain the trend in cloudiness or its regional distribution.

Minnis et al. (2001) performed a similar study with the addition of satellite data and found consistency in trends of cirrus and contrails over the USA but not over Europe. This might point to other important influences on cloudiness that are stronger in Europe than in USA.

Zerefos et al. (2003) took other potential factors into account in their study, namely El Niño Southern Oscillation (ENSO), NAO, and the Quasi Biennial Oscillation (QBO). They de-seasonalized the cirrus time series and removed the ENSO, NAO, and QBO signals. Possible effects of changing tropopause temperatures and convective activity were removed by linear

regression and only the residuals were correlated with air traffic. Cirrus frequency was found to increase, sometimes with statistical significance in regions with heavy air traffic; however, an overall decrease in cirrus frequency was found. Consistent with Minnis et al. (2001), the most significant correlations were found over North America (winter season) and over the NAFC (summer season), whereas the correlations over Europe were insignificant (at a 95% level).

Stubenrauch and Schumann (2005) studied satellite data (1987-1995) for trends of effective high cloud frequency. They introduced a new element in these studies by grouping their data into three classes according to the retrieved upper tropospheric UTH_i (an average of relative humidity over a thick layer in the upper troposphere, say from 200 to 500 hPa). These three classes were grouped as: (1) UTH_i high enough for cirrus formation, (2) UTH_i insufficient for cirrus formation but sufficient for contrail formation and (3) clear sky. This additional classification of the data led to a clear positive trend, +3.7%/decade over Europe and +5.5% over NAFC in effective high cloud amount while the overall trend for all classes combined was weak.

Stordal et al. (2005) found from an analysis of satellite data (1984-2000) that the time series of cirrus coverage C(t) and air traffic density D(t) (flown distance per km^2 per hour) are generally positively correlated. The correlation is inferred from a linear relation: $dC/dt = b\, dD/dt$. Estimated correlations are not strong, partly because other influences mentioned above, have been left in the C(t) time series. They conclude that aviation over Europe produces an extra cirrus coverage of 3 to 5%.

Mannstein and Schumann (2005) also correlated C(t) with D(t), however for 2 months of cirrus data from METEOSAT and actual air traffic data from EUROCONTROL. For relating cirrus cover and traffic density they used a representation that takes overlapping of contrails and saturation effects (e.g. finite size of ice-supersaturated regions) into account: $C(t) = Ci(t) + C_{pot}[1-\exp(-D/D^*)]$, where Ci(t) is cover of natural cirrus, C_{pot} is the potential coverage of persistent contrails (Sausen et al., 1998), and the term in square brackets is the fraction of C_{pot} that is actually covered by contrails. It was shown that the relation between additional cirrus coverage and air traffic density indeed followed roughly the exponential model. The main result of this study was that over Europe aviation is responsible for an additional cirrus coverage of 3% (consistent with the result of Stordal et al.). Unfortunately, it later turned out that the studied data are subject to a serious selection effect which produces an apparent correlation of unknown size (Mannstein and Schumann, 2007).

2.2.2 *Range of radiative forcing calculated for a given contrail coverage and what atmospheric processes govern this range*

Once formed, a contrail's direct radiative impact is through scattering of solar radiation and absorption and scattering of longwave thermal radiation. Contrail time of formation, lifetime, size, shape, altitude and crystal optical properties all affect the radiation field. The background atmosphere, especially cloud fields and surface albedo, also affect the radiative forcing by the contrails.

Sensitivity studies have been carried out to explore the importance of many of these factors and to test the impact of using different radiative schemes (e.g. Meerkötter et al., 1999). Contrails' reflection of solar radiation lead to a negative forcing but absorbed/trapped longwave radiation leads to a positive forcing. The overall effect of a contrail, i.e. its net forcing, is expected to be a positive forcing; however, since the net effect is a result of a cancellation of shortwave and longwave terms of roughly equal magnitude, the contrail net forcing is very sensitive to errors in either term. Zhang et al. (1999) have demonstrated that for a given ice water path the net forcing of cirrus clouds is basically determined by ice particle size and that it potentially changes sign from warming to cooling with decreasing particle size. This suggests the possibility that contrails and contrail-induced cirrus, when they are dominated by very small ice crystals, would act climatically opposite to natural cirrus clouds and cool the climate. However, for realistic ice crystal sizes and IWC, contrails are expected to give a net warming effect.

Sensitivity studies like those by Meerkötter et al. (1999), (see Figure 13 and Table 7) show that the determination of ice crystal size, ice water content and optical depth is key after the contrail coverage is known. These three quantities are all related and the size of the contrail radiative forcing varies more or less proportionally to all of these. Constraining at least two of these

quantities is needed before an accurate estimate of contrail forcing can be made. [See Section 2.3.4.]

Other sensitivity issues include:

Radiative models: Different plane parallel radiation schemes employing different background atmospheres and cloud cover but similar input parameters for contrails give very similar forcings (Tables 2 and 3). Note that a comparison of results from previous work (Table 2, Models N, L, M, and Table 3) indicates that, provided when contrail coverage and optical properties are known the contrail forcing should be readily calculable; however, because they are optically thin, radiation schemes need to account for scattering in the longwave as well as the shortwave to correctly model contrail forcing. Furthermore, all previous estimates of global radiative forcing employ radiation schemes that adopt the plane-parallel approximation and use the same underlying contrail ice particle size distribution proposed by Strauss et al. (1997). This raises the question whether the studies noted in Table 3 are truly independent. Given that contrails are thin lines of cloud three dimensional effects and scattering from the sides of contrails can become important, especially when the Sun is low in the sky and the contrail less than a kilometer in width (Gounou and Hogan, 2007). Generally the 3D effects on individual shortwave and longwave forcings are modest (10%); however, as the net forcing is a cancellation of two terms with opposite sign, these authors found that in certain instances the net forcing could double or change sign.

Background clouds. From an examination of Table 3 it would seem that background clouds, although having a large effect on shortwave and longwave terms, have no effect on net radiative forcing and can be ignored in contrail forcing calculations; however, Stuber and Forster (2007) point out that when considering diurnal variations in aviation, excluding clouds leads to a 10% or greater overestimate of the net radiative forcing.

Diurnal cycle of air traffic. As most flights and contrails occur during daylight they contribute more negative radiative forcing than a diurnal average would suggest. Excluding the diurnal cycle can lead to roughly an overall 20% overestimation of the net forcing, although this varies with location depending on the time of day aircraft are typically overhead (Stuber and Forster, 2007).

Ice crystals optical properties. In radiation calculations contrails are typically assumed to be composed of small, spherical, hexagonal column or aggregate ice crystals. Often, and for convenience, they are assumed to have the same shape as those in typical cirrus clouds used in radiation models, only smaller with an effective radius typically about 10 microns. An assumption of aspherical particles of the same effective radius as a spherical particle will slightly reduce the radiative forcing while the uncertainty in crystal habit could lead to errors on the order of 10% (e.g. Table 7). An open issue in modeling the radiative properties of ice clouds in general is the lack of accurate light scattering models for the size parameter, defined as crystal size divided by the wavelength of the incoming radiation, between 10 to 100. Below this range approximate solutions like the Discrete Dipole Approximation (Draine and Flatau, 1994) or Finite Time Difference Methods (e.g. Yang and Liou, 1996) are applicable. Larger size parameters are covered by the Geometric Optics Approximation (e.g. Mishchenko and Macke, 1999). The effect on the overall radiative forcing by particles with size parameters in this mid-range can be estimated once experimentally derived optical properties are determined for these aspherical crystals; however, there is a significant lack of observations to constrain the uncertainty that crystals in this size range represent.

Other effects. Uncertainties in the contrail height and surface albedo can lead to 10% uncertainties in the magnitude of the radiative forcing but these can be reasonably constrained using detailed flight information and a good surface climatology.

In summary, whilst several factors could lead to 10-20% uncertainty in the radiative forcing by contrails, it is the contrail coverage and the crystal size that are key to providing an accurate forcing estimate. Global estimates of contrail radiative forcing and their impact will be discussed in Section 2.5.1

2.2.3 *How well are aviation-related subscale processes represented in large-scale global models?*

Global models that predict local contrail formation employ the SAC based on grid cell temperatures and humidities or suitable corrections thereof (Ponater et al., 2002; Rädel and Shine, 2008). The frequently applied concept of potential contrail coverage was introduced by Sausen et al. (1998) because of the inability to simulate contrail development in global models. Potential contrail coverage defines the maximum coverage by contrail clouds in a given region if sufficient air traffic was available and meteorological conditions were favourable for persistence. Therefore, it may be viewed as a proxy for ice supersaturated areas in global models which generally do not resolve ice supersaturation on the grid scale. No effort has been made so far to validate simulated potential contrail coverage.

Another important factor that needs to be parameterized in large-scale models is the mass and number of contrail ice particles that survive the vortex phase. This information is needed as an initialization in global models that track the time evolution of contrails, models that are not yet available. The same holds for any other parameter affecting the contrail-to cirrus transition, such as mesoscale wind shear, vertical winds and relative humidity, because the contrail life cycle is not included in current large-scale models. The latter atmospheric parameters could in principle be used to validate future global models simulating contrail cirrus; however, any aircraft-specific processes related to vortex break-up are difficult to consider because aircraft inventories employed in such models do not provide the necessary information.

Given the above, and that radiative effects of contrails depend on their microphysical evolution, radiation modules of climate models can only be fed with assumed contrail optical properties, in particular the effective ice crystal size. Those are determined in part by the competition of contrail cirrus with natural cirrus for condensable water, which constitutes yet another potentially significant subgrid process that remains unconsidered in current large-scale models. Off-line estimates of contrail radiative forcing have used advanced radiation codes, but lack geophysical variability in optical depth and often rely on simple scaling arguments to compute global contrail coverage.

2.2.4 *How well have contrail microphysical and optical properties been measured in past, in-situ observational studies?*

The properties of contrail particles can be described by their size distributions, water content, total number concentration, sulfate and carbon chemistry and light scattering phase function. Hydrometeor optical and microphysical properties have been measured directly or derived using five, fundamentally different techniques: impaction, phase change, light scattering from individual particles, light scattering from an ensemble of particles and imaging. Aerosol particle properties are derived from light scattering and incandescence, condensation chambers, counter-flow virtual and wire impactors and aerosol mass spectrometers.

Table 4 lists the types of airborne measurement methods that have been used to characterize contrails, the properties that they detect and the name of the instrument that incorporates a specific technique. Table 5 lists the majority of measurement campaigns when contrails have been measured, the instruments that were used, the principal investigator who was responsible for the instrument and some of the key publications that describe the instrument and significant results. A description of the most commonly employed techniques for measuring cloud properties is found in Baumgardner (2002) and the majority of aerosol instruments are described by McMurray (2000) and Willeke and Baron (2001). A brief description of all the instruments listed in these tables is given here primarily to highlight the advantages and disadvantages of each of them for measuring contrail properties.

Impaction devices are those that are exposed, either intermittently or continuously, to the air stream. The wire impactors have wires with diameters of 70 μm or 200 μm, depending on the size range of particles to be collected (Goodman et al., 1998) and are exposed for periods of several minutes, depending on the ambient concentration of collected particles. The wires are stored for subsequent evaluation of the captured particles with X-ray dispersion analysis (SEM or TEM). The video ice particle sampler (VIPS) uses a moving, 8 mm transparent tape that is coated with silicone oil and exposed to the particle-laden air stream. After exposure the magnified images are recorded digitally as the tape moves in front of two video cameras. The limitation of these types of devices is

the break-up of ice crystals larger than approximately 50 μm and the wire impactors have a very limited sample volume.

A method for deriving water mass by evaporation is to measure water vapor formed from vaporization of the hydrometeors. The Counterflow Virtual Impactor (CVI) utilizes this technique (Twohy et al, 1997). At the CVI inlet tip cloud droplets or ice crystals larger than some aerodynamic diameter (usually about 5 to 10 μm diameter depending on airspeed and density) are separated from the interstitial aerosol and water vapor and are "virtually" impacted into dry nitrogen gas. This separation is possible via a counter-flow stream of nitrogen out the CVI tip, which assures that only larger hydrometeors are sampled. The water vapor and non-volatile, residual nuclei that remain after droplet evaporation are sampled downstream of the inlet with selected instruments. These may include a hygrometer to determine water content, a condensation nucleus counter, an optical particle counter, or particle filters for various chemical analyses. Since droplets or crystals in a large sampling volume converge into a smaller sample stream within the instrument, concentrations within the CVI are significantly enhanced, which leads to a better detection limit. The CVI has the disadvantage that its lower size threshold of approximately 5 μm rejects a large fraction of the ice crystals that are found in young contrails whose median volume diameter is typically less than 5 μm (e.g. Baumgardner and Gandrud, 1998). The Fast In situ Stratospheric Hygrometer (FISH), developed at the Forschungszentrum Jülich (Germany), is another device that has recently been employed to measure ice water content. It measures water vapor from all hydrometeors evaporated in the heated inlet using a hygrometer based on the Lyman-a photofragment fluorescence technique (Zöger et al., 1999.

Optical particle counters detect the light scattered when a particle passes through a focused light beam. Instruments that convert the light amplitude into a size, using Mie scattering theory, are called single-particle spectrometers. Several such instruments for measuring particle sizes and concentrations are the Forward Scattering Spectrometer Probe models 100 and 300 (FSSP-100, -300), the Passive Cavity Aerosol Spectrometer Probe (PCASP), the Multiangle Aerosol Spectrometer Probe (MASP) and the Cloud and Aerosol Spectrometer (CAS). As droplets in the free air stream pass through a laser beam and scatter light, these instruments collect this light over a solid angle that depends on the instrument and convert the photons into an electrical signal with a photodetector. The MASP and CAS collect light separately over forward and backward angles. Comparison of light measured at two angles provides information on either refractive index (Baumgardner et al., 1996) or ice crystal shape (Baumgardner et al., 2005). The advantage of the instruments is that they are very fast response and measure particle sizes with high resolution. The disadvantage is that they have relatively small sample volumes and the accuracy of the measurement is decreased when measuring non-spherical particles. The information is also ambiguous in certain size ranges as a result of the multivalued nature of the relationship between light scattering and size that stems from the complexity of light refraction.

Light scattering from an ensemble of hydrometeors is the technique used by two of the instruments, one that derives IWC, extinction coefficient, and effective radius from the measurement and the other that derives the asymmetry coefficient and extinction coefficient. The Particle Volume Meter (PVM) measure the diffracted component of scattered light (Gerber et al., 1998). The PVM illuminates an ensemble of hydrometeors with a collimated laser and focuses the near-forward scattered light onto two detectors that are masked with variable-transmission filters. The filters have been designed to provide transmission functions that are mathematically derived to approximate inversions of the integral equations that relate particle surface area (PSA) or LWC to the flux of light scattered by the ensemble of hydrometeors. An instrument that has been specifically designed to measure the asymmetry coefficient, g_λ, is the Cloud Integrating Nephelometer (CIN). The CIN consists of a collimated laser beam that passes through an ensemble of hydrometeors and four detectors that are positioned to measure scattered light in the forward and backward directions The detectors have optical masks that cosine-weight the collected scattered light so that after suitable corrections for the angles over which light is not being collected, the ratio of forward to backward scattered light provides an approximation to the asymmetry factor. The advantage of these techniques is that they measure over larger sample volumes than the single particle instruments and the optical properties are measured directly rather than derived from a size distribution. There remain questions, however, about the sensitivity of the PVM to cloud particles

larger than 30 μm (Wendisch et al., 2002) and the robustness and fidelity of the large angle correction for the CIN measurements (Heymsfield et al., 2006).

One of the first methods in cloud physics research of optically measuring hydrometeor size was by imaging onto a linear diode array the shadow of a particle that passed through a laser. The on/off state of the diodes in the array is recorded at a rate proportional to the velocity of the particles passing through the laser and the images can be subsequently reconstructed to show the features of the hydrometeors. This type of instrument, called a two-dimensional optical array probe (2D-OAP), can typically measure in the size range from 10 μm to greater than several millimeters, depending on the magnification. This technique has been refined to measure hydrometeors at a higher resolution, down to 2.5 μm, with the Cloud Particle Imager (CPI) by using a pulsed laser and a two dimensional photodetector array to capture the particle image (Lawson et al., 2001). In addition, 256 gray levels are measured in the CPI as opposed to the binary levels in the 2D-OAPs. The primary disadvantage of the imaging probes is that the depth of field (DOF) decreases with the square of the particle diameter, e.g. particles with diameters of 20 μm and 10 μm have DOFs of 0.8 mm and 0.2 mm, respectively. Hence, an imaging probe with sufficient resolution to measure contrail particles whose diameters are less than 5 μm would have a very small sample volume.

The perils of measuring ice crystals with optical particle spectrometers have been recognized since the mid 1980s. Studies have identified conclusively that size spectra measured with optical spectrometers that have inlets are contaminated by ice crystal fragments, even in the presence of very low concentrations of larger ice crystals. Gardiner and Hallett (1985) were the first to publicize the effect of ice crystal break-up on the inlet of the FSSP and showed that size distributions in these conditions were broadened and number concentrations were unreasonably large. Later studies by Field et al. (2006) reinforced the conclusions of Gardiner and Hallett by analyzing the distribution of interarrival times of particles measured by the FSSP. McFarquhar et al. (2007) showed that the CAS also suffers from ice fragmentation on its shroud and inlet. In recent projects the flow straightening shroud has been removed to minimize the crystal shattering problem; however, this has not completely eliminated the problem as shown in Fig. 14. These size distributions are compiled from measurements made with the CAS and CIP during the Tropical Composition, Cloud and Climate Coupling (TC4) project. The images below the size distributions are representative measurements with the CIP that indicate the average size and shape of the ice crystals. Whereas the CAS has an inlet with a diameter of approximately 5 cm, the CIP has no inlet and is minimally affected by crystal break up, although there can be some contamination that can be removed by looking at the interarrival times of particle images in these types of instruments (Korolev and Isaac, 2005). In these figures, we show that when the ice crystals are small, the CAS and the CIP concentrations are relatively well matched in the overlapping size range. As the ice crystals become larger, however, the CAS shows increasingly larger concentrations than the CIP. It is assumed that these are a result of fragments formed from ice crystals shattering on the CAS inlet. Fortunately, given that there are rarely any crystals larger than 20 μm in young contrails, ice crystal shattering is probably not a factor to take into account when analyzing FSSP or CAS measurements in early stages of contrail development. Thereafter, as contrails develop into contrail cirrus, shattering becomes a major source of artifacts (Section 2.1.5.2).

2.3 *Present state of modelling capability / best approaches*

2.3.1 *Representation of aviation-related subscale processes in large-scale global models*

As introduced in subsection 2.3.3 most contrail-related subscale processes are not represented in current large-scale models, with the notable exception of the thermodynamic conditions for contrail formation, the most advanced approach having been formulated by Ponater et al. (2002). In their approach contrails are reinitialized every model time step hence, they show no atmospheric life cycle and assumed to share their ice water content with cirrus in proportion to a contrail coverage that was tuned to a specific region using a globally constant tuning coefficient. Contrails are assigned the same optical properties as natural cirrus.

All existing studies address coverage by line-shaped contrails only, constituting only a subset of the total coverage by contrail-cirrus. Even if an advanced global model approach was available

there is a scarcity of in-situ and remote sensing observations that could be used for model evaluation, in particular for contrail cirrus older than about 30 min.

2.3.2 *Modelling of the spreading of ice crystals generated by aircraft*

Lidar observations of the vortex phase of contrails and numerical studies show that the early evolution of a contrail is sensitive to ambient conditions and aircraft performance parameters. Recent numerical experiments (Unterstrasser et al., 2007) show that the number of ice crystals surviving the vortex phase is a power-law function of the ambient supersaturation whose parameters depend on ambient temperature, stability and turbulence level. The surviving number fraction varies from less than one percent at ice saturation to 100% at about 130% ambient supersaturation. The surviving crystal number is important for the evolution of microphysical and optical properties of the developing contrail-cirrus.

2.4 *Current (or model-) estimates of climate impacts and uncertainties*

As emphasized in subsection 2.2.2 radiative forcing from contrails depends on many factors, including contrail coverage, ice water path, optical properties, geometry, time of day, size and location, age and persistence, background cloudiness and surface albedo. After coverage, a poorly known quantity, ice water path and optical properties are the largest sources of uncertainty. Here we perform a literature review of previous forcing studies and the weaknesses and strengths of each to explain differences between findings. In particular, all studies seem to show similar ranges and variability but they also all make similar assumptions, such as the restriction to linear contrails and the use of a constant contrail optical depth. A second part of this section will evaluate the role of spreading contrails and aviation induced cirrus and the last two parts examine the climate impact beyond radiative forcing.

2.4.1 *Persistent linear contrail radiative forcing*

To date global radiative forcing estimates have employed similar simple diagnostic techniques, i.e. combining estimates of 1) contrail coverage and 2) contrail optical properties to get the contrail radiative forcing.

1) Contrail coverage estimates rely on first estimating regions of the Earth where contrails might form, given suitable background conditions of ice supersaturation, and then using a suitable database of flights to estimate when an aircraft forms a contrail. Assumptions are then needed about contrail lifetime and width so that a suitable estimate of coverage can be made. Given the uncertainty in estimating ice supersaturation a large range might be expected from modeling studies; however, all studies to date have employed a "normalization" step that mutes the effect of any differences in their previous assumptions. This normalization linearly scales the contrail coverage found with that estimated using satellite observations of persistent linear contrails over a particular region. Nearly always the scaling is obtained by normalizing to the 1992 European observations of Bakan et al., (1994). The derived normalization factor can be as large as an order of magnitude, thus having a major impact on results. This also means that all results obtained are actually scaled for line-shaped contrails in 1992; hence, it is likely that this normalization is a major reason for the agreement between otherwise disparate methodologies. It is important to note, however, that even when applying the scaling the modeled global contrail coverage can still differ by a factor of two (Table 6) so the other assumptions remain significant as well.

2) Contrail optical depth is either simply assumed (e.g. Stuber and Forster, 2007) or obtained as a diagnostic from a climate model (e.g. Ponater et al, 2002). Until recently GCMs have not included ice supersaturation so estimates of available ice have had to be obtained from parameterisations that assume that ice exists above a relative humidity threshold less than 100%. These schemes are also diagnostic as there is no contrail history, i.e. one timestep does not know about contrails at any previous time steps; therefore, assumptions are also needed about contrail lifetime. In general, following the contrail optical depth used for the IPCC (1999) calculations, the estimate of average optical depth has been reduced, and this, along with reduced estimates of global persistent contrail cover, have been the major reasons for the reduced estimates for the global mean radiative forcing

by contrails (Marquart and Mayer, 2002; Mayer et al., 2002, Ponater et al., 2002, Marquart et al., 2003 and Table 6).

Results from previous studies are shown in Table 6 where the radiative forcing is estimated in the radiative transfer models by combining steps 1) and 2). Radiative forcing can either be estimated within a climate modelling context (e.g. Ponater et al., 2002) or offline (e.g. Myhre and Stordal, 2001, Stuber and Forster, 2007). Offline calculations have the advantage, perhaps, of employing better, observationally-based, background climatology of humidity and temperature to determine ice supersaturation. They can also employ more sophisticated radiative transfer schemes; for example, the Ponater et al., (2002) study using a GCM did not account for scattering in the longwave. On the other hand, offline schemes have the major disadvantage that they have no information of the degree of ice-supersatuation and are therefore unable to estimate the optical depth of contrails. The latest GCMs, such as the European Centre for Medium Range Forecast (ECMWF) model, can now estimate ice supersaturation and it may be possible to obtain a climatology of likely optical thicknesses in the future (see Rädel and Shine, 2008).

The IPCC fourth assessment based their persistent contrail forcing estimate on Sausen et al. (2005) and estimated the contrail forcing for 2005 to be 0.01 Wm^{-2} with a factor of three uncertainty and a low level of scientific understanding (Forster et al., 2007). Although the forcing best estimate is considerably reduced from the 1999 report, which estimated a forcing about three times larger when scaled by fuel use, the uncertainty remains large and confidence low due to the pronounced flaws in the methodology described above.

2.4.2 *Aviation induced cloudiness (AIC)*

Aviation can potentially have several additional effects on cirrus clouds apart from forming linear contrails and there is some confusion as to precisely which effects are being evaluated in the different literature studies. Firstly, persistent linear contrails can shear and spread into large areas of cirrus cloud. Secondly, aerosol, especially soot, can also act as IN that potentially can alter cirrus cloud evolution (see Section 2.1.4). Studies that have estimated the radiative forcing from such changes likely include all forms of cirrus modification including that from persistent linear contrails. IPCC-1999 did not put a best estimate on this radiative forcing but suggested it could range from 0.0 to 0.04 Wm^{-2}. This was based on a study by Boucher (1999) that looked at differing cirrus trends in regions of high and low aviation traffic (see Section 2.2.1). Since then two further studies have adopted similar techniques (Stordal et al., 2005; Zerefos et al., 2003) as discussed in Section 2.2.1. Here we focus on their radiative forcing estimates.

Cirrus trend estimates that compared high and low aviation use areas were used to estimate radiative forcing by Stordal et al., (2005), assuming standard cirrus optical properties. For the calendar year 2000 a range of 0.01-0.08 Wm^{-2} was suggested. Minnis et al. (2004) used surface and satellite cloud observations to derive a suggested upper estimate for the AIC radiative forcing of around 0.03Wm^{-2}. The AR4 IPCC report adopted the Stordal et al. (2005) range, neither providing a best estimate nor attributing the AIC forcing to particular causes. Overall it gave the AIC forcing a very low level of scientific understanding. Therefore, in summary, studies to date suggest that the total radiative forcing of aviation on cirrus, including linear contrail formation, is 2-10 times larger than its role solely in the formation of linear persistent contrails; however, the studies have been unable to place a realistic best estimate or even upper bounds on this.

2.4.3 *Climate impact of contrails on temperature*

Two modeling groups, using three climate models, have examined the climate impact of contrails and AIC beyond that of radiative forcing. Rind et al. (2000) increased cirrus frequency along aircraft flight paths by various amounts in a version of the GISS climate model. For a 1% worldwide increase in cirrus the global surface temperature increased by 0.4 K. The source of this estimate was from an increase in radiative forcing of around 0.1W^{-2} and a climate sensitivity of 0.9 K/Wm^{-2}; this compared to the models' sensitivity to well mixed greenhouse gases of 1.2 K/Wm^{-2}. This study also found a pronounced hemispheric difference in the climate response. Because most

of the forcing was in the Northern Hemisphere, the Northern Hemisphere and especially the Arctic exhibited the greatest response; however, within each hemisphere the geographic variation of temperature response was more-or-less independent of where the aircraft perturbed the cirrus. The maximum temperature response was in the upper troposphere – at a height of 10 km the warming was about twice that at the surface. The recent study with the ECHAM4 model by Ponater et al. (2005) confirmed these findings, i.e. that the response considerably smoothed out the geographical variation of forcing (Fig. 15). Their findings are also consistent with perturbations of other forcing agents in a similar model (Hansen et al. 2005) and other perturbations within different climate models (Forster et al., 2007).

Minnis et al. (2004) used the results of Rind et al. (2000) to infer a possibly very large temperature response over the US in its tropospheric temperatures. They suggested that a modest, observationally based trend in combined contrails and AIC of 1%/decade over the United States would result in a tropospheric temperature warming of 0.3 K/decade; however, Shine et al. (2005) pointed out several errors in their argument and showed that their estimate of warming was likely two orders of magnitude too large. This was confirmed when Hansen et al. (2005) placed the Minnis et al. (2004) contrail observations into the latest version of the GISS model and found a temperature response that was too small to quantify accurately, even when the cloud cover changes were scaled by a factor of 10. These results are shown in Fig. 16.

The findings of Rind et al. (2000) and more recently Ponater et al. (2005) suggest that the response of the Earth's climate to contrails and AIC is probably smaller than suggested by a simple evaluation of radiative forcing. The concept of "efficacy" (Hansen et al., 2005; Forster et al., 2007) compares the global mean temperature response for a given amount of forcing, from a particular agent, to an equivalent radiative forcing from carbon dioxide. If the efficacy is larger than 1.0 then the climate will be more sensitive to the forcing agent than it is to perturbations in carbon dioxide. On the other hand if the efficacy is smaller than 1.0 then the climate is not as sensitive to perturbations in the forcing agent. The preliminary study of Rind et al. (2000) suggested an efficacy smaller than 1.0 and Ponater et al. (2005) suggest an efficacy of only 0.6 for contrail changes. These small efficacies are because contrail and/or cirrus perturbations have a relatively larger effect on the upper tropospheric temperatures compared to those at the surface.

2.4.4 *Impact on diurnal temperature range*

After the 11 September 2001 terrorist attacks in the U.S. civil aviation flights were grounded for three days. The diurnal temperature range (DTR) during this time was observed to be several degrees larger than days immediately before and after these groundings. The DTR was also higher than similar time periods during different years (Travis et al. 2002). Further work described in Travis et al. (2004) suggests that locations where maximum DTR changes were observed also coincide with regions of typically high contrail frequency and air traffic (Fig. 16). Daytime maximum temperatures also appeared to be more affected than the night time minimum. Hansen et al. (1995) do suggest a role for high cloud changes in affecting DTR and a clear DTR decrease is seen across the US in Fig. 15; however, this figure suggests that changes would be small, less than 1 K. Furthermore it has been proposed that unusually clear weather across the U.S. during those three days could have been responsible for the DTR response (Kalkstein and Balling Jr., 2004). Therefore, although a large impact on DTR remains a possibility, more work is certainly needed to investigate these possibilities.

2.5 *Interconnectivity with other SSWP theme areas*

Strong relation with theme 3–supersaturation and theme 5–climate issues. These will be worked out in the February meeting.

3 OUTSTANDING LIMITATIONS, GAPS AND ISSUES THAT NEED IMPROVEMENT

3.1 *Science*

3.1.1 *Uncertainties in contrail formation conditions*

Knowledge of contrail formation conditions is sufficient for most applications including contrail forecasting or climate modeling. Crucial parameters that should be known with high accuracy include the ambient relative humidity and the aircraft propulsion efficiency.

3.1.2 *Chemical and microphysical mechanisms that determine the evolution of emissions from the engine exit to plume dispersion*

As discussed in Section 2 we think that our current understanding of the properties of young contrails, up to the vortex regime, is sufficient for most applications in models in the near future; nevertheless, there are several aspects of plume dynamics and microphysics that warrant a more complete understanding, in part because of their potential implications for persistent contrail development and subsequent influence on contrail-cirrus formation.

The dynamics of aerosol and ice particles at the point of contrail formation is highly complex according to numerical model simulations (Kärcher, 1998). Some features of the underlying physical and chemical processes are not well covered by observations. For example, the ultrafine liquid particle mode is predicted to take up substantial amounts of nitric acid (HNO_3) during water activation, resulting in the formation of supercooled, ternary ($H_2SO_4/HNO_3/H_2O$) droplets (STS) after ice nucleation that subsequently interact with contrail ice. Nitric acid also interacts directly with contrail ice crystals, potentially forming NAT particles (Kärcher, 1996) such as are observed in polar stratospheric clouds (Dye et al., 1990). Contrails composed of NAT and/or STS particles persist at lower relative humidities than traditional contrails composed of pure water ice particles; however, because the NAT phase is only stable at very low temperatures (< 205 K) at subsonic cruise altitudes, this is mainly an issue for the high latitudes in winter. The global consequences of aviation-induced NAT formation has been discussed in the context of a planned fleet of supersonic aircraft (Peter et al., 1991), but has not received sufficient attention in the case of the subsonic fleet. Besides the potential chemical implications, the global, radiative impact of NAT contrails is probably small, but such processes may enhance cloudiness regionally in the Arctic.

Another factor that could become relevant at low temperatures is the formation of cubic ice. While it is becoming increasingly clear that ice nucleates in cubic form and slowly transforms into hexagonal ice, depending on the chemical composition of the ice-forming aerosol particle precursors (Murray et al., 2007), virtually nothing is known about the relevance of cubic ice in contrail formation. As cubic ice has a higher vapour pressure (by about 15%) than hexagonal ice (Murphy, 2003), it may be speculated that contrails composed of cubic ice have smaller ice particles than traditional contrails for at least part of their lifetime (Gao et al., 2004). As in the case of NAT, the cubic ice issue is likely of limited global importance as it becomes relevant only in regions with low air traffic density; however, given the lack of understanding of the fundamental physics of ice formation at low temperatures and high supersaturations, improving our understanding of this process is important from strictly a scientific perspective.

As mentioned above, microphysical and optical properties of persistent contrails and contrail-cirrus are sensitive to conditions and processes during the vortex phase, i.e. about 20 to 120 s of plume ageing. Adiabatic compression and heating due to the vortex's downward migration leads to ice evaporation and the surviving fractions can be as small as one per mille by number. Simulations for one aircraft type (a wide-body) led to the following results (Unterstraßer et al., 2007):

- The fraction of ice number and mass that survives the vortex phase has a power law sensitivity to the ambient supersaturation with respect to ice. The dependence is strongest for the highest temperature that allows contrail formation and becomes weaker with decreasing temperature.

- Only the ice in the secondary vortex survives at low supersaturation, giving rise to a persistent yet very faint contrail.
- The stratification of the atmosphere and its turbulence level have a strong impact on the fraction of the surviving ice via their dynamical effect on the sinking vortex pair. Strong turbulence leads to fast vortex decay, whereas weak turbulence allows the vortex pair to travel a long distance downward. Hence, in situations of strong turbulence, more ice is rendered to the atmosphere than in weakly turbulent conditions. The downward travelling distance of the vortex increases with decreasing strength of stratification; hence, more crystals survive in more stable situations and vice versa. Additionally, more ice is detrained into the secondary wake in more stable situations.
- The variation of the initial circulation with varying aircraft weight during a flight, details of the spatial distribution and the temperature profile within the vortices have only a minor influence on the surviving ice fraction.
- The initial number of ice crystals has an influence on the surviving fraction. The initial number increases with decreasing ambient temperature within a range of about an order of magnitude. At the warmest temperatures that allow contrail formation the surviving fraction is larger when less ice crystals are formed initially; however, the total number of surviving crystals and the surviving ice mass can be larger when more crystals are formed initially.
- The relative position of the engines to the wing tips has a small influence on the contrail properties; nevertheless, the aircraft type plays an important role, but merely for the almost trivial reason that different aircraft types burn different amount of fuel per meter of flight path, which can also vary between one order of magnitude (Sussmann and Gierens, 2001).

None of the factors that are listed here, and that are determined from numerical simulations, have been validated with observational studies. The modeled sensitivities seem reasonable from the perspective of the fundamental physics, yet without targeted studies to compare observations with predictions, there will always remain doubt as to the validity of the simulations and hence, the predictions of environmental impact.

3.1.3 *How do the microphysical and optical properties of natural cirrus differ from naturally occurring cirrus?*

From detailed particle imagery acquired during the SUCCESS field campaign in 1996, and from the Knollenberg (1972) and Atlas et al. (2006) observations, we surmise that contrail crystal shapes develop to habits similar to those found in natural cirrus that develop under the same conditions when the environment is strongly ice supersaturated. These studies indicate that concentrations of ice crystals >100 microns in cirrus and contrail cirrus are comparable, of the order 10's per liter. The ice water content in contrails and natural cirrus are driven by the ambient supersaturation (e.g., Fig. 7). More studies are needed to determine whether the IWC's in cirrus and aged contrail cirrus are comparable.

As noted in Section 2.1.5, issues related to the measurement of small ice crystals in the presence of large ones has confounded our ability to distinguish natural from contrail cirrus based on their radiative properties or median volume diameter. Specifically,

- Shattering of ice crystals on the inlets of probes that have measured contrail ice crystal concentrations with sizes < 50 μm in maximum dimension, e.g. the FSSP, CAS, MASP, and CPI, can account for ice concentrations of 10's per cm^{-3} or greater under conditions where there are even small concentrations of ice crystals > 50 μm. This occurs some 10-20 minutes following contrail formation, depending upon the temperature and supersaturation.
- Because of shattering, previous comparisons of N_t and population mean diameter or median volume diameter of contrail cirrus that has evolved into natural cirrus are likely unreliable.
- This issue of measurement contamination from shattered ice fragments renders differentiation of contrail cirrus from natural cirrus, using extinction alone, nearly impossible at the present time.

3.1.4 *What is the role of soot emissions in altering cirrus and how does soot-induced cirrus relate to contrail-cirrus?*

While most of the above-mentioned sub-themes address issues associated with contrail-cirrus, it was pointed out in section 2.1.4 that aviation may also affect cirrus via emissions of soot particles. Although the role of soot emissions in contrail formation seems to be reasonably well understood (see 2.1.2 and 2.1.3), the question of cirrus formation or modification induced by soot particles (soot-cirrus) remains largely unresolved.

Many tools are available for modeling the formation of soot-induced cirrus, just as there are for modeling the activation of any atmospheric IN and the photochemical and microphysical mechanisms that might affect the ice nucleation ability of aging soot emissions (Kärcher et al., 2007); however, a number of factors limit our understanding of the potential implications for cirrus modification. First of all, there is a paucity of in-situ observations of processes evolved in the dispersing of plumes and of direct and tractable plumes interactions with actively forming cirrus. Secondly, and equally important, is the lack of laboratory studies to investigate how ice forms on soot-containing particles and how this process may be altered with aging in the upper troposphere.

In-situ ice nucleation measurements of exhaust soot particles, under cirrus formation conditions, have yet to be carried out and current laboratory evidence is inconclusive. Likewise, relatively poor knowledge exists of the IN activity of the ambient aerosol that competes with aircraft soot in ice formation at cirrus temperatures. Therefore, atmospheric validation of the interplay of heterogeneous and homogeneous ice formation in cirrus, gleaned from laboratory studies and numerical modeling, remains an unachieved goal.

As a consequence of these gaps in our knowledge of fundamental physical and chemical atmospheric processes, global model studies that address soot-induced cirrus can only provide preliminary parametric studies exploring possible uncertainties of changes in cirrus properties (Hendricks et al., 2005). The number of cirrus ice crystals could potentially be enhanced or reduced in dispersing aircraft plumes relative to unperturbed cirrus formation conditions, depending on assumed ice nucleation scenarios (Kärcher et al., 2007), with the subsequent consequence probably being one of significant regional or global impact.

Whereas contrail effects are fairly evident, it remains unclear whether soot particles exert an additional effect on radiative forcing (and thus contribute to AIC). However, contrail and soot effects may not act in isolation. Contrails need ice supersaturated air masses to persist; in such an environment, soot particles from aviation could preferentially trigger ice formation if they form ice at significantly lower relative humidities than natural particles.

3.2 *Measurements and Analysis*

3.2.1 *How can measurements of contrail microphysical and optical properties be improved?*

Reliable measurements of the size distributions of small ice crystals, and the shapes of these crystals, hinder our ability to accurately model the radiative properties of contrails.

3.2.2 *Aviation's share of cirrus trends*

It is currently not clear how much of the correlation between air traffic and cirrus cloudiness is actually due to a causal relationship. Hence the determination of the radiative forcing of contrail cirrus is fraught with large uncertainties; studies to resolve the differences and to constrain the error margins are certainly needed. All studies suggest that air traffic actually induces additional cirrus clouds, which seems plausible. However it is extremely difficult to demonstrate and prove such a correlation because the variation of cirrus cloudiness due to natural influences is much larger than the possible aviation effect. Hence, to look for the latter is like looking for a signal hidden in strong noise.

3.2.3 *Measurement needs*

An array of research and measurements needs is suggested by limitations and gaps in the state of scientific knowledge of soot impacts on ice formation in cirrus.

- Fundamental laboratory studies are required to ascertain what makes certain soot particles more active than others and what role contrail and atmospheric processing might play in making exhaust soot more or less active as cirrus ice nuclei.
- Direct sampling to test the ice nucleation ability of real exhaust particles during ground-level emissions studies would be fruitful. Alternately, studies using collected samples of real exhaust emissions for laboratory studies would complement the ground level studies.
- New studies of the ice nucleating properties of aircraft exhaust and other ambient ice nuclei measured in-situ for conditions in the cirrus temperature and water vapor regimes are needed. This could be done independently, but would be most useful within the context of a measurement effort to convincingly relate the ice activation properties of aerosols to the microphysical composition of cirrus clouds that form on them. Subsidiary needs for such a study include:
    - A fast IN sensor for atmospheric studies that operates at much lower temperatures than present aircraft systems and that can run unattended to take full advantage of various manned or unmanned high altitude aircraft platforms. A number of new ice nuclei sensors for aircraft use are under development as evidenced by participation in the workshop ICIS 2007 (http://lamar.colostate.edu/~pdemott/IN/INWorkshop2007.htm). It is possible that some of these or other new devices will meet the specifications required for cirrus and contrail studies.
    - A need to sample aerosol particles without heating so as not to impact their chemical phase states and states of hydration since potential "preactivation" may be destroyed during sampling through standard inlets.
    - Purposeful "seeding" of developing cirrus with aircraft exhaust could be a component of the strategy for such studies.
- New studies of cirrus formation would be useful to take advantage of new or improved high resolution measurements of aerosol composition, particle activation to ice, relative humidity, vertical motion, and cloud ice particle size distributions. All of these aspects present varying levels of technical challenge. Nevertheless, instrumentation is steadily becoming available and improving that should be applicable to this task in atmospheric studies.

3.3 *Modelling capability*

3.3.1 *How can we improve prediction of persistent contrails in weather forecast?*

The upper limit on contrail and contrail-cirrus coverage is largely driven by the upper level humidity structure, i.e. the amount of ice-supersaturated regions (ISSRs) in the upper troposphere. Unfortunately, measurements of relative humidity in these levels by radiosondes (strong negative biases), aircraft (airframe distortions) and satellite instruments (insufficient vertical resolution) are notoriously difficult. This is an area of investigation with strong links to theme 3.

Although the knowledge about ISSRs has increased considerably during the last decade or so, most what has been learned is climatological in nature, i.e., we have compiled statistical information (Gierens et al., 1999, 2000, 2004; Gierens and Spichtinger, 2000; Spichtinger et al., 2002, 2003a,b; Gettelman et al., 2006); however, what we need for forecasting of contrail occurrence and persistence is to know more about single ISSR cases. Two case studies of ISSRs have been conducted by Spichtinger et al. (2005a,b). In one case an ISSR that lasted for at least 24 hours was caused by slow large-scale uplift of an airmass in a frontal system. In the second case the ISSR, lasting only a couple of hours, was caused by small-scale uplift due to a superposition of orographic waves and waves induced by strong curvature of the nearby jet stream.

Weather forecast models, that up to now have ignored ice supersaturation, should be able to predict upper tropospheric ice supersaturation in order to predict contrail formation. Some weather models use higher cut-offs of RHi than 100%; however, as long as there is any cut-off, it will be artificial. A notable exception to the standard weather forecast models is the Integrated Forecast Model of the European Centre for Medium-Range Weather Forecast (ECMWF) which has had

upper-tropospheric ice supersaturation included since September, 2006 (Tompkins et al., 2007). Initial evaluation of the skill of the new cloud scheme for contrail prediction, using a confined south England based observation data base, show that it is significantly superior to the old scheme which, like most other models, had a RHi cut-off at ice saturation (Tompkins et al., 2007).

3.3.2 *Contrails in climate models*

The lack in climate models of physical and radiative interaction between contrails and their moist environment (as described in Theme 5) renders a solid determination of global contrail effects on the water budget in the upper troposphere currently impossible. The consequences of a changing background atmosphere, resulting from climate change, cannot be evaluated until simulated contrail cirrus undergo similar interactions as those modeled for natural clouds. Advances in the development of such process-based global models that enable the simulation of these and other relevant contrail processes are the subject of key theme 5 but are also linked to the objectives and priorities of key theme 4.

3.4 *Interconnectivity with other SSWP theme areas*

This will be done in February.

4 Recommendations and Prioritization for Tackling Outstanding Issues

This white paper has identified areas where global climate models can improve the treatment of aircraft effects on climate. These include better specification of contrail coverage and day/night differences, representing the whole life cycle of contrails, allowing contrails to interact with their environment, and resolving ice supersaturation and how it is affected by natural and aircraft-induced ice cloud. Rather than focusing on these model-related areas, we will focus on recommendations that focus on measurements that are needed to improve the treatment of contrails and natural ice clouds in global climate models.

Section 2 argues that the net radiative effect of contrails results from a near-cancellation of the shortwave and longwave terms and because of this cancellation between two forcings of roughly equal magnitude the net contrail forcing is very sensitive to any error in either term. Hence, the highest priorities are associated with decreasing the uncertainties associated with evaluating the short and longwave radiative interactions with contrail and cirrus particles.

High Priority – Near term: Field campaigns are needed that employ new technologies to measure the detailed microphysical and chemical structure of aircraft exhaust plumes and contrails during their initial development and subsequent evolution into mature systems that disperse and age.

High Priority – Near term: Develop improved in situ sensors to measure contrail and cirrus particle properties and ice nuclei concentrations and composition.

New measurement capabilities are available that were not in operation during the previous campaigns designed to study contrail physics, chemistry and dynamics. These had to do with probe resolution during the early phases of contrail evolution and in the case of contrail cirrus the inability to identify and separate artifacts produced by shattering of large particles on the probes' inlets from real ice crystals. Secondly, the measurement of size stratified aerosol composition, particularly black carbon and black carbon coated with sulfate was not available during these earlier research programs. Recently, however, there have been aerosol mass spectrometers, single particle soot photometers and fast response optical spectrometers that can distinguish the shapes of very small ice crystals by their depolarization signals. These instruments, deployed on multiple airborne platforms on a program design similar to that of SUCCESS, would provide new information that would constrain cloud parameterizations in models and greatly decrease uncertainties that were associated

with previous measurements. There remains, however, a number a serious technological obstacles to be hurdled. There have been some new developments, e.g. of inlet-less optical spectrometers, that hold promise for circumventing the issue of crystal breakup. These are only now being used operationally and detailed evaluation is necessary to assess if they are free of the problems that limited the earlier technology. In addition, direct collections of contrail crystals during the pre-vortex and vortex phases may be necessary as probes that digitally image crystals smaller than about 30 microns, with high enough resolution to delineate the microstructure, have not yet been developed for airborne use.

The A-train satellite constellation, especially CALIPSO, provides an opportunity to study the backscattering behavior of natural and contrail cirrus in coordination with the targeted, airborne research missions that are a high priority recommendation. Especially useful would be to examine the vertical structure of the volume extinction coefficient, deduced from lidar backscatter, and the depolarization ratio, a measure of particle shape, from case-studies and statistically, to determine whether there are fundamental differences between cirrus and contrail cirrus extinction coefficients. The interpretation of these satellite-derived optical properties is highly dependent on validation with in-situ measurements. Once validated, application of the integrated remote and in situ measurements in state-of-the-art radiative transfer models will provide the net radiative forcing of both natural and aircraft induced cirrus for a wide range of synoptical and climatological conditions.

High Priority – Near term: Implementation of a "closure" experiment to evaluate the sensitivity of cirrus cloud formation and evolution to soot particles emitted by aircraft.

Most studies of ice nucleation by soot have been focused at temperatures warmer than 235K and have used idealized soot particles of unknown relevance to aircraft exhaust soot. A "closure" experiment suitable to make headway in this area requires high-resolution measurements of aerosol composition, their activation to ice, relative humidity, vertical motion, and cloud ice particle size distribution. Carefully developed research aircraft flight patterns that target specific cloud-formation conditions can be used to elucidate the ice-nucleating ability of soot aerosols under certain conditions and their competition with ice formation by ambient aerosols. Specifically, orographic wave clouds provide an excellent environment to characterize the ice-forming activity of soot particles heterogeneously—when environmental temperatures are above -35C, and in competition with homogeneous freezing when below this temperature. Aircraft tracks upwind of these clouds can dispense the soot aerosols and subsequent in-situ and remote sampling of the clouds can discern changes in the ice microphysics. Confirmation of the ice-nucleating behavior of the soot aerosols would involve direct measurement of emitted aerosols using ice nuclei activation instrumentation, and measurements of the composition and ice activation properties of the wave cloud residual aerosols following their sampling by a CVI. Cloud chamber and other fundamental laboratory studies can be used to further elucidate the ice-nucleating properties of soot aerosols and their potential changes with atmospheric aging. Further, laboratory studies could be used in conjunction with carefully designed flight profiles to assess the role of "preactivation" on the ice-forming ability of soot.

High priority – Medium Term: Deploy and acquire sounding of temperature and water vapor from the current generation of radiosondes – the Vaisala RS90 and RS92 that do not have the strong negative biases found in earlier sondes.

The upper limit on contrail and contrail-cirrus coverage is largely driven by the amount and spatial extent of ice-supersaturation (ISS) in the upper troposphere. Over the next several years as long-term data sets acquired with these sensors become available, more robust estimates of layering and spatial extent of ice supersaturations will become available for the upper troposphere. Continued acquisition and analysis of data from the MOZAIC project and from satellite-borne instruments (AIRS) will complement the sonde measurements and should be encouraged, although the relative humidities derived from satellites remain highly uncertain.

High priority – Medium Term: Deploy ground-based remote sensors for measuring upper tropospheric water vapor concentrations, specifically Raman lidar, in areas with a high likelihood of ISS in the upper troposphere.

Medium priority – Long Term: Equip commercial airliners (like MOZAIC) with humidity probes that are designed especially for use in the upper troposphere (including AMDAR, Aircraft Meteorological Data Reporting to the weather centers) and cloud sensors that detect cirrus layers and contrail plumes.

New developments in the capability of meteorological models, such as the ECMWF (European Centre for Medium-Range Weather Forecasts) operational model, to predict ice supersaturated regions means that it may be possible in the near future to predict whether persistent contrails can form in a specific region at a specific time. Unfortunately the meteorological analyses (including the ECMWF one) which serve as initial conditions for forecast runs and for archiving/documenting the atmospheric state still do not represent ISS since radiosonde readings are not operationally corrected and satellite data assimilation suffers from the low vertical resolution in the water vapor bands. Simple cloud sensors would provide a useful contribution to cloud coverage along with basic information on effective radius and number concentration.

5. RECOMMENDATIONS FROM THE CURRENT 'PRACTICAL' PERSPECTIVE

Can our current body of knowledge presented in Section 2 be used in the near term to improve the representation of commercial aircraft influences on climate? Specifically, what can be done using the data collected to date on contrail and cirrus cloud microphysics, their radiative properties, the ice nucleating properties of soot aerosols, and the results of detailed (e. g., LES) modeling of contrail thermodynamics, dynamics and microphysics be used in the near term to improve estimates of the effects of aircraft on climate?

Central to this question is whether the global distribution of ice supersaturation can be better predicted in forecast and climate models and whether it can be evaluated using the existing body of global data on upper tropospheric relative humidity and ice supersaturation. Models will have to carry water vapor and allowing the build up of ice supersaturations rather than condensing and then unloading the condensate from one time step to the next. Ice supersaturation and ice condensate must be carried from one time step to the next and for it to be removed realistically. A physically consistent treatment of ice supersaturation and contrail/cirrus coverage in global models, however, is probably not achievable in the near term, because it requires fundamental changes in cloud parameterization schemes. Meanwhile, substantial progress in global models is still possible in the near future by adapting and validating the subgrid-scale parameterizations of supersaturation and cloud fraction to contrail cirrus that are currently in use to predict natural clouds.

Accurate, high quality information on the vertical structure of water vapor as a function of time of day and season are needed on a global basis for model evaluation and for developing a reliable data base and for evaluating space-borne estimates of water vapor (e. g., AIRS). Improving existing radiosonde water vapor measurements to correct for biases resulting from sensor time lag, 'icing" of the sensor, solar radiative effects, and vertical averaging are now achievable. This is especially true for sonde measurements made with sensors developed and deployed over the past five years that are less influenced by time lag and icing. The correction algorithms should be and could immediately be used in the operational work of the weather centers. This would allow, in the short term, the representation of ice supersaturation in the analyses via data assimilation, not only in the forecasts. With the corrected relative humidity (water vapor) measurements, there is now the ability and also a strong need for performing a comparison of ice supersaturated regions from sondes with weather forecast (e. g., ECMWF) and climate models.

Improvements in the representation of cirrus microphysical and radiative properties in global models are desirable in that they feed back into the upper tropospheric water vapor budget. Improved representations of the scattering properties of natural cirrus ice crystals—scattering models,

have recently become available. Improvements in knowledge of cirrus crystal nucleation—homogeneous and heterogeneous processes and how those can be parameterized for use in large scale model, have become available during the past several years. A consideration of recent laboratory studies, if parameterized in models, can be used at least to bracket minimum and maximum potential impacts of soot emissions on cirrus nucleation.

Several flights into contrails at various stages of their development have been acquired but have not been mined. These include observations in the US from MiDCiX and additional observations from CRYSTAL-FACE, among others. Because the contrails in these cases were generated by the research aircraft, they acquired high-quality water vapor and particle microphysical measurements, and several eventually developed into contrail cirrus, analysis of those data would provide information on the properties of contrail cirrus and provide data sets to evaluate contrail microphysical models.

A global database of upper-level cloudiness and information on vertical profiles of extinction through the upper parts of high clouds is now available from the CALIPSO satellite. These data can be scrutinized with a goal of differentiating cirrus from contrail microphysical (extinction) and radiative properties and may help to evaluate how, when and where contrails evolve into contrail cirrus.

6. REFERENCES

Abbatt, J. P. D., Benz, S., Cziczo, D. J., Kanji, Z., Lohmann, U., and Möhler, O., 2006: Solid ammonium sulfate aerosols as ice nuclei: A Pathway for cirrus cloud formation, *Science*, 313, 5794, 1770–1773.

Appleman, H., 1953: The formation of exhaust condensation trails by jet aircraft. *Bull. Am. Meteorol. Soc*., *34*, 14–20.

Archuleta, C.A., P.J. DeMott, and S.M. Kreidenweis, 2005: Ice nucleation by surrogates for atmospheric mineral dusts and mineral dust/sulfate particles at cirrus temperatures. *Atmos. Chem. Phys.*, 5, 2617–2634.

Atlas, D., Z. Wang, D.P. Duda, 2006: Contrails to cirrus - morphology, microphysics, and radiative properties. *J. Appl. Meteorol. Climatol.*, 45, 5-19.

Bakan, S., M. Betancor, V. Gayler, H. Graßl, 1994: Contrail frequency over Europe from NOAA-satellite images. *Ann. Geophysicae*, 12, 962-968.

Baumgardner, D., J.E. Dye, B. Gandrud, K. Barr, K. Kelly, K.R. Chan, 1996: Refractive indices of aerosols in the upper troposphere and lower stratosphere, *Geophys. Res. Lett*, 23, 749-752.

Baumgardner, D. and. B. Gandrud, 1998: A comparison of the microphysical and optical properties of particles in an aircraft contrail and mountain wave cloud, *Geophys. Res. Lettr.*, 25, 1129-1132.

Baumgardner, D., H. Jonsson, W. Dawson, D. O'Connor and R. Newton, 2001: The cloud, aerosol and precipitation spectrometer (CAPS): A new instrument for cloud investigations, *Atmos. Res.*, 59-60, 251-264.

Baumgardner, D., J.F. Gayet, H. Gerber, A. Korolev, and C. Twohy, 2002: Clouds: Measurement Techniques In-Situ, in the *Encyclopaedia of Atmospheric Science*, Eds. J, Curry, J. Holton and J. Pyle, Academic Press, U.K., ISBN: 0-12-227090-8

Baumgardner, D., H. Chepfer, G.B. Raga, G.L. Kok, 2005: The Shapes of Very Small Cirrus Particles Derived from In Situ Measurements, *Geophys. Res. Lett.,*32, L01806, doi:10.1029/2004GL021300, 2005

Beaver, M. R., Elrod, M. J., Garland, R. M., and Tolbert, M. A., 2006: Ice nucleation in sulfuric acid/organic aerosols: Implications for cirrus cloud formation, *Atmos. Chem. Phys.*, 6, 3231–3242.

Boucher, O., 1999: Air traffic may increase cirrus cloudiness. *Nature*, 397, 30-31.

Brock, C. A., F. Schröder, B. Kärcher, A. Petzold, R. Busen, M. Fiebig, 2000: Ultrafine particle size distributions measured in aircraft exhaust plumes, *J. Geophys. Res.*, 105(D21), 26555-26568, 10.1029/2000JD900360.

Busen, R., U. Schumann, 1995. Visible contrail formation from fuels with different sulfur contents. *Geophys. Res. Lett.*, 22, 1357–1360.

Campos, T. L., and 15 coauthors, 1998: Measurements of NO and NO_y emission indices during SUCCESS. *Geophys. Res. Ltrs*., **25**, 1713-1716.

Carleton, A.M., P.J. Lamb, 1986: Jet contrails and cirrus cloud: A feasibility study employing high-resolution satellite imagery. *Bull. AMS*, 67, 301-309.

Chen, Y., S.M. Kreidenweis, L.M. McInnes, D.C. Rogers, P.J. Demott, 1998: Single particle analysis of ice nucleating aerosols in the upper troposphere and lower stratosphere, *Geophys. Res. Lettr.*, 25, 1391-1394.

Cziczo, D. J., Murphy, D. M., Hudson, P. K., and Thomson, D. S., 2004: Single particle measurements of the composition of cirrus ice residues during CRYSTAL-FACE, *J. Geophys. Res.*, 109, D04201, doi:10.1029/2004JD004032.

Demirdjian, B. , D. Ferry, J. Suzanne, O.B. Popovicheva, N.M. Persiantseva and N.K. Shonija, 2007: Heterogeneities in the microstructure and composition of aircraft engine combustor soot: impact on the water uptake. *J. Atmos. Chem.*, 56, 83, doi: 10.1007/s10874-006-9043-9.

DeMott, P.J., 1990: An exploratory study of ice nucleation by soot aerosols. *J. Appl. Meteor.*, 29, 1072-1079.

DeMott, P. J., Rogers, D. C., and Kreidenweis, S. M., 1997: The susceptibility of ice formation in upper tropospheric clouds to insoluble aerosol components, *J. Geophys. Res.*, 102, 19 575–19 584.

DeMott, P. J., Chen, Y., Kreidenweis, S. M., Rogers, D. C., and Sherman, D. E., 1999: Ice formation by black carbon particles, *Geophys. Res. Lett.*, 26, 2429–2432.

DeMott, P. J., 2002: Laboratory studies of cirrus cloud processes, In *Cirrus*, D.K. Lynch, K. Sassen, D.O.C Starr, G. Stephens Eds., Oxford University Press, New York, 102-135.

DeMott, P.J., A.J. Prenni, C.A. Archuleta, and S.M. Kreidenweis, 2002: Some aerosol effects on cirrus ice formation. *American Meteorological Society Conference on Cloud Physics*, Ogden, UT, June, 2002 (on CD-ROM).

DeMott, P. J., K. Sassen, M. Poellot, D. Baumgardner, D. C. Rogers, S. Brooks, A. J. Prenni, and S. M. Kreidenweis, 2003a: African dust aerosols as atmospheric ice nuclei. *Geophys. Res. Lett.*, **30**, No. 14, 1732, doi:10.1029/2003GL017410.

DeMott, P. J., D. J. Cziczo, A. J. Prenni, D. M. Murphy, S. M. Kreidenweis, D. S. Thomson, R. Borys and D. C. Rogers, 2003b: Measurements of the concentration and composition of nuclei for cirrus formation. *Proceedings of the National Academy of Sciences*, 100, No. 25, 14655-14660.

DeMott, P. J., M.D. Petters, A.J. Prenni, C.M. Carrico, and S.M. Kreidenweis, 2008: Ice nucleation behavior of biomass combustion particles, in preparation for submission to *Atmos. Chem. and Phys.*

Denman, K.L., G. Brasseur, A. Chidthaisong, P. Ciais, P.M. Cox, R.E. Dickinson, D. Hauglustaine, C. Heinze, E. Holland, D. Jacob, U. Lohmann, S Ramachandran, P.L. da Silva Dias, S.C. Wofsy and X. Zhang, 2007: Couplings Between Changes in the Climate System and Biogeochemistry. In: *Climate Change 2007: The Physical Science Basis. Contribution of Working Group I to the Fourth Assessment Report of the Intergovernmental Panel on Climate Change* [Solomon, S., D. Qin, M. Manning, Z. Chen, M. Marquis, K.B. Averyt, M.Tignor and H.L. Miller (eds.)]. Cambridge University Press, Cambridge, United Kingdom and New York, NY, USA.

Diehl, K. and Mitra, S. K., 1998: A laboratory study of the effects of a kerosene burner exhaust on ice nucleation and the evaporation rate of ice crystals, *Atmos. Environ.*, 32, 3145–3151.

Draine, B.T., and P.J. Flatau. Discrete dipole approximation for scattering calculations. *J. Opt. Soc. Am. A*, 11:1491-1499, 1994.

Duda, D.P., P. Minnis, L. Nguyen, R. Palikondra, 2004: A case study of the development of contrail clusters over the Great Lakes. *J. Atmos. Sci.,* 61, 1132-1146.

Dürbeck, T., T. Gerz, 1995: Large-eddy simulation of aircraft exhaust plumes in the free atmosphere: effective diffusivities and cross-sections. *Geophys. Res. Lett*., 22, 3203-3206.

Dürbeck, T., T. Gerz, 1996: Dispersion of aircraft exhausts in the free atmosphere. *J. Geophys. Res.*, 101, 26,007-26,015.

Dye, J.E., B.W. Gandrud, D. Baumgardner, K.R. Chan, G.V. Ferry, M. Loewenstein, K.K. Kelly, and J.C. Wilson, 1990: Observed particle evolution in the polar stratospheric cloud of January 24, 1989. *J. Geophys. Res.*, 17, 413-416.

Dymarska, M., Murray, B. J., Sun, L., Eastwood, M. L., Knopf, D. A., and Bertram, A. K., 2006: Deposition ice nucleation on soot at temperatures relevant for the lower troposphere, *J. Geophys. Res.*, 111, D04204, doi:10.1029/2005JD006627.

Fahey, D.W. et al., 1995. Emission measurements of the Concorde supersonic aircraft in the lower stratosphere. *Science* 270, 70-74.

Field, P. R., A. J. Heymsfield, and A. Bansemer , 2006: Shattering and Particle Interarrival Times Measured by Optical Array Probes in Ice Clouds, *J. Atmos. and Oceanic Tech.,* 23, 1357–1371.

Forster, P., Ramaswamy, V., Artaxo, P., Berntsen, T., Betts, R., Fahey, D.W., Haywood, J., Lean, J., Lowe, D.C., Myhre, G., Nganga, J., Prinn, R., Raga, G., Schulz, M. and Van Dorland, R., 2007: Changes in Atmospheric Constituents and in Radiative Forcing. In: Climate Change 2007: The Physical Science Basis. Contribution of Working Group I to the Fourth Assessment Report of the Intergovernmental Panel on Climate Change. Cambridge University Press, Cambridge, United Kingdom and New York, NY, USA.

Freudenthaler, V., F. Homburg, H. Jäger, 1995: Contrail observations by ground-based scanning lidar: cross-sectional growth. *Geophys. Res. Lett.*, 22, 3501-3504.

Gao, R. S., and coauthors, 2004: Evidence that nitric acid increases relative humidity in low-temperature cirrus clouds. Science, 303, 516-520.

Gardiner, B. A., and J. Hallett, 1985: Degradation of in-cloud forward scattering spectrometer probe measurements in the presence of ice particles, *J. Atmos. Oceanic Technol.*, 2, 171– 180.

Gayet, J. G., G. Febvre, and H. Larsen, 1996: The reliability of the PMS FSSP in the presence of small ice crystals, *J. Atmos. Oceanic Technol*., 13, 1300– 1310.

Gerber, H., C.H. Twohy, B.W. Gandrud, A.J. Heymsfield, G. M. McFarquhar, P.J. Demott and. D.C. Rogers, 1998: Measurements of wave-cloud microphysical properties with two new aircraft probes, *Geophys. Res. Lettr*, 25, 1117-1120.

Gettelman, A., et al., 2006, The Global Distribution of Supersaturation in the Upper Troposphere from the Atmospheric Infrared Sounder. *J. Climate,* 19, 6089–6103.

Gierens, K.M., 1998: How the sky gets covered with condensation trails. *Meteorol. Z.*, 7, 181-187.

Gierens, K., U. Schumann, 1996: Colors of contrails from fuels with different sulfur contents. J. Geophys. Res. 101, 16731-16736.

Gierens, K., E. Jensen, 1998: A numerical study of the contrail-to-cirrus transition. *Geophys. Res. Lett.* 55, 4341-4344.

Gierens, K., U. Schumann, M. Helten, H.G.J. Smit, A. Marenco, 1999: A distribution law for relative humidity in the upper troposphere and lower stratosphere derived from three years of MOZAIC measurements. *Ann. Geophys.* 17, 1218-1226.

Gierens, K., P. Spichtinger, 2000: On the size distribution of ice-supersaturated regions in the upper troposphere and lowermost stratosphere. *Ann. Geophys.* 18, 499-504.

Gierens, K., U. Schumann, M. Helten, H. Smit, P.H. Wang, 2000: Ice-supersaturated regions and sub visible cirrus in the northern midlatitude upper troposphere. *J. Geophys. Res.* 105, 22743-22754.

Gierens, K. 2003: On the transition between heterogeneous and homogeneous freezing. *Atmos. Chem. Phys.*, 3, 437-446.

Gierens, K., R. Kohlhepp, P. Spichtinger, M. Schroedter-Homscheidt, 2004: Ice supersaturation as seen from TOVS. *Atmos. Chem. Phys.*, 4, 539-547.

Gierens, K., 2007: Are fuel additives a viable contrail mitigation option? *Atmospheric Environment* 41, 4548–4552.

Goodman, J., R.F. Pueschel, E.J. Jensen, S. Verma, G.V. Ferry, S.D. Howard, S.A. Kinne, and D. Baumgardner, 1998: Shape and size of contrail particles, *Geophys. Res. Lettr.*, 25, 1327-1330.

Gorbunov, B., Baklanov, A., Kakutkina, N., Windsor, H. L., and Tuomi, R., 2001: Ice nucleation on soot particles, *J. Aerosol Sci.*, 32, 199–215.

Gounou, A. and Hogan, R. J., 2007: A sensitivity study of the effect of horizontal photon transport on the radiative forcing of contrails, J. Atmos. Sci., 64, 1706–1716.

Haag, W., Kärcher, B., Schaefers, S., Stetzer, O., Möhler, O., Schurath, U., Krämer, M., and Schiller, C., 2003: Numerical simulations of homogeneous freezing processes in the aerosol chamber AIDA, *Atmos. Chem. Phys.*, 3, 195–210.

Haag,W. and Kärcher, B., 2004: The impact of aerosols and gravity waves on cirrus clouds at midlatitudes, *J. Geophys. Res.*, 109, D12202, doi:10.1029/2004JD004579.

Hansen J et al. 2005: Efficacy of climate forcings. J.Geophys.Res., 110:D18104

Heintzenberg, J., K. Okada, and J. Ström, 1996: On the composition of non-volatile material in upper tropospheric aerosols and cirrus crystals. *Atmos. Res.*, 41, 81-88.

Hendricks, J., Kärcher, B., Lohmann, U., and Ponater, M., 2005: Do aircraft black carbon emissions affect cirrus clouds on the global scale? *Geophys. Res. Lett.*, 32, L12814, doi:10.1029/2005GL022740.

Heymsfield, A.J., and R.M. Sabin, 1989: Cirrus crystal nucleation by homogeneous freezing of solution droplets. *J. Atmos. Sci.*, 46, 2252-2264.

Heymsfield, A. J., R. P. Lawson, and G. W. Sachse, 1998: Growth of ice crystals in a precipitating contrail. *Geophys. Res. Lett.*, *25*(9), 1335–1338.

Heymsfield, A.J., C. Schmitt, A. Bansemer, G-J van Zadelho, M. J. McGill, C. Twohy, D. Baumgardner, 2006: Effective Radius of Ice Cloud Particle Populations Derived from Aircraft Probes, *J. Atmos. Oceanic Tech.* 23, No. 3, pp. 361–380.

Heymsfield, A.J., 2007: On Measurements of Small Ice Particles in Clouds, *Geophys. Res. Lettr*, VOL. 34, L23812, doi:10.1029/2007GL030951, 2007

Hung, H.-M., S. T. Malinowski, and S. T. Martin, 2003: Kinetics of heterogeneous ice nucleation on the surfaces of mineral dust cores inserted into aqueous ammonium sulfate particles, *J. Phys. Chem. A,* 107, 1296–1306.

Intergovernmental Panel on Climate Change (IPCC 1999), *Aviation and the Global Atmosphere*. J. E. Penner, D. H. Lister, D. J. Griggs, D. J. Dokken, and M. McFarland (eds.), Cambridge University Press. Cambridge, UK, 1999.

Jensen E.J., and O.B. Toon, 1997: The potential impact of soot particles from aircraft exhaust on cirrus clouds. *Geophys. Res. Lett.*, 24, 249-252.

Jensen, E.J., O.B. Toon, R.F. Pueschel, J. Goodman, G.W. Sachse, B.E. Anderson, K.R. Chan, D. Baumgardner, R.C. Miake-Lye., 1998: Ice crystal nucleation and growth in contrails forming at low ambient temperatures, *Geophys. Res. Lettr.*, 25, 1371-1374.

Jensen et al., 2005: Ice supersaturations exceeding 100% at the cold tropical tropopause: implications for cirrus formation and dehydration. *Atmos. Chem. Phys.*, 5, 851-862.

Jonsson, H.H., J.C. Wilson, C.A. Brock, R.K.Knollenberg, R. Newton, J.E. Dye, D. Baumgardner, S. Borrmann, G.V. Ferry, R. Pueschel, D.C. Woods, M.C. Pitts, 1995: Performance of a Focused cavity aerosol spectrometer for measurements in the stratosphere of particle size in the 0.06 - 2.0 mm-Diameter range, *J. Ocean. Atmos. Tech.*, 12, 115-129.

Kanji, Z. A. and Abbatt, J. P. D., 2006: Laboratory studies of ice formation via deposition mode nucleation onto mineral dust and n-hexane soot samples, *J. Geophys. Res.*, 111, D16204, doi:10.1029/2005JD006766.

Kärcher, B., 1996: Aircraft-generated aerosols and visible contrails. *Geophys. Res. Lett. 23 (15)*, 1933-1936.

Kärcher, B., Th. Peter and R. Ottmann, 1995: Contrail formation: Homogeneous nucleation of H_2SO_4 / H_2O droplets. *Geophys. Res. Lett. 22,* 1501-1504.

Kärcher, B., T. Peter, U.M. Biermann, and U. Schumann, 1996: The initial composition of jet condensation trails. *J. Atmos. Sci.*, 53, 3066-3083.

Kärcher, B., 1998: Physicochemistry of aircraft generated liquid aerosols, soot, and ice particles, 1. Model description. *J. Geophys. Res. 103 (D14)*, 17111-17128.

Kärcher, B., R. Busen, A. Petzold, F.P. Schröder, U. Schumann, and E.J. Jensen, 1998: Physicochemistry of aircraft generated liquid aerosols, soot, and ice particles, 2. Comparison with observations and sensitivity studies. *J. Geophys. Res. 103 (D14)* , 17129-17148.

Kärcher, B., and U. Lohmann, 2003: A parameterization of cirrus cloud formation: Heterogeneous freezing, *J. Geophys. Res.*, 108, 4402, doi:10.1029/2002JD003220.

Kärcher, B. and Ström, J., 2003: The roles of dynamical variability and aerosols in cirrus cloud formation, *Atmos. Chem. Phys.*, 3, 823–838.

Kärcher, B., Hendricks, J., and Lohmann, U., 2006: Physically based parameterization of cirrus cloud formation for use in global atmospheric models, *J. Geophys. Res.*, 111, D01205, doi:10.1029/JD006219.

Kärcher, B., O. Möhler, P.J. DeMott, S. Pechtl, and F. Yu, 2007: Insights into the role of soot aerosols in cirrus cloud formation, *Atmos. Chem. Phys.*, **7**, 4203–4227.

Knollenberg, R.G., 1972: Measurements of the growth of the ice budget in a persisting contrail. *J. Atmos. Sci.*, 29, 1367-1374.

Knopf, D. A., and T. Koop, 2006: Heterogeneous nucleation of ice on surrogates of mineral dust. J. *Geophys. Res.*, 111, D12201, doi:10.1029/2005JD006894.

Koehler, K., M. D. Petters, P. J. DeMott, S. M. Kreidenweis, and O. B. Popovicheva, 2008: Hygroscopicity, cloud condensation nuclei activity and ice nucleation ability of selected combustion soot particles. In preparation for submission to *Atmos. Chem. Phys.*

Koop, T., B, Luo, A. Tsias, and T. Peter, 2000: Water activity as the determinant for homogeneous ice nucleation in aqueous solutions. *Nature*, 406, 611-614.

Koop, T., 2004: Homogeneous nucleation in water and aqueous systems. *Z. Phys. Chem*. 218, 1231-1258.

Korolev, A., and G. A. Isaac, 2005: Shattering during sampling by OAPs and HVPS. part I: Snow particles, *J. Atmos. Oceanic Technol*., 22, 528–543.

Kuhn, M., A. Petzold, D. Baumgardner, and F.P. Petzold, 1998: Particle composition of a young condensation trail and of upper tropospheric aerosol, *Geophys. Res. Lettr.*, 25, 2679-2682.

Kuhn, P.M., 1970: Airborne observations of contrail effects on the thermal radiation budget. J. Atmos. Sci., 27, 937-942.

Lawson, R. P., A. J. Heymsfield, S. M. Aulenbach, and T. L. Jensen, 1998: Shapes, sizes, and light scattering properties of ice crystals in cirrus and a persistent contrail during SUCCESS, *Geophys. Res. Lett.*, *25*(9), 1331–1334.

Lawson, R.P., Baker, B.A., Schmitt, C.G., and Jensen, T.L., 2001: An overview of microphysical properties of Arctic clouds observed in May and July during FIRE.ACE. *J. Geophys. Res.*, **106**, 14,989-15,014.

Lawson, R. P., O'Connor, D., Zmarzly, P., Weaver, K., Baker, B. A., Mo, Q., and Jonsson, H.: The 2D-S (Stereo) probe, 2006: design and preliminary tests of a new airborne, high speed, high-resolution particle imaging probe, *J. Atmos. Oceanic Technol.*, 23, 1462-1477.

Lewellen, D. C., and W. S. Lewellen, 2001: The effects of aircraft wake dynamics on contrail development. *J. Atmos. Sci.,* **58,** 390–406.

Lin, R-F., D.O.C Starr, P.J. DeMott, R. Cotton, K. Sassen, E. Jensen, B. Karcher, and X. Liu, 2002: Cirrus parcel model comparison project phase 1: The critical components to simulate cirrus initiation explicitly, *J. Atmos. Sci.*, 59, 2305-2329.

Lohmann, U., 2002: Possible aerosol effects on ice clouds via contact nucleation. *J. Atmos. Sci.*, 59, 647-656.

Lohmann, U. and K. Diehl, 2006: Sensitivity studies of the importance of dust ice nuclei for the indirect aerosol effect on stratiform mixed-phase clouds. *J. Atmos. Sci.*, 63, 968-982.

Mannstein, H. and U. Schumann, 2005: Aircraft induced contrail cirrus over Europe. *Meteorol. Z. 14*, 549-554.

Marquart, S. and Mayer, B., 2002: Towards a reliable GCM estimation of contrail radiative forcing, Geophys. Res. Lett., 29(8), 20-1–20-4, doi:10.1029/2001GL014075.

Marquart, S., Ponater, M., Mager, F., and Sausen, R., 2003: Future development of contrail cover, optical depth and radiative forcing: Impacts of increasing air traffic and climate change, J. Climate, 16, 2890–2904.

McFarquhar, Greg M. Junshik Um, Matt Freer, Darrel Baumgardner, Gregory L. Kok, and Gerald Mace, 2007: Importance of small ice crystals to cirrus properties: Observations from the Tropical Warm Pool International Cloud Experiment (TWP-ICE), *Geophys. Res. Lettr.*, 34, L13803, doi:10.1029/2007GL029865

McMurray, P.H., 2000: A review of atmospheric aerosol measurements, *Atmospheric Environment*, 34, 1959-1999

Meerkötter, R., U. Schumann, D. R. Doelling, P. Minnis, T. Nakajima, and Y. Tsushima, 1999: Radiative forcing by contrails. *Ann. Geophys.*, **17**, 1080–1094, 1999.

Meyer, R., Mannstein, H., Meerk¨otter, R., Schumann, U., and Wendling, P., 2002: Regional radiative forcing by line-shaped contrails derived from satellite data, J. Geophys. Res., 107(D10), ACL 17- 1–ACL 17-15, doi:10.1029/2001JD000426

Minnis, P., V. Chakrapani, D. Doelling, L. Nguyen, R. Palikonda, D. Spangenberg, T. Uttal, R. Arduini, and M. Shupe (2001), Cloud coverage and height during FIRE ACE derived from AVHRR data, J. Geophys. Res., 106(D14), 15215-15232.

Minnis P, Ayers JK, Palikonda R. Phan D. 2004: Contrails, Cirrus Trends, and Climate. J. Climate, 17, 1671-1685

Mishchenko, M. I. and A. Macke, 1999: " How Big Should Hexagonal Ice Crystals be to Produce Halos?," Appl. Opt. **38**, 1626-1629.

Möhler, O., Stetzer, O., Schaefers, S., Linke, C., Schnaiter, M., Tiede, R., Saathoff, H., Krämer, M., Mangold, A., Budz, P., Zink., P., Schreiner, J., Mauersberger, K., Haag, W., Kärcher, B., and Schurath, U., 2003: Experimental investigations of homogeneous freezing of sulphuric acid particles in the aerosol chamber AIDA, *Atmos. Chem. Phys.*, 3, 211–223.

Möhler, O., Büttner, S., Linke, C., Schnaiter, M., Saathoff, H., Stetzer, O., Wagner, R., Krämer, M., Mangold, A., Ebert, V., and Schurath, U., 2005a: Effect of sulfuric acid coating on heterogeneous ice nucleation by soot aerosol particles. *J. Geophys. Res.*, 110, D11210, doi:10.1029/2004JD005169.

Möhler, O., Linke, C., Saathoff, H., Schnaiter, M., Wagner, R., Mangold, A., Krämer, M., and Schurath, U., 2005b: Ice nucleation on flame soot aerosol of different organic carbon content. *Meteorol. Z.*, 14, 477–484.

Möhler, O., P. R. Field, P. Connolly, S. Benz, H. Saathoff, M. Schnaiter, R. Wagner, R. Cotton, M. Krämer, A. Mangold, and A. J. Heymfield, 2006: Efficiency of the deposition mode ice nucleation on mineral dust particles. *Atmos. Chem. Phys.*, 6, 3007-3021.

Murphy, D.M., 2003: Dehydration in cold clouds is enhanced by a transition from cubic to hexagonal ice. *Geophys. Res. Lett.*, 30(23), 2230, doi: 10.1029/2003GL018566.

Murray, B. J., and A. K. Bertram 2007: Strong dependence of cubic ice formation on droplet ammonium to sulfate ratio. Geophys. Res. Lett. 34, L16810, doi:10.1029/2007GL030471.

Myhre, G. and Stordal, F., 2001: On the tradeoff of the solar and thermal infrared radiative impact of contrails. Geophysical Research Letters, 28, 3119-3122.

Next Generation Air Transportation System, Federal Aviation Administration report to the U.S. Congress, 2004.

Peter, T., C. Marcolli, P. Spichtinger, T. Corti, M. B. Baker, and T. Koop, 2006: When Dry Air Is Too humid. *Science*, 314, 1399-1402.

Peter, T., C. Bruhl, and P. J. Crutzen 1991: Increase in the PSC-formation probability created by high-flying aircraft. *Geophys. Res. Lett.*, 18, 1465-1468.,

Murray, B. J., and A. K. Bertram 2007: Strong dependence of cubic ice formation on droplet ammonium to sulfate ratio. Geophys. Res. Lett. 34, L16810, doi:10.1029/2007GL030471.

Petzold, A., R. Busen, F.P. Schroeder, R. Baumann, M. Kuhn, J. Stroem, D. Hagen, P. Whitefield, D. Baumgardner, F. Arnold, and U. Schumann, 1997: Near field measurements on contrail properties from fuels with different sulfur content, *J. Geophys. Res.,* 102, 29,867-29,880.

Petzold, A., J. Ström, S. Ohlsson and F. P. Schröder, 1998a.: Elemental composition and morphology of ice-crystal residual particles in cirrus clouds and contrails, *Atmos. Res.*, *49, 21-34*

Petzold A., J. Ström, F. P. Schröder and B. Kärcher, 1998b: Carbonaceous aerosol in jet engine exhaust: emission characteristics and implications for heterogeneous chemical reactions, *Atmos. Environ.*, *33, 2689-2698.*

Petzold, A., A. Döpelheuer, C. A. Brock, F. Schröder, 1999: In situ observations and model calculations of black carbon emission by aircraft at cruise altitude, *J. Geophys. Res.*, 104(D18), 22171-22182, 10.1029/1999JD900460.

Petzold, A., M. Gysel, X. Vancassel, R. Hitzenberger, H. Puxbaum, S. Vrochticky, E.Weingartner, U. Baltensperger, and P. Mirabel, 2005: On the effects of organic matter and sulphur-containing compounds on the CCN activation of combustion particles. *Atmos. Chem. Phys.*, 5, 3187–3203.

Poellot, M. R., W. P. Arnott, and J. Hallett, 1999: In-situ observations of contrail microphysics and implications for their radiative impact. *J. Geophys. Res.*, 1**04**, 12,077–12,084.

Ponater, M., Marquart, S., and Sausen, R., 2002: Contrails in a comprehensive global climate model: Parameterization and radiative forcing results, J. Geophys. Res., 107(D13), ACL 2-1–ACL 2-15, doi:10.1029/2001JD000429.

Ponater, M., Marquart, S., Sausen, R., Schumann, U., 2005: On contrail climate sensitivity. Geophysical Research Letters 32, L10706, doi:10.1029/2005GL022580

Popovicheva O. B., Persiantseva N. M., Shonija N. K., P. J. DeMott, K. Koehler, M. D. Petters, S. M. Kreidenweis, V. Tishkova, B. Demirdjian, J. Suzanne, 2007: Water interaction with hydrophobic and hydrophilic soot particles, in preparation for submission to *Phys. Chem. Chem. Phys.*

Rädel G., and K. Shine, 2008. Radiative forcing by persistent contrails and its dependence on cruise altitudes. *J. Geophys. Res*., (in press).

Richardson, M. S., P. J. DeMott, S. M. Kreidenweis, D. J. Cziczo, E. Dunlea, J. L. Jimenez, D. S. Thompson, L. L. Ashbaugh, R. D. Borys, D. S. Westphal, G. S. Cassucio and T. L. Lersch, 2007: Measurements of heterogeneous ice nuclei in the Western U.S. in springtime and their relation to aerosol characteristics. *J. Geophys. Res.*, 112, D02209, doi:10.1029/2006JD007500.

Rind D., Lonergan P. and Shah K., 2000: Modeled impact of cirrus cloud increases along flight paths. Journal of Geophysical Research 105, 19927-19940

Roberts, P. and J. Hallett, 1968: A laboratory study of the ice nucleating properties of some mineral particulates. *Quart. J. Royal Meteorol. Soc.*, 94, 25–34 (1968).

Rogers, D.C., P.J. DeMott, S.M. Kreidenweiss and Y. Chen, 1998: Measurements of ice nucleating aerosols during SUCCESS, *Geophys. Res. Lettr.*, 25, 1383-1386.

Rogers, D.C., P.J. DeMott, S.M. Kreidenweis and Y. Chen, 2001: A continuous flow diffusion chamber for airborne measurements of ice nuclei, *J. Atmos. Oceanic Technol.*, 18, 725-741.

Rogers, D.C., P.J. DeMott, and S.M. Kreidenweis, 2008: An exploratory field study of the production of ice nucleating aerosol particles by jet aircraft. In preparation for submission to *J. Geophys. Res.*

Sassen, K., and G.C. Dodd, 1988: Homogeneous nucleation rate for highly supercooled cirrus cloud droplets. *J. Atmos. Sci.*, 45, 1357-1369.

Sassen, K., P. J. DeMott, J. M. Prospero, and M. R. Poellot, 2003: Saharan dust storms and indirect aerosol effects on clouds: CRYSTAL-FACE results, *Geophys. Res. Lett.*, 30 (12), 1633, doi:10.1029/2003GL017371.

Sausen, R., K. Gierens, M. Ponater, and U. Schumann, 1998: A diagnostic study of the global distribution of contrails part I: Present day climate. *Theor. Appl. Climatol*., **61**, 127–141.

Sausen, R., Isaksen, I., Grewe, V., Hauglustaine, D., Lee, D., Myhre, G., Kohler, M., Pitari, G., Schumann, U., Stordal, F. and Zerefos, C. , 2005: Aviation radiative forcing in 2000: An update on IPCC (1999). Meteorologische Zeitschrift, 14, 4, 555-561. doi: 10.1127/0941-2948/2005/0049.

Sausen, R., et al., 2005: Aviation radiative forcing in 2000: An update on IPCC (1999). *Meteorol. Z.*, **14**, 1–7.

Schiller, C., M. Krämer, A. Afchine, N. Spelten: An in-situ climatology of ice water content in Arctic, mid latitude and tropical cirrus, JGR, in press.

Schmidt, E., 1941: Die Entstehung von Eisnebel aus den Auspuffgasen von Flugmotoren. In: *Schriften der Deutschen Akademie der Luftfahrtforschun.* Verlag R. Oldenbourg, Munich and Berlin, Germany, Vol. 44, pp. 1-15.

Schröder, F. P., B. Kärcher, A. Petzold, R. Baumann, R. Busen, C. Hoell, U. Schumann, 1998: Ultrafine aerosol particles in aircraft plumes: In situ observations, Geophys. Res. Lett., 25(15), 2789-2792, 10.1029/98GL02078.

Schröder, F., C. A. Brock, R. Baumann, A. Petzold, R. Busen, P. Schulte, M. Fiebig, 2000: In situ studies on volatile jet exhaust particle emissions: Impact of fuel sulfur content and environmental conditions on nuclei mode aerosols, J. Geophys. Res., 105(D15), 19941-19954, 10.1029/2000JD900112.

Schröder, F., and Coauthors, 2000: On the transition of contrails into cirrus clouds. *J. Atmos. Sci.,* **57,** 464–480.

Schumann U., Ström, J., Busen, R., Baumann, R., Gierens, K., Krautstrunk, M., Schröder, F.P., Stingl, J., 1996. In situ observations of particles in jet aircraft exhausts and contrails for different sulfur-containing fuels. J. Geophys. Res. 101, 6853-6869.

Schumann, U., 2000: Influence of Propulsion Efficiency on Contrail Formation, *Aerospace Science and Technology* 4 391-401.

Schumann, U., R. Busen, and M. Plohr, 2000: Experimental Test of the Influence of Propulsion Efficiency on Contrail Formation, J. Aircraft 37 (2000) 1083-1087.

Schumann, U., 2002: Contrail cirrus, in D. K. Lynch et al. (eds.), *Cirrus*, Oxford University Press, pp. 231–255.

Schumann U., F. Arnold, R. Busen, J. Curtius, B. Kärcher, A. Kiendler, A. Petzold, H. Schlager, F. Schröder, and K.-H. Wohlfrom, 2002: Influence of fuel sulfur on the composition of aircraft exhaust plumes: The experiments SULFUR 1–7, *J. Geophys. Res.*, 107 (D15), doi:10.1029/2001JD000813.

Seifert, M., J. Ström, R. Krejci, A. Minikin, A. Petzold, J.-F. Gayet, H. Schlager, H. Ziereis, U. Schumann, and J. Ovarlez, 2004: Thermal stability analysis of particles incorporated in cirrus crystals and of non-activated particles in between the cirrus crystals: comparing clean and polluted air masses. *Atmos. Chem. Phys.*, 4, 1343–1353.

Shilling, J. E., Fortin, T. J., and Tolbert, M. A., 2006: Depositional ice nucleation on crystalline organic and inorganic solids, *J. Geophys. Res.*, 111, D12204, doi:10.1029/2005JD006664.

Shine, K.P., 2005: Comment on 'Contrails, cirrus, trends, and climate'. *J. Clim.*, **18**, 2781–2782.

Spichtinger, P., K. Gierens, W. Read, 2002: The statistical distribution law of relative humidity in the global tropopause region. *Meteorol. Z.* 11, 83-88.

Spichtinger, P., K. Gierens, U. Leiterer, H. Dier, 2003a: Ice supersaturation in the tropopause region over Lindenberg, Germany. *Meteorol. Z.*, 12, 143-156.

Spichtinger, P., K. Gierens, W. Read, 2003b: The global distribution of ice-supersaturated regions as seen by the Microwave Limb Sounder. *Q. J. R. Meteorol. Soc.*, 129, 3391-3410.

Spichtinger, P., K. Gierens, H. Wernli, 2005a: A case study on the formation and evolution of ice supersaturation in the vicinity of a warm conveyor belt's outflow region. *Atmos. Chem. Phys.*, 5, 973-987.

Spichtinger, P., K. Gierens, A. Dörnbrack, 2005b: Formation of ice supersaturation by mesoscale gravity waves. *Atmos. Chem. Phys.*, 5, 1243-1255.

Strauss, B.; Meerkötter, R.; Wissinger, B.; Wendling, P.; Hess, M. (1997): On the Regional Climate Impact of Contrails - Microphysical and Radiative Properties of Contrails and Natural Cirrus Clouds. Annales Geophysicae, Vol. 15, S. 1457 – 1467

Ström, J. and Ohlsson, S., 1998: In-situ measurements of enhanced crystal number densities in cirrus clouds caused by aircraft exhaust, *J. Geophys. Res.*, 103, 11 355–11 361.

Ström, J., M. Seifert, B. Kärcher, J. Ovarlez, A. Minikin, J.-F. Gayet, R. Krejci, A. Petzold, F. Auriol, W. Haag, R. Busen, U. Schumann, and H. C. Hansson, 2003: Cirrus cloud occurrence as function of ambient relative humidity: a comparison of observations obtained during the INCA experiment. *Atmos. Chem. Phys.*, 3, 1807–1816.

Stubenrauch, C.J., and U. Schumann, 2005: Impact of air traffic on cirrus coverage. Geophys. Res. Lett., 32, L14813, doi:10.1029/2005GL022707.

Sussmann, R., K. Gierens, 1999: Lidar and numerical studies on the different evolution of a contrail's vortex system and its secondary wake. *J. Geophys. Res.* 104, 2131-2142.

Stuber, N. and Forster, P., 2007: The impact of diurnal variations of air traffic on contrail radiative forcing, Atmos. Chem. Phys., 7, 3153-3162.

Stordal F, Myhre G, Stordal EJG, Rossow WB, Lee DS, Arlander DW, Svenby T 2005: Is there a trend in cirrus cloud cover due to aircraft traffic? Atmospheric Chemistry and Physics 5:2155 – 2162.

Sussmann, R., K. Gierens, 1999: Lidar and numerical studies on the different evolution of a contrail's vortex system and its secondary wake. *J. Geophys. Res.* 104, 2131-2142.

Sussmann, R., K. Gierens, 2001: Differences in early contrail evolution of 2-engined versus 4-engined aircraft. Lidar measurements and numerical simulations. *J. Geophys. Res.* 106, 4899-4911.

Thomson, D. S., M. E. Schein, D. M. Murphy, 2000*:* Particle Analysis by Laser Mass Spectrometry WB-57F Instrument Overview, *Aerosol Science and Technology, 3,153 – 169.*

Tompkins, A.M., K. Gierens, G. Rädel, 2007: Ice supersaturation in the ECMWF Integrated Forecast System. *Q. J. R. Meteorol. Soc.*, 133, 53-63.

Toon, O.B. and R.C. Miake-Lye, 1998: Subsonic Aircraft: Contrail and Cloud Effects Special Study (SUCCESS), *Geophy. Res. Lettr.,* 25, 1109-1112.

Travis, D.J., Carleton, A.M., and Lauritsen, R.G., 2002: Contrails reduce daily temperature range. Nature, 418, 601-602.

Travis, D.J., Carleton, A.M., and Lauritsen, R.G., 2004: Regional variations in U.S. diurnal temperature range for the 11-14 September 2001 aircraft groundings: evidence of jet contrail influence on climate. J. Clim., 17, 1123-1134

Twohy, C.H., Schanot, A.J. and W.A. Cooper, 1997: Measurement of condensed water content in liquid and ice clouds using an airborne counterflow virtual impactor, *J. Atmos. Oceanic Technol.*, 14, 197-202, 1997.

Twohy, C.H. and B.W. Gandrud, 1998: Electron microscope analysis of residual particles from aircraft contrail, *Geophy. Res. Lettr.*, 25, 1359-1362.

Unterstraßer, S., K. Gierens, P. Spichtinger, 2007: The evolution of contrail microphysics in the vortex phase. *Meteorol. Z.,* accepted.

Wendisch, M., T.J. Garrett and J.W. Strapp, 2002: Wind tunnel tests of the airborne PVM-100A response to large droplets, *J. Atmos. Oceanic tech.*, 19, 1577-1584.

Willeke, K. and Baron, P.A., 2001: Aerosol measurement: Principles, Techniques, and Applications. Second addition: Van Norstrand Reinhold, N.Y..

Wilson, C. W., A. Petzold, S. Nyeki, U. Schumann, and R. Zellner, 2004: Measurement and Prediction of Emissions of Aerosols and Gaseous Precursors from Gas Turbine Engines (PartEmis): An Overview, *Aerospace Sci. Technol.*, 8, 131–143.

Wuebbles, D., 2006: Workshop on the Impacts of Aviation on Climate Change: A Report of Findings and Recommendations June 7-9, 2006, Cambridge, MA, REPORT N0. PARTNER-COE-2006-004, Joint Planning & Development Office Environmental Integrated Product Team, 64 pp

Yang, P. and K. N. Liou, 1996: Finite-difference time domain method for light scattering by small ice crystals in three-dimensional space, J. Opt. Soc. Am. A **13**, 2072-2085.

Zerefos CS, Eleftheratos K, Balis DS, Zanis P, Tselioudis G, Meleti C, 2003: Evidence of impact of aviation on cirrus cloud formation. Atmos. Chem. Phys., 3:1633-1644

Zhang, Y., Macke, A., and F. Albers, 1999: Effect of crystal size spectrum and crystal shape on stratiform cirrus radiative forcing, Atm. Res., 52, 59-75.

Zobrist, B., Marcolli, C., Koop, T., Luo, B. P., Murphy, D. M., Lohmann, U., Zardini, A. A., Krieger, U. K., Corti, T., Cziczo, D. J., Fueglistaler, S., Hudson, P. K., Thomson, D. S., and Peter, Th., 2006: Oxalic acid as a heterogeneous ice nucleus in the upper troposphere and its indirect aerosol effect, *Atmos. Chem. Phys.*, 6, 3115–3129.

Zöger, M., A. Afchine, N. Eicke, M.-T. Gerhards, E. Klein, D. S. McKenna, U. Mörschel, U. Schmidt, V. Tan, F. Tuitjer, T. Woyke, and C. Schiller, 1999: Fast in situ stratospheric hygrometers: A new family of balloonborne and airborne Lyman- photofragment fluorescence hygrometers, *J. Geophys. Res.*, 104, 1807-1816.

Zuberi, B., Bertram, A. K., Koop, T., Molina, L. T., and Molina, M. J., 2001: Heterogeneous nucleation of aqueous particles induced by crystallized (NH4)2SO4-H2O, ice and letovicite, *J. Phys. Chem., A* 105, 6458–6464.

Zuberi, B., Bertram, A. K., Cassa, C. A., Molina, L. T., and Molina, M. J., 2002: Heterogeneous nucleation of ice in (NH4)2SO4-H2O particles with mineral dust immersions, *Geophys. Res. Lett.*, 29, 1504, doi:10.1029/2001GL014289.

TABLES

Table 1: KEY CONTRAIL MICROPHYSICAL MEASUREMENTS

Study	Contrail Type/numbers	Key Findings	Particle Probe[1]
Knollenberg (1972)	Contrail>cirrus uncinus	Unexpectedly large IWC --*Contrail evolved into natural cirrus* --Some crystals developed to >0.5 mm	1D-C (75 μm-2.175 mm)
Gayet et al. (1996)	Contrail cirrus	N_t (>50 μm) up to 0.175 cm^{-3}, larger than natural cirrus	2D-C (25-800 μm)
Goodman (1996)	Contrail	1 min. after generation --N_t~5-10 cm^{-3} -- $\bar{D}_v$ 4-5 μm --Habits predom. plates --Shapes formed when crystals D>0.5 μm	Wire Impactor (>0.5 μm)
Heymsfield et al (1998)	Contrail>cirrus	N_t=10-100 cm^{-3} $\bar{D}$=1-10 μm Contrail visible for >6 hours	MASP (0.3-20 μm) VIPS (20-200 μm) PI (50-1000 μm) 2D-C (50-1600 μm)
Lawson et al. (1998)	Contrail>cirrus	Crystal habits: columns and bullet rosettes *When time>40 minutes, 1-20 micron crystals in contrail core with N_t~1 cm^{-3}*	MASP (0.3-20 μm) PI (50-1000 μm)
Poellot et al. (1999)	21 contrail clouds	N_t > 10 cm^{-3} $\bar{D}$ ~10 μm	FSSP-100 (2-47 μm) 1D-C (20-600 μm) 2D-C (33-1056 μm)
Schröder et al. (2000)	12 Contrail Flights --Sampled up to 30 min. from generation	N_t > 100 cm^{-3} $\bar{D}$=1-10 μm Ice Particles Spherical	FSSP-300 (0.3-20 μm) FSSP-100 (6–98 μm) 2D-C (20-650 μm) Replicator (>2 μm)
Schumann (2002)	Contrail>cirrus	Compilation of contrail IWC estimates	Many instruments
Gao et al. (2004)	Cold contrail	Presence of new class of HNO_3 containing ice crystals at T<202K	MASP [TDL]
Atlas et al. (2006)	Contrail cirrus	Tracked contrails with satellite and lidar	Ground-based Lidar MODIS

Footnote 1:

1D-C: One-dimensional Optical Array Probe **2D-C** Two-dimensional Optical Array Probe

FSSP: Forward Scattering Spectrometer Probe **MASP**: Multi-angle Aerosol Spectrometer Probe

MODIS: Moderate-Resolution Imaging Spectroradiometer **PI**: Particle Imaging Nephelometer

Replicator: Continuous impactor-type probe producing ice crystal crystal replicas **TDL**: Tunable Laser Diode Hygrometer
VIPS: Video Ice Particle Sampler- continuous impactor-type probe producing videos of ice crystals
Wire Impactor: Impactor-type ice crystal replication technique

	Longwave	*Shortwave*	*Net*
Meerkotter et al. (1999)	51.5	−22.0	29.5
Myhre and Stordal (2001)	45.6	-25.2	20.4
Stuber and Forster (2007)	44.2	-20.3	23.9

	Myhre and Stordal (2001)		*Stuber and Forster (2007)*	
	All-sky	*Clear-sky*	*All-sky*	*Clear-sky*
Longwave	0.21	0.27	0.19	0.25
Shortwave	-0.09	-0.15	-0.06	-0.12
Net	0.12	0.12	0.13	0.13

Table 2. Top: Radiative forcing [W/m2] at the top of the atmosphere due to a 100% contrail cover (τvis =0.52) in a continental mid-latitude summer atmosphere (three different radiative transfer schemes are employed).

Table 3: Bottom: Annual mean, global mean radiative forcings [W/m2] at the top of the atmosphere due to a 1% contrail cover (τvis =0.3) for all-sky and clear sky conditions (: different radiative transfer schemes, background atmosphere and background clouds are employed. From Stuber and Forster, 2007)

Table 4 Contrail Properties Measurement Techniques

N = total number concentration, M = total mass concentration, $P_{\lambda,\theta}$ = Phase function
SD = size distribution, σ_e = Extinction coefficient, R_e = Effective radius

Sensing Technique	Particle Property	Instruments
Impaction	N: Directly SD: Directly M: Size distribution integration $P_{\lambda,\theta}$: Size distribution integration R_e: Size distribution integration σ_e: Size distribution integration	Wire impactor SEM grid behind Counterflow Virtual Impactor Video Ice Particle Sampler (VIPS)
Phase change of hydrometeors	N: From CVI only M: Directly	Counterflow Virtual Impactor (CVI)[3] FISH[4]
Single particle light scattering	N: Directly SD: Directly M: Size distribution integration $P_{\lambda,\theta}$: Size distribution integration R_e: Size distribution integration σ_e: Size distribution integration	Forward Scattering Spectrometer Probe Models 100 a (FSSP-100, 300)[1] Passive Cavity Aerosol Spectrometer Probe (PCASP) Cloud and Aerosol Spectrometer (CAS)[1] Multiangle Aerosol Spectrometer (MASP)[1] Focussed Cavity Aerosol Spectrometer (FCAS)[5]
Hydrometeor Ensemble Light Scattering	M: Direct from PVM $P_{\lambda,\theta}$: Partial information from CIN R_e: Direct from PVM σ_e: Direct from CIN	Particle Volume Monitor (PVM)[6] Cloud Integrating Nephelometer (CIN)[2]
Non-Intrusive optical imaging	N: Directly SD: Directly M: Size distribution integration $P_{\lambda,\theta}$: Size distribution integration R_e: Size distribution integration σ_e: Size distribution integration	Cloud Imaging Probe (CIP)[1] Cloud Particle Imager (CPI)[7] 2D Optical Array Probe[1] Small ice detector (SID)[8]
Condensation + light scattering	N: Directly	Condensation Nucleus Counter (CNC)[9] Ice Nucleus Counter[10]
Incandescence and scattering	N: Directly M: Directly (light absorbing carbon) SD: Directly $P_{\lambda,\theta}$: Size distribution integration R_e: Size distribution integration σ_e: Size distribution integration	Single Particle Soot Photometer (SP2)[1]
Laser ionization and mass spectrometery	N: Directly M: Directly (dependent on technique)	Particle Analysis by Laser Mass Spectrometry (PALM

[3] Droplet Measurement Technologies, Boulder, CO
[4] Institute for Chemistry and Dynamics of the Geosphere 1: Stratosphere, Forschungszentrum Jülich, Germany
[5] Denver University, DEnver, CO.
[6] Gerber Scientific Inc., Reston, VA, USA
[7] Stratton Park Engineering, Boulder, CO, USA
[8] Manufacturer?
[9] TSI Inc., Minneapolis, MN
[10] Colorado State University, Ft. Collins, CO

Table 5 Instrumentation on Contrail Measurement Projects

Project Name	Instrumentation	Principal Investigator (responsible for instruments	References
Sulfur I-V	TSI 3067 CN counter	A. Petzold,	Petzold et al. (1997; 1998a,b; 1999)
	N-MASS	C. Brock	Brock et al. (2000)
	PCASP	F. Schröder	Schröder et al (1998, 2000)
	FSSP-300	S. Borrmann	Schumann et al. (1996; 2002)
	CVI	J. Ström	
	MASP	M. Kuhn, D. Baumgardner	Kuhn et al. (1998)
ASHOE/MAESA	CN counter (In-House)	C. Brock	Fahey et al. (1995)
	FCASP	J. Wilson	Jonsson et al. (1995)
	MASP	D. Baumgardner	Baumgardner et al. (1996)
SUCCESS	Wire impactors	J. Goodmann	Goodmann et al. (1998)
	CN	D. Hagen	
	CCN	L. Radke,W.A. Cooper	
	IN (CFD)	D.C. Rogers, P. Demott	Chen et al. (1998), Rogers et al. (1998)
	FSSP-300	R. Pueschel	
	MASP	D. Baumgardner, B. Gandrud	Baumgardner and Gandrud (1998)
	PCASP	J. Anderson	
	CVI	C. Twohy	Twohy and Gandrud (1998), Twohy et
	PVM	H. Gerber	al. (2007)
	VIPS	A. Heymsfield	
			Gerber et al. (1998)
			Toon, O.B. and R.C. Miake-Lye, 1998
AEROCONTRAIL	TSI 3067 CN counter	A. Petzold, C. Brock	
	PCASP	F. Schröder	
	FSSP-300	S. Borrmann	
	CVI	J. Ström	
	MASP	M. Kuhn, D. Baumgardner	
SONIC	?		
CRYSTAL/FACE	CN counters (In-House)	M. Freeman	
	NMASS	M. Freeman	
	PALMS	D. Murphy	Thompson et al. (2000)
	FCAS	J. Wilson	Jonsson et al. (1995)
	CAS	D. Baumgardner, G. Kok	Baumgardner et al. (2001),
	CIP	D. Baumgardner, G. Kok	Baumgardner et al. (2005)
	CPI	P. Lawson	Lawson et al. (2001)
	FSSP-100	P. Lawson	
	VIPS	A. Heymsfield	
CR-AVE	CN counters (In-House)	M. Freeman	
	NMASS (CN In House)	M. Freeman	
	PALMS	D. Murphy	Thompson et al. (2000)
	FCAS	J. Wilson	Jonsson et al. (1995)
	CAS	D. Baumgardner	Baumgardner et al. (2001),
	CIP	D. Baumgardner	Baumgardner et al. (2005)
	CVI	C. Twohy	Twohy et al. (2007)
	CPI	P. Lawson	Lawson et al. (2001)
	2D-S	P. Lawson	Lawson et al. (2006)
CIRRUS-III	CN counters (In-house)		
	FSSP-100		
	CIP		
	FISH		Zöger et al. (1999)
	SP2	G. Kok and D. Baumgardner	

Table 6*: Contrail radiative forcing studies from Stuber and Forster, 2007*

Table 5. Comparison of contrail radiative forcing RF (in mW/m^2) calculated in this study with results from earlier studies. "Scaled" indicates values that have been linearly scaled with contrail cover (in %). For the two studies with a variable optical depth, the mean value of τ is given.

study	contrail cover	τ	diurnal cycle air traffic	RF
this study	0.04	fixed, 0.1	yes	2.0
this study	0.04	fixed, 0.3	yes	5.0
MS2001	0.09	fixed, 0.3	yes	9.0
this study, scaled	0.09	fixed, 0.3	yes	11.3
this study	0.04	fixed, 0.1	no	2.4
Marquart et al. (2003)	0.06	variable, 0.15	no	3.5
this study, scaled	0.06	fixed, 0.1	no	3.6
Fichter et al. (2005)	0.047	variable, 0.15	no	3.2
this study, scaled	0.047	fixed, 0.1	no	2.8

TABLE 7*: CONTRAIL RADIATIVE FORCING SENSITIVITY STUDY FROM MERKOTTER ET AL., 1999*

Table 6. Sensitivity of the daily mean net TOA flux change by contrails to various parameters for 100% contrail with given optical depth τ at 0.55 μm. Results from models N, FL, and M, where available

Case/parameters	Parameter range	τ	Net forcing in Wm^{-2}		
			N	FL	M
Reference		0.52	37.1	37.2	37.2
Different aspherical particles	Spherical – aspherical	0.4	37–22	37–34	37–36
Solar zenith angle	60°–21°	0.52	37–48	37–45	37–46
Ice water content (IWC)	7.2–42 mg m^{-3}	0.2–1.0	19–51	18–53	19–52
Particle radius	5–20 µm	0.85–0.21	41–20	–	–
Surface temperature	289–299 K	0.52	34–39	36–39	35–40
Optical depth of low-level clouds	0–23	0.52	37–40	37–39	37–40
Surface albedo	0.05–0.3	0.52	31–40	34–39	34–40
Relative humidity	Reference – 80%	0.52	37–31	37–31	37–31
Contrail depth (for fixed ice water path)	200 m–1 km	0.52	37–37	–	37–37
Lower contrail top (for fixed IWC)	11–10 km	0.52	37–31	37–32	37–31
Lower contrail top (increased IWC)	11–10 km	0.52–1.32	37–45	–	37–41

FIGURES

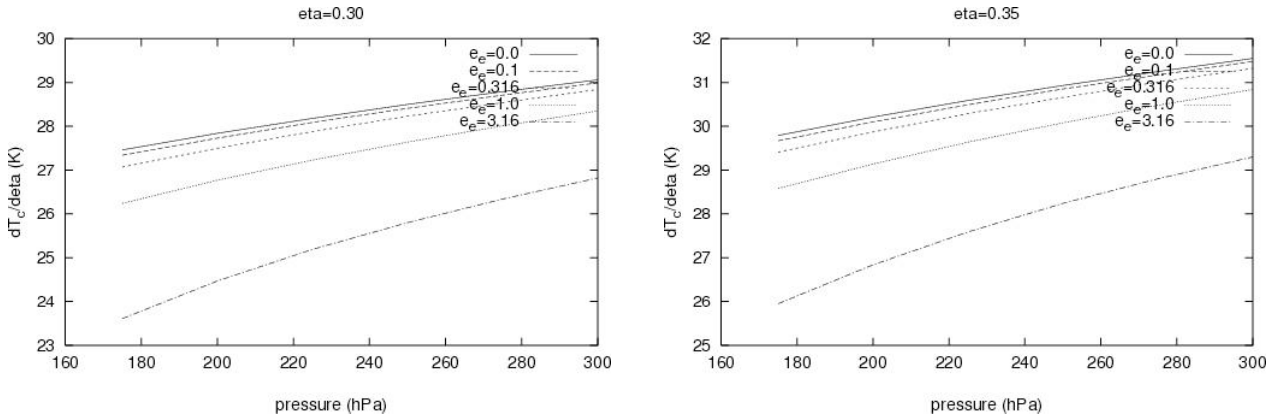

Figure 1: Error in the determination of the contrail formation threshold temperature T_c due to uncertainties in the determination of the overall propulsion efficiency, η, for older aircraft with η=0.3 (left panel) and more modern aircraft with η=0.35 (right panel).

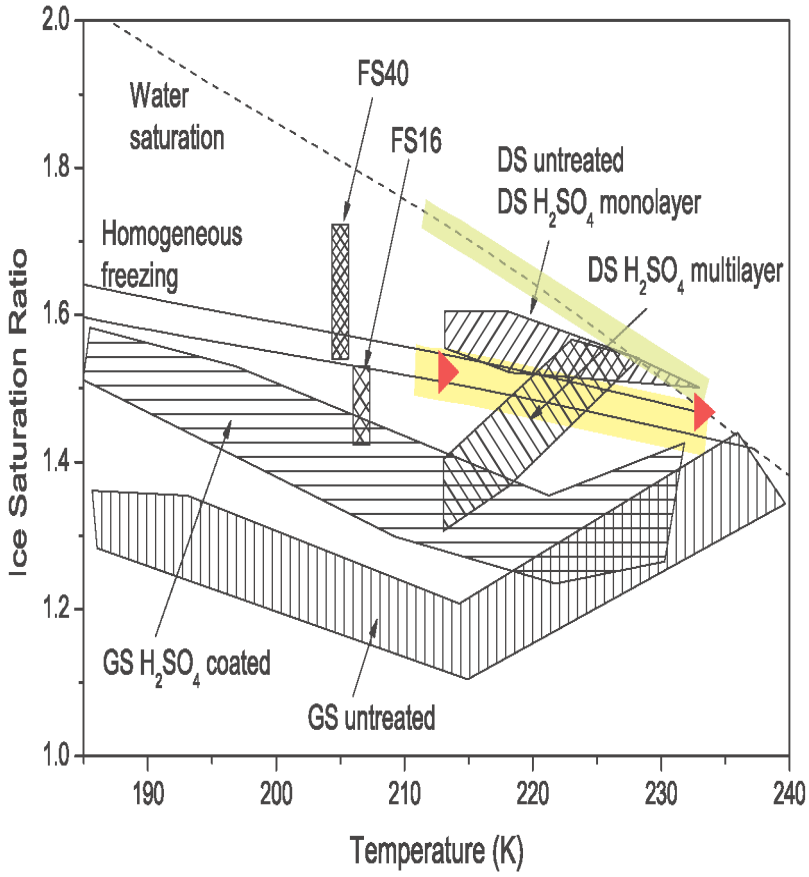

Figure 2: Range of ice formation conditions of some different types of soot particles in the cirrus cloud regime, adapted from Kärcher et al. (2007). All ice formation conditions represent small fractions (<1%) of particles activating for different types. GS represent graphite spark generator soot tested in cloud expansion chamber studies by Möhler et al. (2005a). FSxx represents flame generator soot of xx% organic content in similar chamber studies by Möhler et al. (2005b). DS represent commercial soot particle samples tested in a continuous flow diffusion chamber (CFDC) by DeMott et al. (1998). Yellow shading indicates the range of conditions of low temperature ice formation by fresh biomass combustion particles in a CFDC (DeMott et al. 2008). Red arrow points represent CFDC ice formation conditions for real combustor soot selected at a mobility size of 250 nm (Koehler et al. 2008). Light green shading indicates CFDC ice formation conditions for 50 nm fresh exhaust particles from burning jet fuel in a laboratory burner (DeMott et al. 2002). The lower and upper threshold curves for homogeneous freezing are calculated for 1% of solution particles with radii 1 μm and 0.1 μm freezing within 100 s and 1 s, respectively.

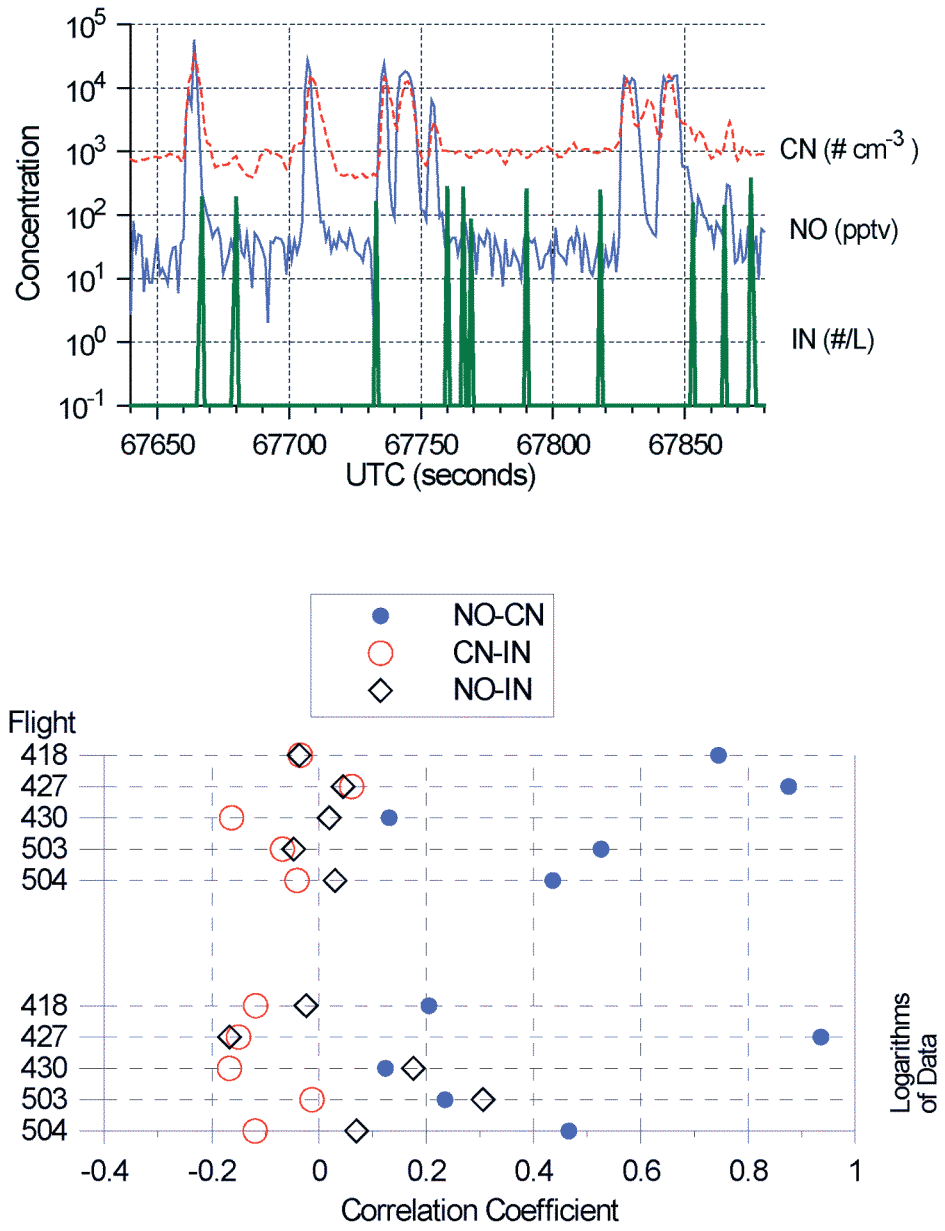

Figure 3: Top panel: Concentrations at 1 Hz of CN (dash line), NO (thin) and IN (thick) for 240 s during several DC-8 aircraft penetrations of a T-39 aircraft exhaust plume on one day during the SUCCESS experiment. IN were processed at -30ºC in the immersion freezing regime (supersaturated with respect to water) in the top panel results. Ambient temperature was -43°C. Bottom panel: Summary of correlation coefficients between NO, IN (T range of 235 to 250K) and CN for five flights, distinguishing (top) all values and (bottom) logarithms of values which excludes seconds when ice nuclei counts were zero.

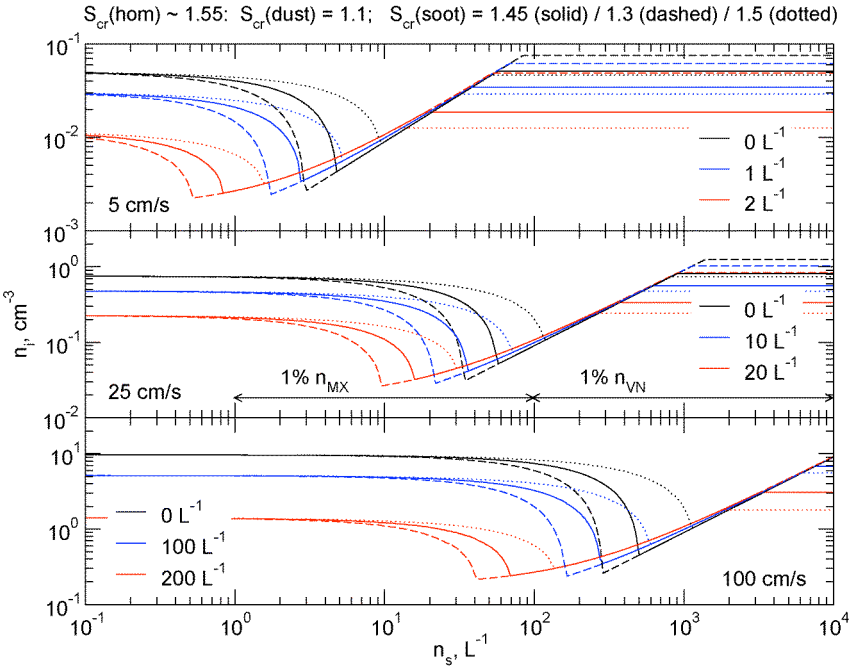

Figure 4: The calculated total number density of nucleated ice crystals as a function of assumed soot particle number density, from Kärcher et al. (2007). The curves result from competition of three particle types during ice formation in adiabatically rising cirrus air parcels. Results are shown for updraft speeds of 5 cm/s (typical synoptic-scale vertical wind), 25 cm/s (corresponding to typically observed background mesoscale temperature fluctuations), and 100 cm/s (strong updrafts in orographic waves or near convection). The air parcels start rising at 250 hPa and 220K at ice saturation and contain natural mineral dust particles with concentrations noted in the legends, a wide range of soot particle concentrations ns as indicated, and 500 cm−3 sulfuric acid particles ("hom" nuclei). The ice nucleation thresholds of these particle types are given at the figure top. The two arrows in the middle panel indicate the range of number concentrations of black carbon-containing type MX (aircraft exhaust coagulated with ambient particles) and VN (volatile/nonvolatile mixed exhaust particles)particles typical for far-field plume ages up to 2 days, assuming that 1% of those are active IN.

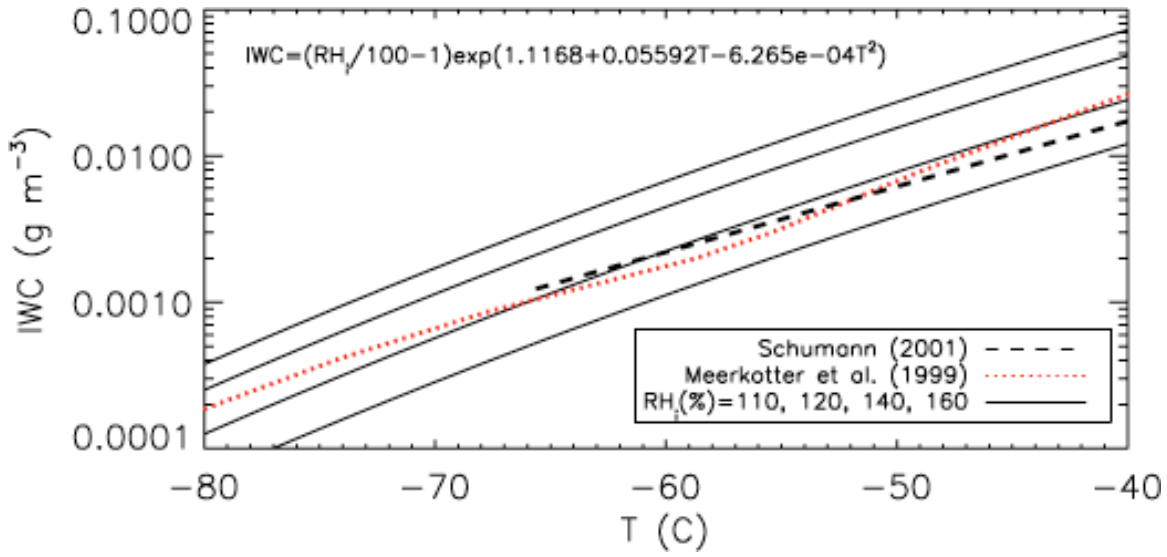

Fig. 5: Contrail ice water content as a function of temperature fitted to observations by Schummann (2002), from the model of Meerkotter et al. (1999) and as given by Eq. 4.

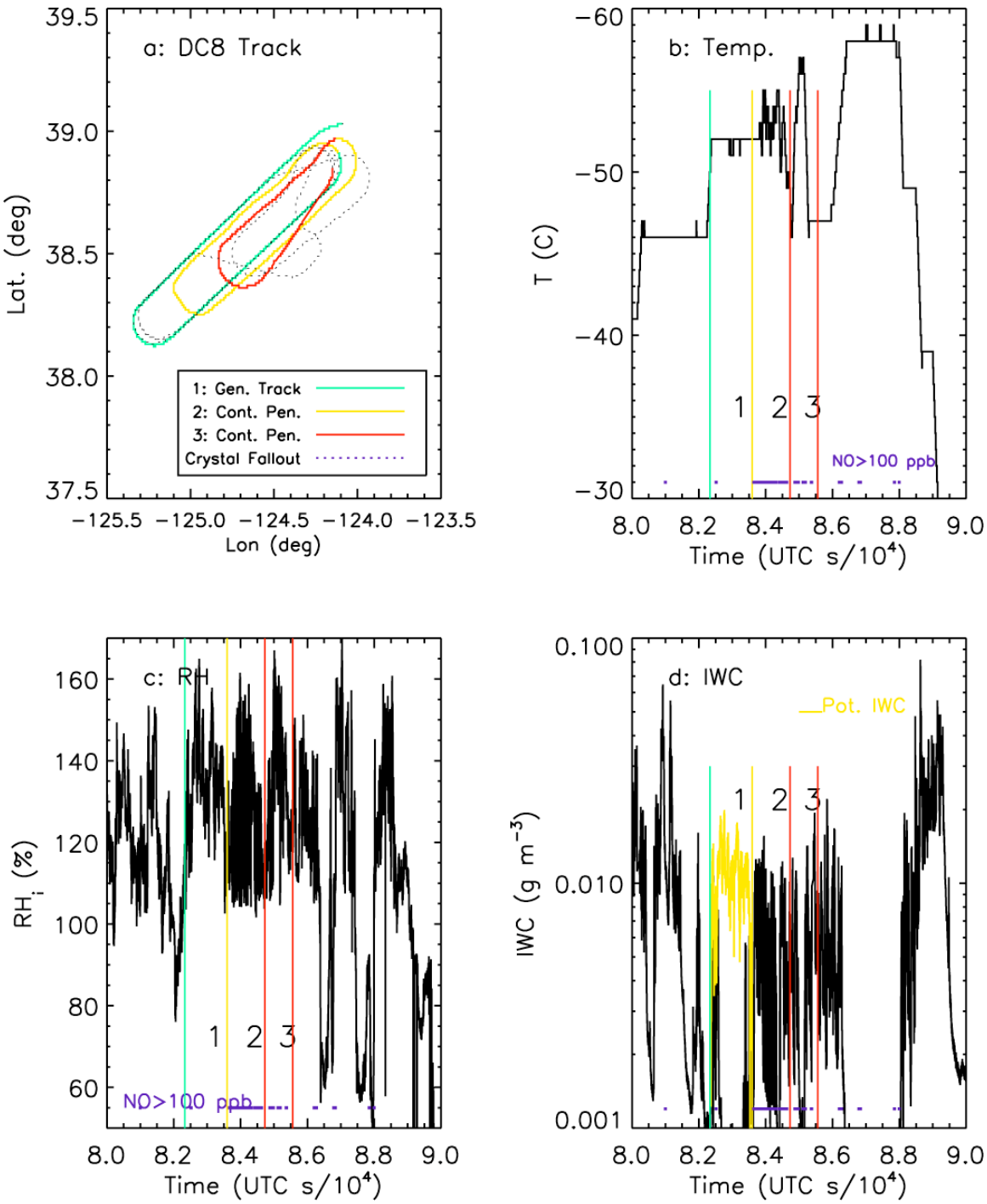

Fig. 6: In-situ observations from contrail produced by NASA DC8 aircraft on 12 May 1996 the SUCCESS field campaign. The contrail was generated in region labelled 1 and was subsequently sampled in regions 2 and 3.

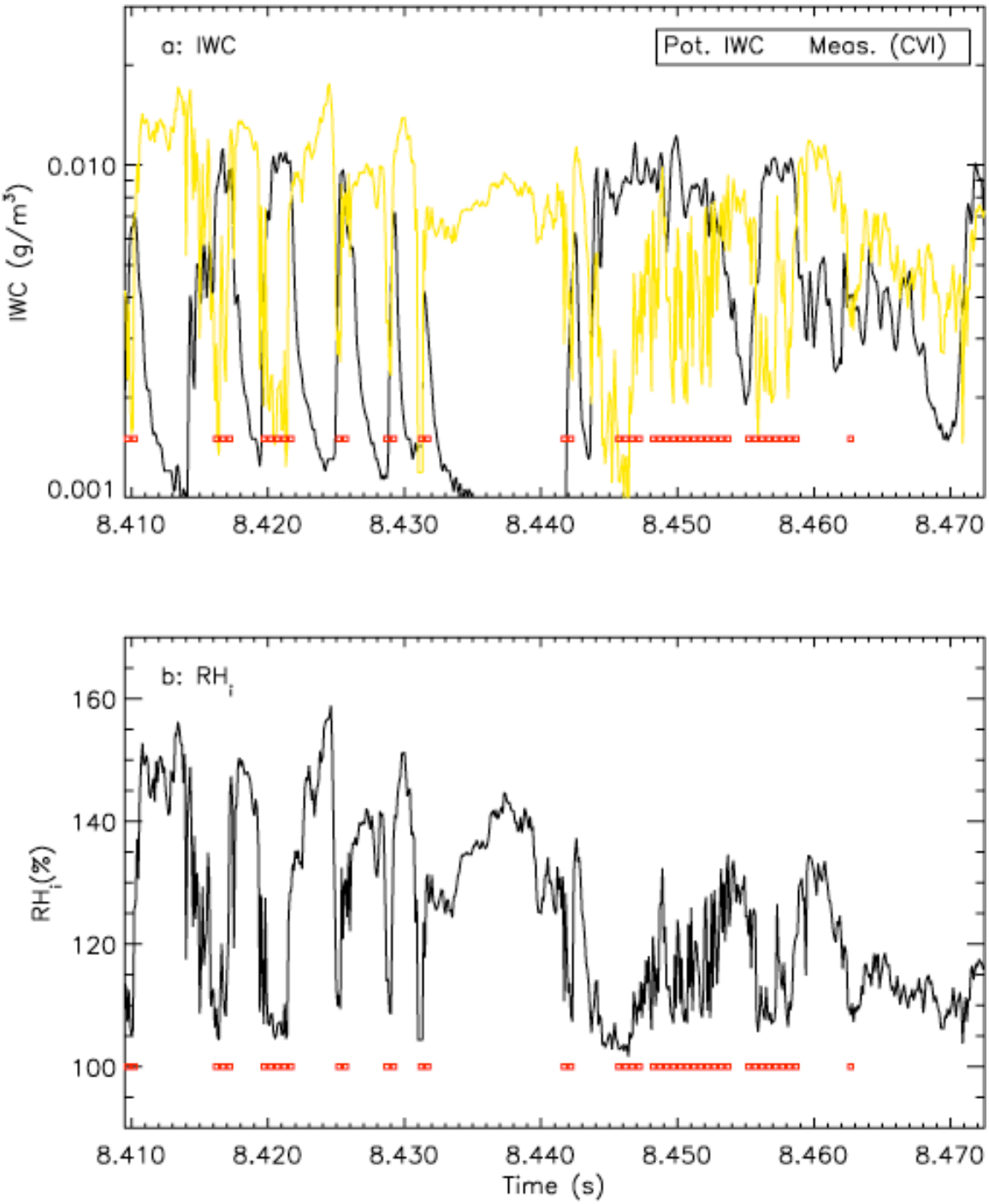

Fig. 7: (a) IWC, both measured and potential (as derived from Eq. 1), and (b) RH_i as function of time during a portion of Pen. 2.

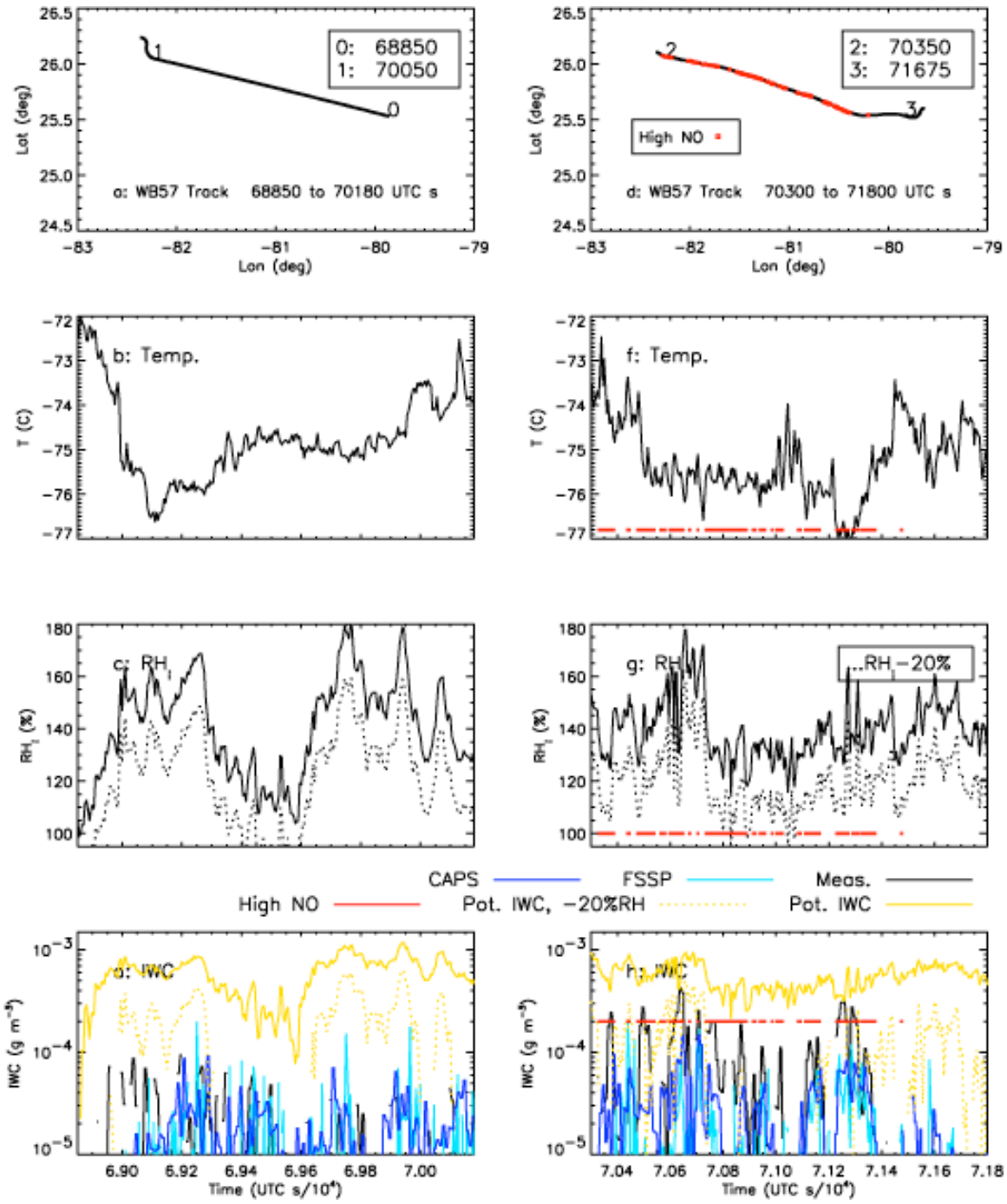

Fig. 8: Measurements from the NASA WB57 aircraft during a penetration into a contrail on 13 July 2002 during the CRYSTAL-FACE field program in southern Florida.

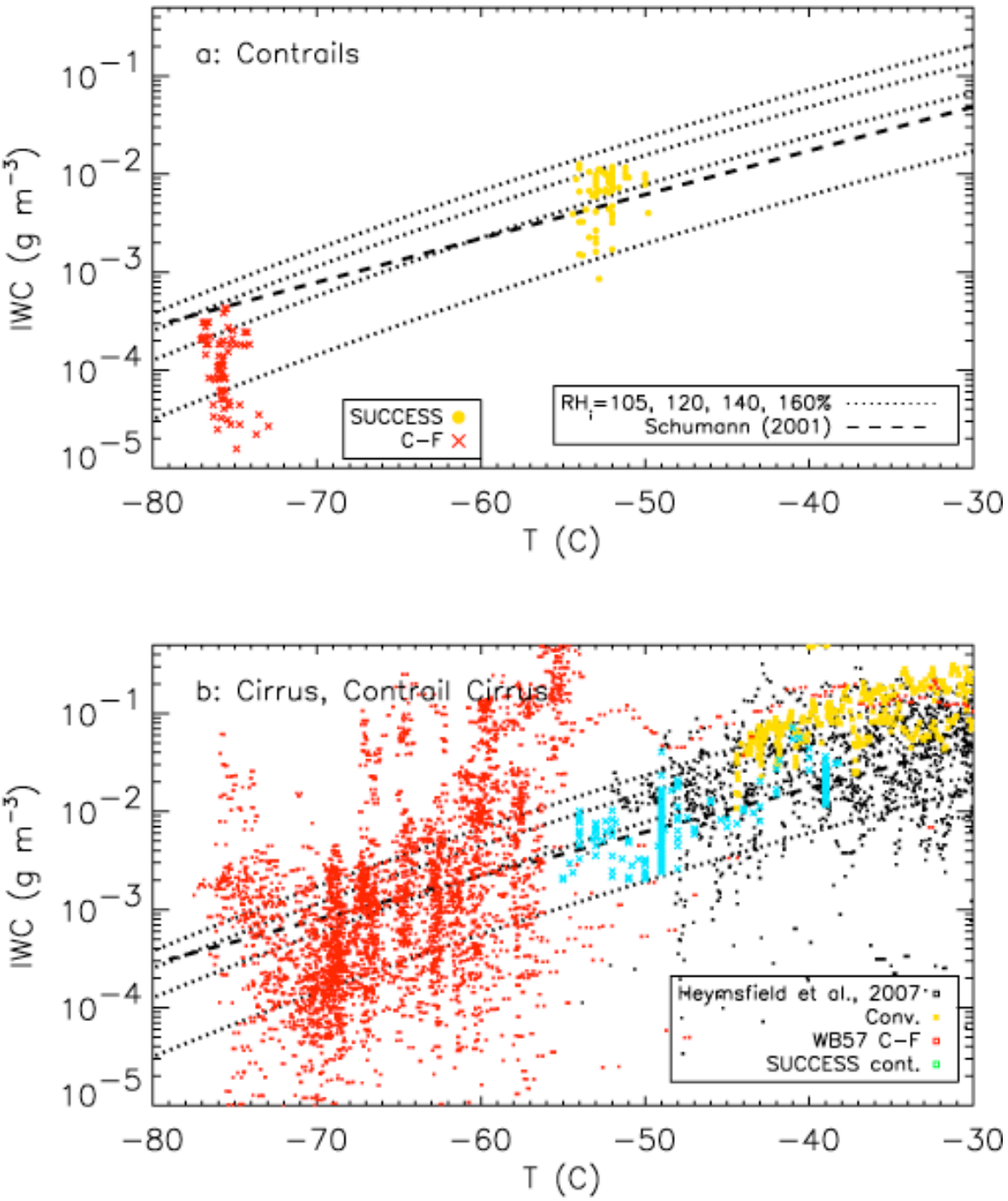

*Fig. 9: (a) Measurements of the IWC as a function of temperature for the SUCCESS and CRYSTAL-FACE contrail observations, and (b) from measurements in cirrus and in cirrus developing from the SUCCESS contrai*l

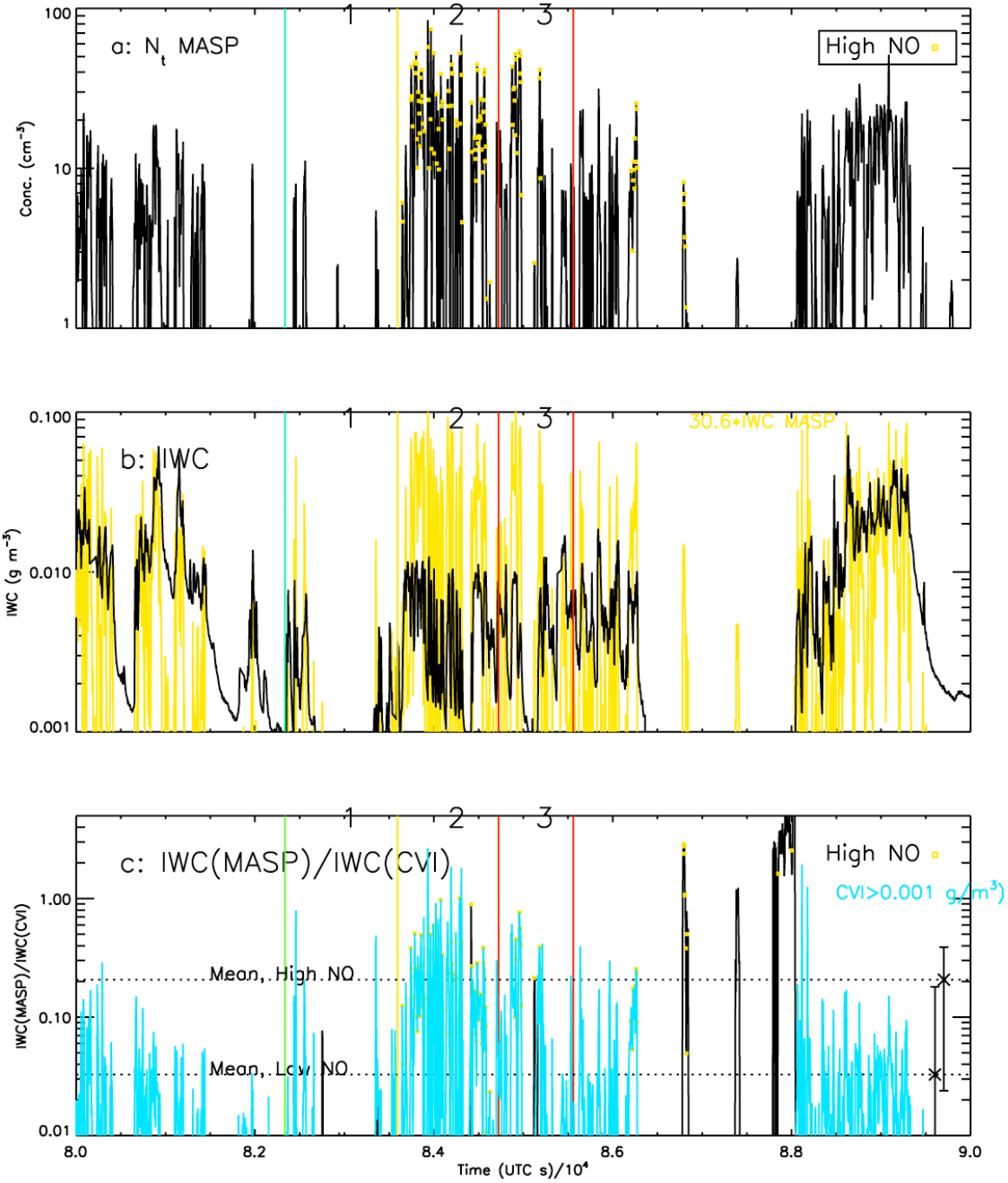

Fig. 10: Particle size distribution observations on 12 May 1996 during the SUCCESS field campaign. Regions of high NO, where contrail particles are sampled, are shown.

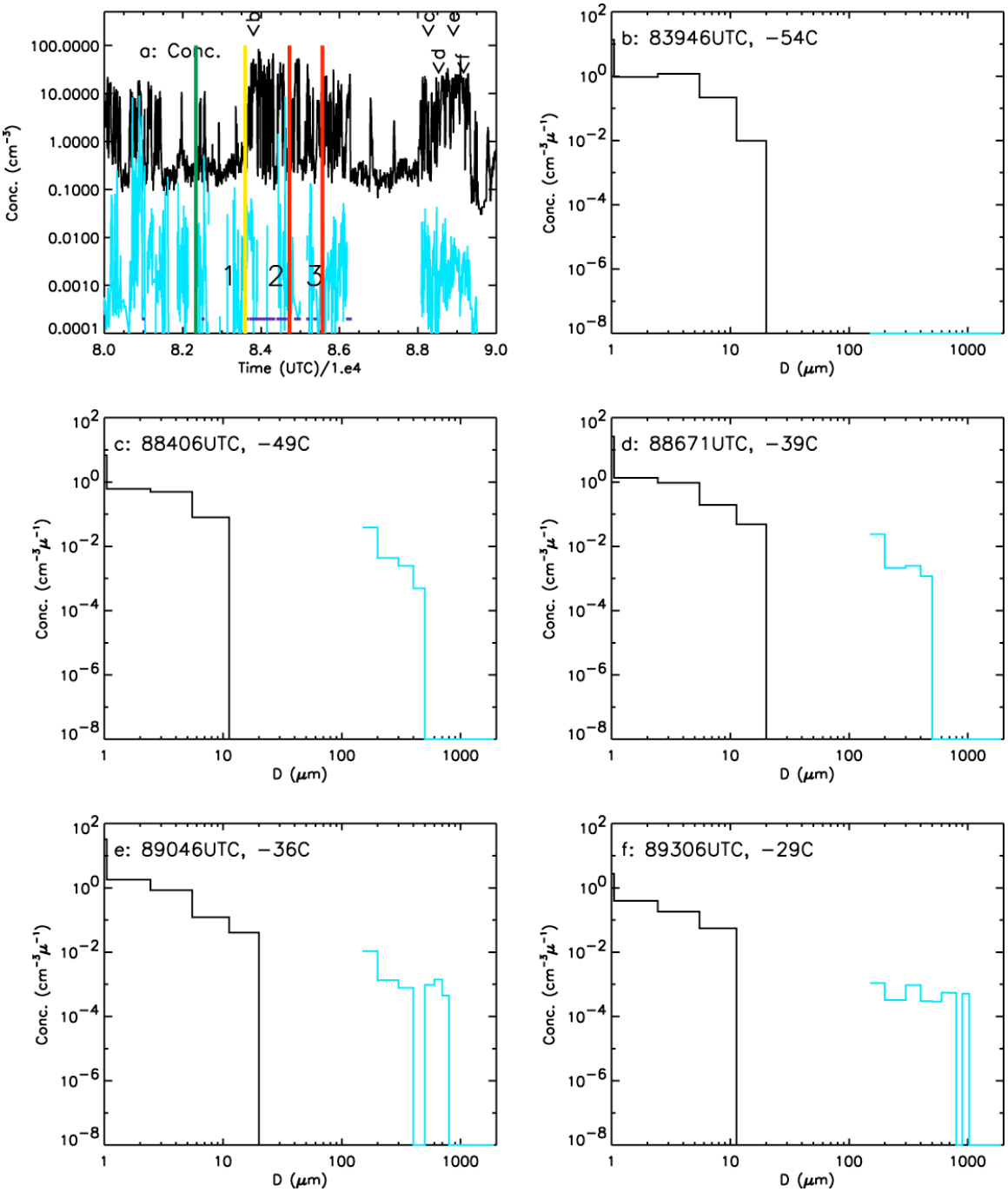

Fig.11: (a) Total concentrations measured by the MASP and 2D-C probes, and (b-f) PSD measured within the contrail plume and in fallout from it, on 12 May 1996 during the SUCCESS field program. In (a), the time of collection of each PSD is shown.

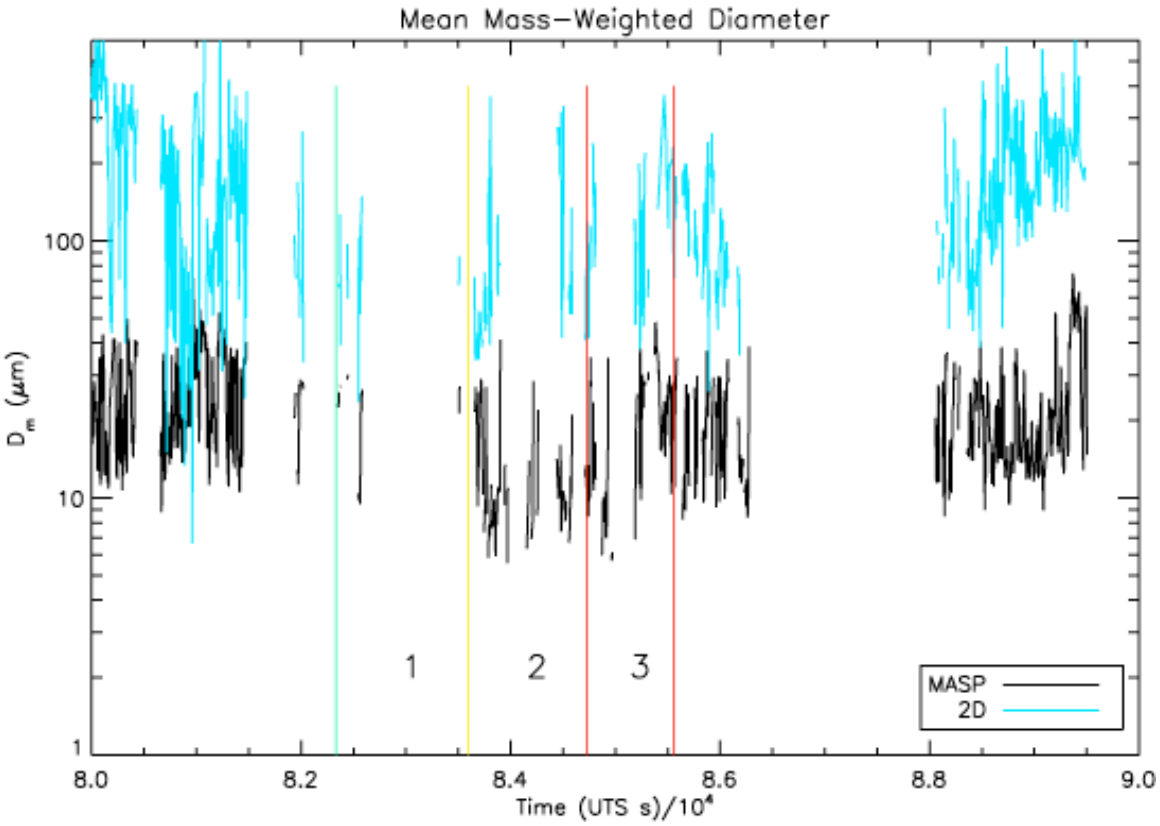

Fig. 12. Mean mass weighted diameter as derived from the CVI IWCs, above the probes cut size, and the total concentrations from the MASP and 2DC probes.

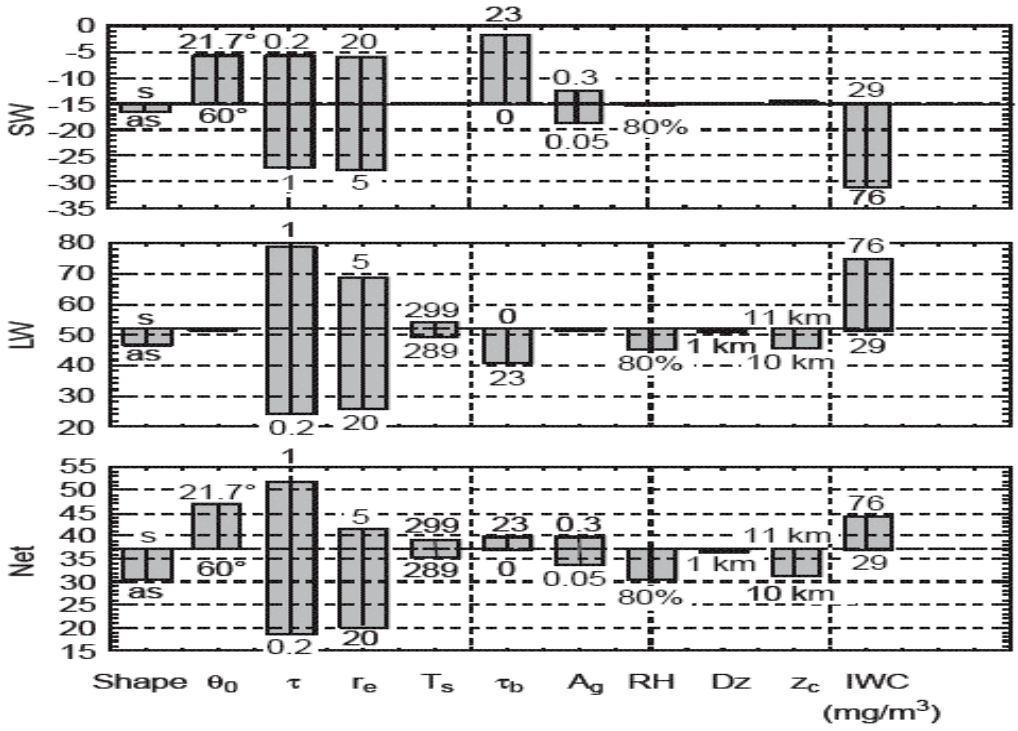

Fig. 6. Results of a sensitivity study using model N. The *bars* indicate the range of variation of shortwave (*SW*), longwave (*LW*) and net (*Net*) flux changes in Wm^{-2} for 100% contrail cover due to the given variation of the parameters: particle shape, solar zenith angle θ_0, IWC or optical depth τ, volume-mean particle radius r_e (in μm), surface temperature T_s (K), optical depth of lower level cloud τ_b, ground albedo A_g, ambient relative humidity *RH* (% of liquid saturation), contrail layer depth *Dz* (km), cloud top level z_c (km), and contrail at 1 km lower level but with increased ice water content *IWC* (mg m^{-3})

Figure 13. Sensitivity study for contrail radiative forcing from Meerkotter et al. (1999)

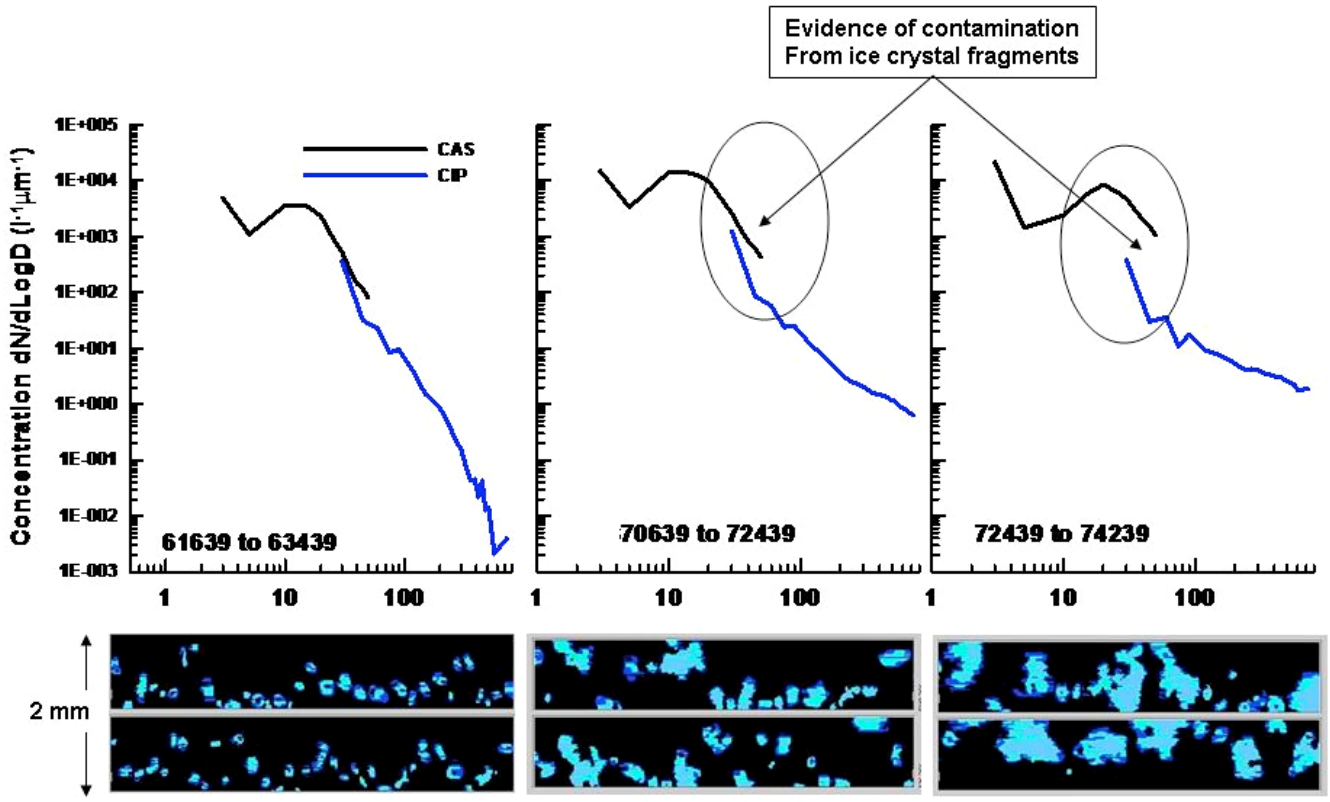

Fig. 14 The size distributions shown here are from the Cloud Aerosol Spectrometer (CAS) in black and the Cloud Imaging Probe (CIP) in blue, showing the agreement in the overlapping size ranges when ice crystals are small, as shown in the images from the CIP (below the size distributions), disagreeing when larger ice crystals are present.

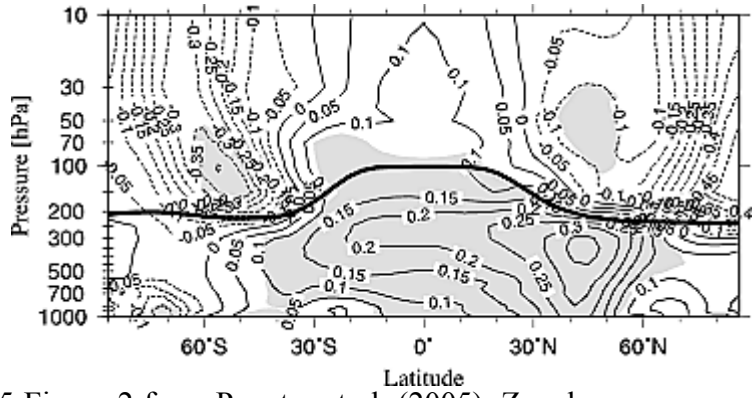

Fig. 15 Figure 2 from Ponater et al. (2005). Zonal mean cross section of annual mean temperature response in the equilibrium climate simulation using enhanced contrail forcing. Thick line displays the tropopause. Shading indicates significance on a 95% level.

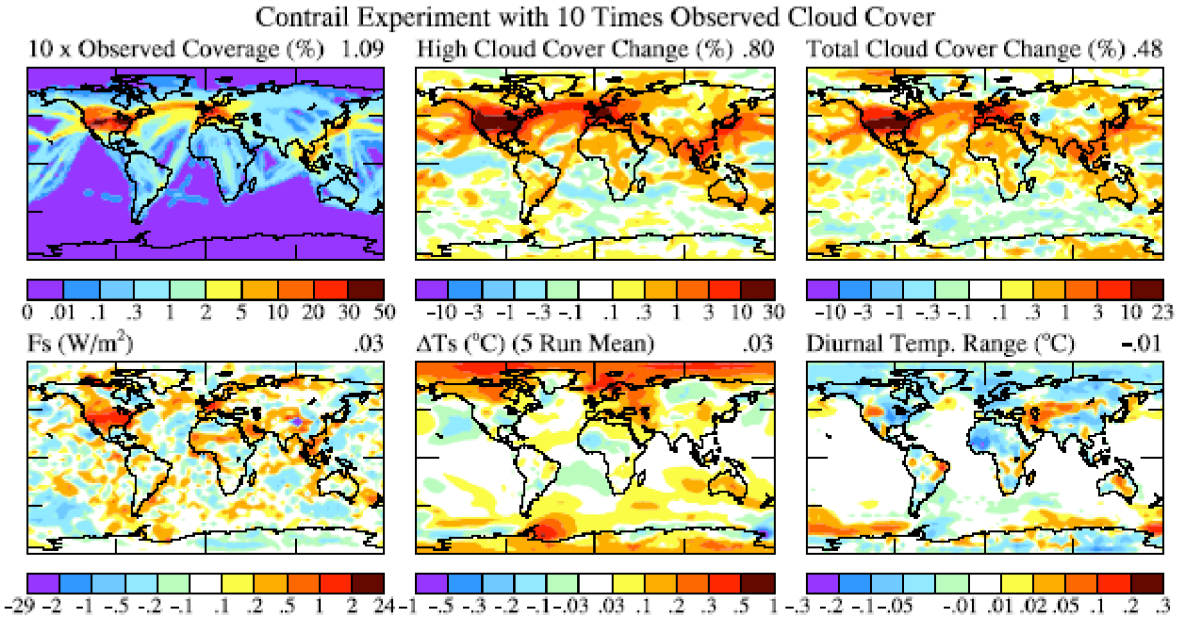

Figure 16. Observed contrail coverage in 1992 from *Minnis et al.* [2004] and simulated impact of the contrails, increased by a factor of 10, on high cloud cover, total cloud cover, Fs, surface air temperature, and the diurnal range of surface air temperature in years 81–120 of the coupled climate model.

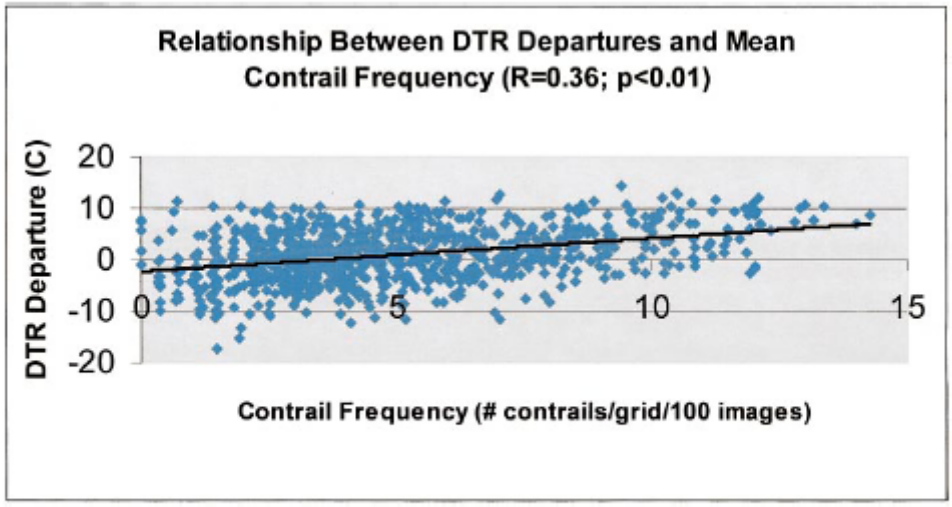

FIG. 4. Scatterplot of the relationship between 11–13 Sep 2001 DTR departures and mean combined 1977–79 and 2000–01 contrail frequency for Oct ($R = 0.36$; $p < 0.01$).

Fig. 17 Results of sensitivity study of net radiative fluxes for varying contrail conditions. From Travis et al. 2004